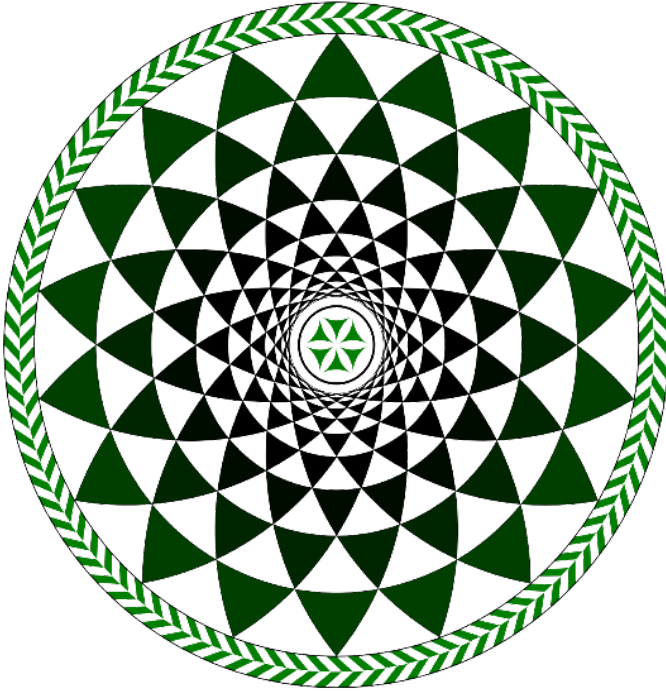


Multis 2022



Multiscale Phenomena in Condensed Matter

Kraków, 27 – 30 June 2022

The Henryk Niewodniczański Institute of Nuclear Physics
Polish Academy of Sciences



Multiscale Phenomena in Condensed Matter

Kraków, 27 – 30 June 2022

Book of abstracts

ORGANIZERS:

Juliusz Chojenka
Dominik Czernia
Magdalena Fitta
Mirosław Gałązka (chair)
Paweł Horodek
Małgorzata Jasiurkowska-Delaporte
Ewa Juszyńska-Gałązka
Piotr Konieczny

Aleksandra Pacanowska
Robert Pełka (co-chair)
Marcin Perzanowski
Marcin Piwowarczyk
Oliwia Polit
Wojciech Sas
Paweł Sobieszczyk
Monika Synowska-Kałuza (secretary)

Honorary Patronage





Dear Colleagues, Dear Friends,

It is our great pleasure and honour to welcome you to the conference **”Multiscale Phenomena in Condensed Matter — Multis 2022”**, the online meeting held on 27 — 30 June. We are happy that you found our idea of a scientific meeting devoted to a wide scope of research into condensed matter interesting and worth joining. We are very grateful to those of you who accepted our invitation to present the opening, keynote or invited lecture: it was an important point at the beginning of organization and helped us a lot, thank you. The rich subject area of the conference, comprising structure, dynamics, relaxation, magnetism and other properties, as well as great diversity of materials, from liquid crystals to molecular nano-magnets, and a variety of experimental techniques — X-ray diffraction, neutron scattering, dielectric, infrared and positron spectroscopy — reflects the investigations we have been conducting in the Henryk Niewodniczański Institute of Nuclear Physics Polish Academy of Sciences for a long time. Our intention is to promote collaborative research among physicists, chemists and natural scientists, which may bring new ideas and important results. For this very purpose, a series of biennial Multis conferences has been initiated.

The conference is organized by the Henryk Niewodniczański Institute of Nuclear Physics Polish Academy of Sciences. The Institute was established in 1955, its founder and first director was Professor Henryk Niewodniczański. Even though the main research stream involves elementary particle and nuclear physics, condensed matter physics together with other disciplines like nano-materials engineering, dosimetry or medical physics, are being explored as well.

We welcome all of you to the conference and firmly hope that Multis 2022 conference will be an important and valuable scientific event. We expect that lectures and posters will initiate valuable and stimulating discussions. During the conference closing session prizes for the best poster and the best oral presentation will be awarded and plans for a follow-up meeting will be announced.

Chairman of the conference

Mieczysław Ostrowski

The historical panorama of Kraków at the Welcome page is a copy of the copperplate engraving by Meriam Matthaus Elder. In 1619 he wrote „Cracovia Totius Poloniae urbs celeberrima atque amplissima regia atque Academia insignis” (Most celebrated and splendid city in all Poland notable by the royal castle and Academia).

Design of our Logo was inspired by the mosaic from Pompeii (Casa degli Amorini Dorati) as it mimics the multiscale path. The T_EX code to draw the mosaic was first published by Daniel Steger <http://www.texaple.net/tikz/examples/mosaic-from-pompeii>

Programme of the Conference

MONDAY, 27 JUNE 2022

09:00		Opening	
09:10	Opening lecture	B. M. Murphy: Ultra-fast to slow dynamics at liquid interfaces investigated with X-rays	p. 15
10:10	Invited	K. Saito: Small spin clusters mimicking a temperature induced phase transition	p. 16
10:40	Contributed	K. Szałowski: Electric field-controlled spin state in uthrene, [7]uthrene and [8]uthrene molecule: computational study	p. 17
11:00	Break		
11:30	Keynote	S. Thomas: Circular economy: new opportunities in sustainable soft nano materials and polymer bio-nanocomposites	p. 19
12:10	Contributed	S. Urban: Dielectric studies of systems influenced by the ionic conductivity	p. 21
12:30	Contributed	S. Pawlus: Is adding a large atom important for the relaxation dynamics of monohydroxy alcohols?	p. 22
12:50	Contributed	D. Sonaglioni: Fast differential scanning calorimetry: new perspectives in data reduction and applications to organic samples	p. 23
13:10	Break		
14:10	Keynote	S. Chorazy: Molecular magnetism meets optical thermometry in heterometallic systems linking lanthanide and transition metal complexes	p. 24
14:50	Invited	S. Ferlay: Assembling functional molecular crystals	p. 26

15:20 **Contributed** M. Ceglarska: Relaxation processes in a single crystal of $\text{Co}(\text{NCS})_2(4\text{-methoxypyridine})_2$ spin chain p. 27

15:40 **Contributed** P. Danylchenko: Rotational magnetocaloric effect in $\text{Ni}(\text{en})(\text{H}_2\text{O})_4 \cdot 2\text{H}_2\text{O}$ p. 28

16:00 **Break**

Flash talks (16:10 – 16:50)

16:10 J. Chudzik: Formation of crosslinked functional Poly (4-vinylpyridine)- CoBr_2 in both static and dynamic conditions p. 30

16:15 P. Dąbczyński: Dendrites formation on poly(methylmetacrylate) surface reactively sputtered with cesium ion beam p. 32

16:20 J. Chojenka: Magnetism and transport studies of thin iron films deposited on anodized titanium oxides p. 33

16:25 W. Sas: Bilayers and double-shell nanotubes of Prussian blue and its Cr analog — the synthesis and magnetic properties p. 35

16:30 S. Yefimova: UV-light activated $(\text{Gd},\text{Y})\text{VO}_4 \cdot \text{Eu}^{3+}$ nanoparticles as nano radio enhancers p. 36

16:35 V. Seminko: Luminescent ceria nanoparticles with controlled ROS scavenging activity p. 38

16:40 S. Pastukh: Investigation of electronic and magnetic properties of copper pyrophosphat p. 39

16:45 M. S. Shakeri: The effect of solvent on oxidation behavior of copper during laser irradiation of suspension, a reactive bond molecular dynamics study p. 40

TUESDAY, 28 JUNE 2022

09:00	Keynote	J. Müller: Fluctuation (noise) spectroscopy as a tool to study the dynamics of multi-scale systems in condensed matter	p. 42
09:40	Invited	M. Mihalik: Magnetism in $\text{RMn}_{1-x}\text{Fe}_x\text{O}_3$ orthorhombically distorted perovskite compounds	p. 44
10:10	Contributed	Y. Nakazawa: Thermodynamic properties around the metal-insulator spin phase boundary in the dimer-Mott organic compounds	p. 46
10:30	Break		
11:00	Invited	J. Pallister: Limit shape phase transitions: a merger of arctic circles	p. 48
11:30	Contributed	M. Zentkova: The hole doped perovskite manganites $\text{La}_{0.80}\text{Ag}_{0.15}\text{MnO}_3$ for bioapplications	p. 49
11:50	Contributed	M. Chaika: Surface origin of Laser Induced White Light emission	p. 50
12:10		Poster session I (12:10 – 13:10)	p. 11
13:10	Break		
14:10	Keynote	K. Neyts: 3D liquid crystal structures determined by surface alignment	p. 52
14:50	Invited	S. Napolitano: Slow dynamics facilitates equilibration of liquids and glasses	p. 54
15:20	Contributed	J. F. C. Silva: Intermolecular association in co-amorphous systems and their relaxation to co-crystals	p. 56
15:40		Poster session II (15:40 – 16:40)	p. 13

WEDNESDAY, 29 JUNE 2022

09:00	Keynote	M. Johnson: Neutrons to study multiscale phenomena in energy materials	p. 58
09:40	Invited	A. Ivanov: Atomic dynamics in condensed matter studied by neutron scattering with crystal spectrometers	p. 59
10:10	Contributed	O. Tomchuk: Cluster structure and cluster-cluster interaction in nanodiamond aqueous sols by small-angle scattering	p. 60
10:30	Contributed	O. P. Artykulnyi: Structural studies of surfactant-polymer associations in bulk and at interfaces	p. 62
10:50	Contributed	D. Soloviov: Functional lipid pairs as building blocks of phase-separated membranes	p. 64
11:10	Break	Best Poster Competition Voting Time (11:10 – 11:25)	
11:30	Keynote	S. Stankov: Lattice dynamics of thin europium oxide films: from the ferromagnetic semiconductor EuO to the high- k dielectric Eu ₂ O ₃	p. 65
12:10	Contributed	K. J. Kapcia: Modeling of ultrafast magnetization decrease in cobalt multilayer system under soft X-ray radiation	p. 67
12:30	Contributed	S. Niyogi: Mechanical properties and pore size distribution in athermal porous glasses	p. 69
12:50	Contributed	W. Tomczyk: Computer simulations of mesophases formed by bent-shaped molecules with excluded-volume type interactions	p. 70
13:10	Break		
14:10	Keynote	J. Larionova: Prussian blue type nano-objects: new opportunities for old materials	p. 72

14:50	Invited	P. A. Goddard: Scattering from magnetic monopoles and antiferromagnetic domain manipulation in a frustrated pyrochlore iridate	p. 73
15:20	Invited	A. Zarzycki: Porous Ti/TiO _x /Fe magnetic junction and its magnetotransport properties	p. 74
15:40	Contributed	M. A. Gala: Search for dependency between Verwey and Curie temperatures in magnetite monocrystals doped with Mn, Zn, Al and Ti	p. 75
16:00	Contributed	B. Klebel-Knobloch: Evolution of the Hall-coefficient, dc-resistivity and Fermi-surface in cuprates	p. 77

THURSDAY, 30 JUNE 2022

09:00	Keynote	E. Chrzumnicka: Liquid crystals: smart molecular systems	p. 79
09:40	Invited	D. Cangialosi: Multiple mechanisms for equilibrium recovery in glasses	p. 81
10:10	Invited	A. Drzewicz: Insight into complex crystallization mechanisms of chiral smectogenic liquid crystal	p. 82
10:30	Contributed	K. Chat: Influence of stereoregularity on the glass transition dynamics under high-pressure conditions and geometrical nanoconfinement	p. 84
10:50	Contributed	P. Baloh: Influence of nanoclusters concentration on low-temperature properties of As-S system	p. 85
11:10	Break		
11:30	Invited	S. Pizzanelli: The state of water adsorbed on a MOF: an NMR study	p. 87

12:00	Invited	E. Carignani: Lead Halide Perovskites for energy applications: structural complexity and dynamics revealed by solid state NMR	p. 89
12:30	Contributed	M. Goździuk: Nanovolumes of soybean oil-based biopolymer matrices to the construction of biosensors for trace water pollutants	p. 91
12:50	Contributed	F. Nardelli: Influence of sulfur-curing conditions on the dynamics and crosslinking of rubber networks: a time-domain NMR study	p. 92
13:10	Break		
14:10	Invited	A. Leon: Water electrolysis for hydrogen production — focus on high-temperature steam electrolysis using solid oxide cells	p. 94
14:40	Invited	A. J. Jackson: Self-assembly in deep eutectic solvents: from surfactant aggregation to protein folding	p. 96
15:10	Contributed	K. Lenczewska: Dependence of structural and optical properties on the type of phase structure in the luminescent $\text{BiVO}_4:\text{Tm}^{3+}$	p. 98
15:30	Contributed	M. Perzanowski: Magnetization reversal mechanism in exchange-biased spring-like thin-film composite	p. 100
15:50	Break	Best Talk Competition Voting Time (15:50 – 16:05)	
16:10		Closing of the conference	

Poster session I

Tuesday, 12:10 – 13:10

1. S. Akagi: Crystal structures and magnetic studies of two-types of Ni-W octacyanide bimetal assemblies p. 101
2. M. S. Barabashko: Kinetics of the thermal decomposition of thermally reduced graphene oxide (TRGO) p. 103
3. A. Deptuch: Kinetics of cold crystallization of the chiral fluorinated smectogenic 3F5HPhH6 compound p. 104
4. A. F. Fadilla: Synthesis of lambda-type trititanium pentoxide using a block copolymer p. 106
5. ... p. ...
6. Y. V. Horbatenko: Thermal conductivity of bulk and nanostructured materials in modern concepts framework p. 108
7. S. El Houbbadi, A. Fedorchuk: Multifunctional ordered mesoporous silica-based materials for nanotechnological applications p. 109
8. D. Hurova: Mean squared displacement of molecules from lattice sites in the orientationally ordered phase of $^{15}\text{N}_2$ p. 111
9. G. Inkrataitė: Synthesis and investigation of cerium and boron and/or magnesium doped YAG and LuAG for high quality scintillators application p. 112
10. A. Karachevtseva: Influence of thermoactivate contribution on isochoric thermal conductivity of tetrafluorethane p. 113
11. A. Kizalaite: Synthesis of manganese whitlockite via dissolution-precipitation process p. 115
12. ... p. ...
13. A. V. Nagorny: Structural investigation of ferrofluids by small-angle neutron scattering p. 116

14. S. Nagashima: Observation of surface magnetic domain on magnetic thin films of hexacyanochromium-chromium magnetic film p. 117
15. A. Nykiel: Structure and magnetic properties of FeCo nanowires p. 119
16. A. Pacanowska: Switchable composite materials based on polymers and chain-like molecular magnet p. 121
17. A. Pakalniskis: Investigation of crystal structure and doping driven phase transitions in $\text{Lu}_{(1-x)}\text{Sc}_x\text{FeO}_3$ system p. 123
18. O. Polit: Influence of particles-solvent interactions on composite particles formation during pulsed laser irradiation in liquid process p. 125
19. S. A. Róžański: Influence of finite size effects and surface interactions on the molecular and collective dynamics in confined liquid crystals p. 127
20. V. V. Sagan: Phase $V(T)$ transformations in freons of the ethane series under isochoric conditions p. 129
21. R. Seiki: One-step metal-semiconductor phase transition observed in nanosize tetratitanium heptoxide p. 131
22. V. Seminko: Luminescent ceria nanoparticles with controlled ROS scavenging activity p. 133
23. T. Yamamoto: Phase behaviors of liquid crystal 8CB under steady shear flow p. 134
24. S. Yefimova: UV-light activated $(\text{Gd},\text{Y})\text{VO}_4:\text{Eu}^{3+}$ nanoparticles as nano radio enhancers p. 135

Poster session II

Tuesday, 15:40 – 16:40

- Y. Bahjou: Synthesis, crystal structures of Cu(II), Ni(II), Co(II) and Cd(II) coordination complexes constructed by tetrazole and bi-pyrazole CN junction entities p. 137
25. J. Bujakowska: High magnetic anisotropy induced by unusual coordination in a pentanuclear star-like Ni₄Fe molecule p. 138
26. K. Capała: Inertial Lévy flights in bounded domains p. 140
27. G. P. Costa: Norfloxacin-picolinic acid coamorphous/cocrystal: diffractometric study of a cocrystallization process through amorphous phase p. 141
28. D. Czernia: Effects of plasma irradiation on the three-dimensional cyanide-bridged network based on the Nb(IV) and Mn(II) ions p. 143
29. J. Gatlik: Effect of nonzero temperature on the process of penetration of the potential barrier through the kink p. 145
30. P. O. Ferreira: Menthol-valsartan low transition temperature mixtures (LTTMs): a thermoanalytical study p. 147
31. A. Karczmarzka, M. Adamek: Carbon structures fabricated by a versatile hydrothermal method: controllable synthesis and preliminary material characterization p. 149
32. D. Karoblis: Investigation of structural, morphological and magnetic properties of Bi_{1-x}GdxFe_{0.85}Mn_{0.15}O₃ solid solutions prepared via sol-gel method p. 150
33. L. A. Kotvytska: Thermodynamic studies of the zeolitic imidazolate frameworks p. 152
34. M. Kuniej: Orbach-like which-way spin dephasing in self-assembled and gate-defined quantum dots p. 154
35. S. Lalik: Nanocomposites based on liquid crystalline (S)-MHPOBC matrix and Au nanoparticles p. 156
- 36.

37. V. Lipp: Numerical investigation of radiation-induced dynamics of solids in two-dimensional geometry p. 158
38. N. Osiecka-Drewniak, A. Dziuba: Polymorphism and physical stability of aripiprazole p. 159
39. A. Oulmidi: Environmental-friendly adsorbent based on pyridine blocks for removal of heavy metals p. 160
40. A. M. Piekarska: Emergence of a superglass phase in a Bose-Hubbard model with off-diagonal disorder p. 161
41. M. Piwowarczyk: Phase situation of (E)-4-((4-alkyloxyphenyl)diazenyl)phenyl alkanoates and their mixtures with chiral mesogens p. 163
42. M. S. Shakeri: The effect of solvent on oxidation behavior of copper during laser irradiation of suspension, a reactive bond molecular dynamics study p. 164
43. P. Sobieszczyk: Influence of He⁺ irradiation and surface effects on compensation point in ferrimagnetic TbFe alloys p. 166
44. M. Stawiarz: The analysis of anisotropy in polydispersed multiphase composites p. 167
45. A. Warzybok: Serendipitous formation of a dumbbell-like CN-bridged Ni(II) dimer p. 168
46. O. Vinnik: The lattice specific heat of metal-organic materials with chain-like crystal structure p. 169
47. W. Zając: Luminescent synthetic opals for angle-dependent emissive colour p. 170
48. M. Żurek: The TP-C isotherms of LaNi₅ and LaNi_{4.75}Pb_{0.25} alloy at different temperatures statistical physics modeling of hydrogen sorption onto: microscopic state investigation, interpretation and comparison between alloys p. 172

Ultra-fast to slow dynamics at liquid interfaces investigated with X-rays

B. M. Murphy

Kiel University, Kiel Nano, Surface and Interface Science, Kiel, Germany

email: murphy@physik.uni-kiel.de

Understanding and controlling structure and function of liquid interfaces is a constant challenge in biology, nanoscience and nanotechnology, with applications ranging from molecular electronics to controlled drug release. X-ray reflectivity and grazing incidence diffraction provide an invaluable probe for studying the atomic scale structure at liquid–air interfaces.^(1–4) The new ultra-fast laser system at the LISA liquid diffractometer⁽²⁾ situated at beamline P08 at the PETRA III synchrotron radiation source in Hamburg provides the laser pump with X-ray probe. The femtosecond laser combined with the LISA diffractometer allows unique opportunities to investigate photo-induced structural changes at liquid interfaces on the pico- and nanosecond time scales with pump-probe techniques.⁽⁴⁾ This talk will concentrate on two aspects: the non-equilibrium dynamics due to ion creation under influence of the pump laser along with temperature-dependent capillary wave behaviour⁽³⁾ down to the freezing point for water and NaI solution.

Acknowledgments: We acknowledge financial support by the BMBF through projects K16FK1/K19FK2. We acknowledge DESY (Hamburg, Germany), a member of the Helmholtz Association HGF, for the provision of experimental facilities.

⁽¹⁾ A. Elsen et al. Proc. Natl. Acad. Sci 110 (2013), 6663.

⁽²⁾ B. M. Murphy et al. J. Synchr. Rad. 21 (2014), 45.

⁽³⁾ B. Runge et al. Phys. Rev. B 93 (2016), 165408.

⁽⁴⁾ J. E. Warias et al. "The Laser Pump X-Ray Probe Option at LISA P08 DESY", in preparation.

Small spin clusters mimicking a temperature induced phase transition

K. Saito

University of Tsukuba, Tsukuba, Japan

email: kazuya@chem.tsukuba.ac.jp

Phase transitions usually accompany a change in symmetry and thermodynamic singularities. Although the latter requires the so-called thermodynamic limit of system size, it is not for the former. However, the ordinary models undergoing a phase transition in the thermodynamic limit do not exhibit any change in symmetry in a finite size. Indeed, an octahedral cluster of six spins described by the 3-state Potts model with the antiferromagnetic interaction, for example, gives monotonous temperature dependences of spin correlation functions at different distances while keeping their magnitude order (Figure 1). Since neighbors with the same state are always disfavored, the "averaged" symmetry around any C_4 axes is reduced to twofold irrespective of temperature. The symmetry is the same as the ground state.

Recently, we encountered an interesting phenomenon that ensembles of classical spins exhibit an exotic phase transition between two states of vanishing long-ranged orientational order for a particular combination of the lattice geometry and the interaction between spins.⁽¹⁾ This talk reports that two regular "polyhedra" catching the required geometric characteristics exhibit a change in the averaged symmetry upon temperature variation if the interaction is also exceptional.

Acknowledgments: This work was supported in part by JSPS Grant-in-Aid for Scientific Research on Innovative Areas "Discrete Geometric Analysis for Materials Design" (JP20H04629).

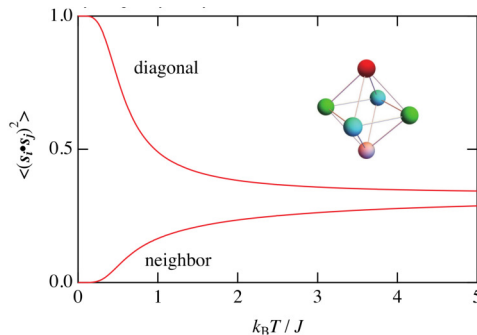


Figure 1. Temperature dependence of spin correlation functions of an octahedral spin cluster of the antiferromagnetic 3-state Potts model: $V_{ij} = -J s_i \cdot s_j$. Inset shows a twofold symmetry of the cluster.

⁽¹⁾ K. Saito et al. J. Phys. Soc. Jpn. 90 (2021), 124003.

Electric field-controlled spin state in uthrene, [7]uthrene and [8]uthrene molecule: computational study

K. Szałowski

University of Łódź, Faculty of Physics and Applied Informatics,
Department of Solid State Physics, Łódź, Poland

email: karol.szalowski@uni.lodz.pl

The recent progress in synthesis of nanographenes (being actually polyaromatic hydrocarbons) with atomic precision invigorates interest in studies of such nanostructures.⁽¹⁾ Particular attention is focused on the structures which exhibit magnetic properties due to their prospective applications in carbon-based spintronics. A recently synthesized zigzag-edged nanographene belonging to this class is [7]uthrene,⁽²⁾ being polyaromatic U-shaped diradical hydrocarbon. For this molecule, as well as for smaller uthrene, a theoretical prediction of spin-triplet ground state is known.^(2,3) Its presence in [7]uthrene molecule has been already confirmed experimentally.⁽²⁾

In the paper we report the computational study of the ground-state magnetic properties of uthrene, [7]uthrene and [8]uthrene nanostructures in external in-plane electric field, with a view to controlling the spin state using the electric field in the nanoscale.⁽⁴⁾

Our predictions are based on the Hubbard model for p^z electrons in the system. The Hamiltonian includes an in-plane electric field of arbitrary orientation as well as a possible exchange splitting as a proximity effect induced by the substrate. The model is solved using a mean-field approximation for half-filling of the cluster energy states. A similar model approach was found consistent with the scanning tunnelling microscopy characterization of the electronic properties of [7]uthrene.⁽²⁾

The complexity of the magnetic ground state diagram increases with the increasing nanostructure size. For low fields, the magnetic ground-state phase diagrams comprise predominantly a ferromagnetic state with spin $S=1$ as well as states with $S=0$. They include both a non-magnetic state and an antiferromagnetic state with spin densities of opposite signs concentrated on both triangular parts of the molecule. The possibility of switching between the $S=1$ and $S=0$ state by applying the electric field is predicted, with pronounced directional anisotropy of the critical electric field and its lowest magnitudes of the order of 0.1 V/\AA . The influence of such factors as the proximity exchange field from the substrate or the uniaxial strain on the constructed phase diagram is discussed. The differences between the results obtained for uthrene, [7]uthrene and [8]uthrene are emphasized.

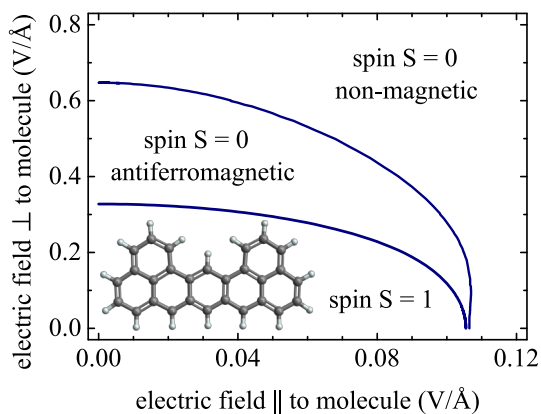


Figure 1. The ground-state magnetic phase diagram of the [7]uthrene molecule in external electric field in the absence of exchange splitting.

- (1) S. Song et al. *Chem. Soc. Rev.* 50 (2021), 3238.
- (2) X. Su et al. *Nano Lett.* 20 (2020), 6859.
- (3) M. Melle-Franco. *Chem. Commun.* 51 (2015), 5387.
- (4) K. Szałowski, *Int. J. Mol. Sci.* 22 (2021), 13364.

Circular economy: new opportunities in sustainable soft nano materials and polymer bio-nanocomposites

S. Thomas

Mahatma Gandhi University, Priyadarshini Hills P. O. Kottayam, Kerala,
India

email: sabuthomas@mgu.ac.in

Green chemistry started for the search of benign methods for the development of nanoparticles from nature and their use in the field of antibacterial, antioxidant, and antitumor applications. Bio wastes are eco-friendly starting materials to produce typical nanoparticles with well-defined chemical composition, size, and morphology. Cellulose, starch, chitin and chitosan are the most abundant biopolymers around the world. All are under the polysaccharides family in which cellulose is one of the important structural components of the primary cell wall of green plants. Cellulose nanoparticles (fibers, crystals and whiskers) can be extracted from agrowaste resources such as jute, coir, bamboo, pineapple leaves, coir etc. Chitin is the second most abundant biopolymer after cellulose, it is a characteristic component of the cell walls of fungi, the exoskeletons of arthropods and nanoparticles of chitin (fibers, whiskers) can be extracted from shrimp and crab shells. Chitosan is the derivative of chitin, prepared by the removal of acetyl group from chitin (Deacetylation). Starch nano particles can be extracted from tapioca and potato wastes. These nanoparticles can be converted into smart and functional biomaterials by functionalization through chemical modifications (esterification, etherification, TEMPO oxidation, carboxylation and hydroxylation etc) due to presence of large amount of hydroxyl group on the surface. The preparation of these nanoparticles includes both series of chemical as well as mechanical treatments; crushing, grinding, alkali, bleaching and acid treatments. Transmission electron microscopy (TEM), scanning electron microscopy (SEM) and atomic force microscopy (AFM) are used to investigate the morphology of nanoscale biopolymers. Fourier transform infra-red spectroscopy (FTIR) and X-ray diffraction (XRD) are being used to study the functional group changes, crystallographic texture of nanoscale biopolymers respectively. Since large quantities of bio wastes are produced annually, further utilization of cellulose, starch and chitins as functionalized materials is very much desired. The cellulose, starch and chitin nano particles are currently obtained as aqueous suspensions which are used as reinforcing additives for high performance environment-friendly biodegradable polymer materials. These nanocomposites are being used as biomedical composites for drug/gene delivery, nano scaffolds in tissue engineering and cosmetic orthodontics. The reinforcing effect of these nanoparticles results from the formation of a percolating network based on hydrogen bonding forces.

The incorporation of these nano particles in several bio-based polymers have been discussed. The role of nano particle dispersion, distribution, interfacial adhesion and orientation on the properties of the ecofriendly bio nanocomposites have been carefully evaluated.

- (1) Sabu Thomas et al. ACS Appl. Mater. Interfaces 10 (23), pp 20032–20043,2018
- (2) Sabu Thomas et al. ACS Sustainable Chemistry & Engineering, 2017
- (3) R Augustine, A Augustine, N Kalarikkal, S Thomas, Progress in Biomaterials 5 (3-4), 223-235, 2016
- (4) SS Babu, S Mathew, N Kalarikkal, S Thomas, Biotech 6 (2), 249,2016
- (5) S Gopi, A Pius, S Thomas, Journal of Water Process Engineering, 2016
- (6) J Joy, P Mathew, S Thomas, S Pillai, Journal of Renewable Materials 4 (5), 351-364, 2016
- (7) E Fortunati, F Luzi, A Jiménez, DA Gopakumar, D Puglia, S Thomas, ...Carbohydrate polymers 149, 357-368, 2016

Dielectric studies of systems influenced by the ionic conductivity

S. Urban

Institute of Physics, Jagiellonian University, Kraków, Poland

email: Stanislaw.urban@uj.edu.pl

Problem of interpretation of the dielectric spectra collected for systems infected by electric charges often arises when the materials like organic liquids, mixtures, liquid crystals, pharmaceuticals, ionic liquids, biologic materials, are studied. Influence of ionic conductivity is manifested as strong increase of the dielectric losses at the low frequency parts of the dielectric spectra. Therefore the dielectric relaxation processes connected with the dipole rotations may be strongly masked by the ionic conductivity. Method of separation of the charge and dipolar relaxations was given by Jadzyn and Świergiel.⁽¹⁾ They proved theoretically and experimentally that two types of currents, the ionic current and displacement current (caused by rotating dipoles) affect the impedance of the measured systems. In this contribution their approach will be demonstrated for the case of dielectric spectra collected for several symmetrical imines in the liquid state⁽²⁾ and for the semi-conducting polymeric P3HT mixed with PCBM and imine SC2 compounds in the form of gels⁽³⁾ (such donor-acceptor systems are used in the organic solar photovoltaic cells).

⁽¹⁾ J. Świergiel et al. *Ind. Eng. Chem. Res.*, 52(34) (2013), 11974 – 11979.

⁽²⁾ S. Urban et al. *J. Mol. Liq.* 328 (2021), 115447.

⁽³⁾ S. Lalik et al. submitted.

Is adding a large atom important for the relaxation dynamics of monohydroxy alcohols?

S. Pawlus, K. Łucak, A. Szeremeta, J. Grelska, K. Jurkiewicz

A. Chelkowski Institute of Physics, University of Silesia in Katowice,
Chorzów, Poland

email: sebastian.pawlus@us.edu.pl

It is well known that in the case of many monohydroxy alcohols not only structural relaxation can be detected in their dielectric spectra. Also additional, a slower and often dominating relaxation process is seen. This exponential in shape process, called Debye, manifests molecular dynamics of supramolecular hydrogen-bonded structures.⁽¹⁾ Depending on the terminal or non-terminal position of the OH group attached to the alkyl chain, these structures can be chain-like or ring-like. Their architecture is reflected in the Debye relaxation intensity, which diminishes for alcohols with non-terminal localization of hydroxyl groups. However, large pendant groups like the phenyl ring attached to the molecule strongly influence the architecture of HB superstructures. E.g. for phenyl alcohols, only a single relaxation process is observed, composed of structural and Debye relaxations, with only slightly different time scales.⁽²⁾

As shown in Fig. 1, the addition of Cl, Br, and I atoms into the molecule structure of propanol influences the intensity of both relaxations. The question arises if adding these large atoms or pendant groups will affect and to what extent the molecular dynamics of these materials? Is, e.g., time scales of relaxations, structural and Debye, modified by modification of the dipole moment of molecules? We will try to answer these questions based on our recent studies of various monoalcohols.

The authors are thankful for the Polish National Science Centre's financial support within the OPUS project (Dec. no UMO-2019/35/B/ST3/02670).

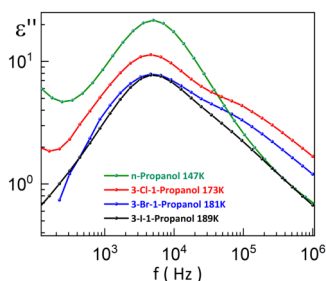


Figure 1. Comparison of the dielectric loss spectra measured for n-propanol and derivatives for the same position of the Debye relaxation.

⁽¹⁾ R. Böhmer et al. *Physics Reports* 545 (2014), 125.

⁽²⁾ A. Nowok et al. *J. Phys. Chem. Lett.* 12 (2021), 2142.

Fast differential scanning calorimetry: new perspectives in data reduction and applications to organic samples

D. Sonaglioni,^{1,2} E. Tombari,³ S. Capaccioli^{1,2}

¹CISUP, Centro per l'Integrazione della Strumentazione dell'Università di Pisa, Pisa, Italy

²Dipartimento di fisica "E. Fermi", Università di Pisa, Pisa, Italy

³Consiglio Nazionale delle Ricerche, Istituto per i Processi Chimico-Fisici (CNR-IPCF), Pisa, Italy

Fast differential scanning calorimetry (FDSC) is a particular kind of calorimetry, also called chip calorimetry, that is based on a thin film of sample deposited on MEMS (micro-electro-mechanical-systems) calorimetric devices, instead of the usual sample held in metallic pans in furnaces as for conventional calorimetry. This switch of paradigm allows the reduction of the involved sample mass and to reach very high heating scan rates, up to 40000 K/s, without losing precision.⁽¹⁾ Even though there are lots of advantages, some drawbacks are present too, which are usually known in literature as thermal lag and heat flow losses. Whereas the latter has been studied intensively in literature,^(2,3) the first is still unexplored. We think that this quantity deserves a systematic investigation, especially when the calorimeter is used to characterize organic compounds: contrary to what obtained with indium, or other reference standards, organic samples show a non-negligible thermal lag, even at low scanning rates.⁽⁴⁾ Starting from the study of some prototypical glass-formers, such as orto-terphenyl (OTP), widely studied in literature^(5,6) even with the FDSC,⁽⁷⁾ glycerol and poly(propylene glycol), and with the help of numerical simulations performed with the TNM model,⁽⁸⁾ we have developed a new method to take into account the thermal lag, and correct the experimental data. We have also shown that this method produces physically meaningful thermograms. We have also discussed such results in terms of energy balance and fictive temperature⁽⁹⁾ of the thermograms. Finally, we show an example of this correction method applied to the FDSC study of compounds of pharmaceutical interest, in particular to those belonging to the class I and II, according to the classification of Baird et al.⁽¹⁰⁾, that show a strong tendency to crystallize on cooling and reheating, respectively.

(1) F. Yi et al. *Appl. Phys. Rev.* 6 (2019), 031302.

(2) E. Zhuravlev et al. *Thermochim. Acta* 505 (2010), 14.

(3) D. N. Bolmatenkov et al. *Thermochim. Acta* 694 (2020), 178805.

(4) X. Monnier et al. *Thermochim. Acta* 648 (2017), 13.

(5) R. Richer et al. *J. Chem. Phys.* 108 (1998), 9016.

(6) R. J. Greet et al. *J. Chem. Phys.* 46 (1967), 1243.

(7) M. I. Yagofarov et al. *Thermochim. Acta* 668 (2018), 96.

(8) I. M. Hodge et al. *Macromol.* 15 (1982), 762.

(9) C. T. Moynihan et al. *J. Am. Ceram. Soc.* 59 (1976), 12.

(10) J. A. Baird et al. *J. Pharm. Sci.* 99 (2010), 3787.

Molecular magnetism meets optical thermometry in heterometallic systems linking lanthanide and transition metal complexes

S. Chorazy,¹ J. J. Zakrzewski,¹ M. Zychowicz,¹ P. Bonarek,¹
M. Liberka,¹ M. Wyczęsany,¹ J. Wang,² K. Nakabayashi,² S. Ohkoshi²

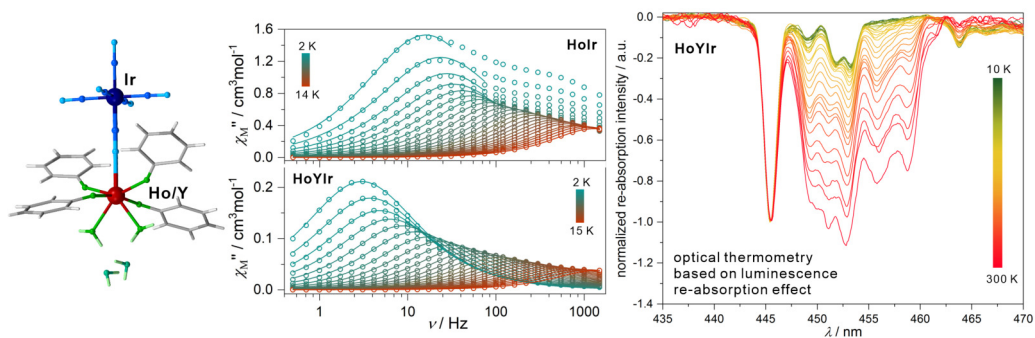
¹Faculty of Chemistry, Jagiellonian University, Kraków, Poland

²Department of Chemistry, School of Science, The University of Tokyo,
Tokyo, Japan

email: simon.chorazy@uj.edu.pl

Molecular nanomagnets, often named single-molecule magnets (SMMs), exhibit strong magnetic anisotropy that leads to the slow relaxation of magnetization and the resulting magnetic hysteresis loop of a molecular origin. These remarkable magnetic objects, which are considered promising candidates for future data storage devices, can be rationally designed using lanthanide(III) complexes with the specific arrangement of charged ligands around the 4f metal center.⁽¹⁾ On the other hand, materials incorporating lanthanide ions are a great source of diverse photoluminescent phenomena; therefore, molecular materials based on 4f metal complexes can provide luminescent SMMs that offer the pathway for useful magneto-optical correlations.⁽²⁾ Recently, the idea of combining optical thermometry effects, applicable for temperature sensing in electronics, medical diagnostics, and chemical reactors, with molecular magnetism appear.⁽³⁾ This opens the extraordinary strategy for achieving smart electro-magnetic SMM-based devices with a self-monitored temperature. In this regard, we present our strategy toward magneto-luminescent heterometallic systems combining molecular magnetism with optical thermometry which is realized by linking lanthanide complexes of Dy^{III}, Ho^{III}, or Yb^{III} with non-innocent metalloligands based on cyanido metal complexes including hexa-cyanidometallates of Co^{III}, Rh^{III}, and Ir^{III}, or less common dicyanidometallates of Ir^{III}.^(4,5) The example of Ho^{III}-[Ir^{III}(CN)₆]³⁻ molecules with their representative opto-magnetic characteristics is shown below.

Acknowledgments: The presented work was financed by the National Science Centre of Poland within the OPUS-15 project (grant no. 2018/29/B/ST5/00337). We also acknowledge the European Research Council through the ERC-StG LUMIFIELD project, no. 101042112. Thus, the part of the work was partially funded by the European Union. Views and opinions expressed are however those of the author(s) only and do not necessarily reflect those of the European Union or the European Research Council. Neither the European Union nor the granting authority can be held responsible for them.



- (1) F.-S. Guo et al. *Science* 362 (2018), 1400.
- (2) S. Chorazy et al. *Chem. Eur. J.* 22 (2016), 7371.
- (3) D. Errulat, et al. *ACS Cent. Sci.* 5 (2019), 1187.
- (4) J. Wang et al. *J. Am. Chem. Soc.* 142 (2020), 3970.
- (5) J. Wang et al. *Chem. Sci.* 12 (2021), 730.

Assembling functional molecular crystals

S. Ferlay,¹ C. Adolf,¹ M. W. Hosseini,¹ L. Shi,² J. Kobylarczyk,^{2,3}
R. Podgajny²

¹University of Strasbourg, CNRS, Strasbourg, France

²Faculty of Chemistry, Jagiellonian University, Krakow, Poland

³Institute of Nuclear Physics PAN, Krakow, Poland

email: ferlay@unistra.fr

The design of complex molecular systems in the crystalline phase may lead to the development of new solid-state task specific materials and devices. For example, the formation of assemblies of molecular crystals displaying physical properties is a step towards the development of smart molecular materials at the millimeter size level.

A molecular strategy based on the use of series of isostructural crystalline compounds (obtained from two or three molecular compounds), held mainly by weak intermolecular bonds,⁽¹⁾ has been performed as a proof of concept for the formation of core-shell and also welded crystals (Fig. 1a).^(2,3) These assemblies of crystals have been built from epitaxial growth.

Then, for the first time, core-shell crystals built from paramagnetic components based on $[(\text{WCN})_8]^{3-}$ and 3d metal ions, displaying competition or interplay of switchable phenomena of spin-crossover (SCO), electron transfer (ET), and charge transfer induced spin transition (CTIST),⁽⁴⁾ are presented (Fig. 1b).

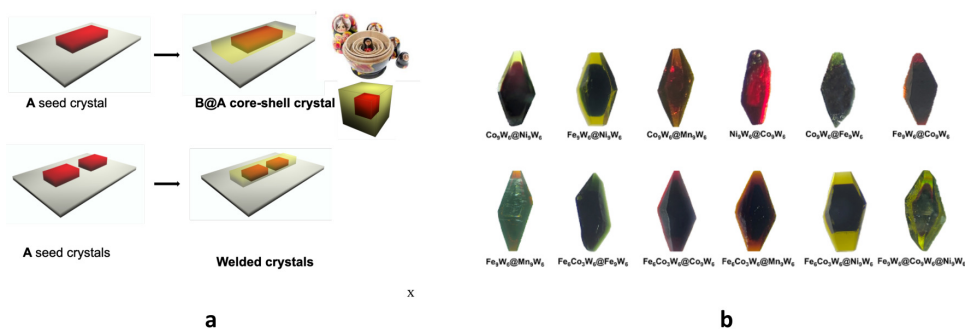


Figure 1. For molecular crystals: a) schematic representation for the formation of core-shell and welded crystals and b) core-shell crystals based on the use of $[(\text{WCN})_8]^{3-}$ and metallic ions displaying magnetic properties.

⁽¹⁾ G. Marinescu et al. Chem. Commun. 49 (2013), 11209.

⁽²⁾ C. R. R. Adolf et al. J. Am. Chem. Soc. 137 (2015), 15390.

⁽³⁾ C. R. R. Adolf et al. Cryst. Eng. Comm. 20 (2018), 2233.

⁽⁴⁾ L. Shi et al. Cryst. Growth Des. 22 (2022), 3413.

Relaxation processes in a single crystal of $\text{Co}(\text{NCS})_2(4\text{-methoxyppyridine})_2$ spin chain

M. Ceglarska,¹ D. Pinkowicz,² C. Näther,³ M. Rams¹

¹Institute of Physics, Jagiellonian University, Kraków, Poland

²Faculty of Chemistry, Jagiellonian University, Kraków, Poland

³Institut für Anorganische Chemie, Christian-Albrechts-Universität zu Kiel, Kiel, Germany

email: magdalena.ceglarska@doctoral.uj.edu.pl

A single crystal of $[\text{Co}(\text{NCS})_2(4\text{-methoxyppyridine})_2]_n$ was synthesized and magnetically investigated. The magnetic measurements were performed along three perpendicular crystallographic directions and compared to the results obtained for a powder sample investigated previously.⁽¹⁾ The inter- and intrachain interactions do not differ between single crystal and powder, however, the change of the energy barrier of the Single Chain Magnet relaxation process is noticeable. Apart from that, the relaxation time of this process is longer. Such a change is associated with the finite chains regime of the temperatures in which we measure the relaxations, where the relaxation time is dependent on the length of the chains. It is confirmed by the measurements performed on the grounded single crystal samples, where we observed a gradual change of the relaxation times (Fig. 1). For the single crystal sample, a second process is also observed, but only close to the critical temperature (3.95 K). The relaxation time of this process is temperature independent, indicating a negligible energy barrier. Such phenomenon was previously not observed for any of the powder samples of compounds from the $[\text{Co}(\text{NCS})_2(\text{ligand})_2]_n$ family, therefore, we associate it with the much lower number of defects in the monocrystalline sample than in polycrystals.⁽²⁾

This project is supported by National Science Centre, Poland (Project Preludium 19 no. 2020/37/N/ST3/02526).

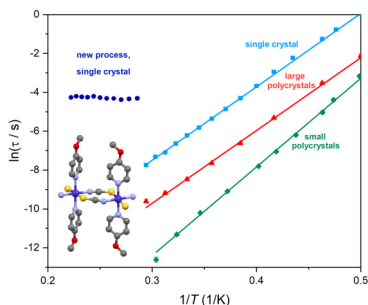


Figure 1. Relaxation times of $[\text{Co}(\text{NCS})_2(4\text{-methoxyppyridine})_2]_n$.

(1) M. Rams et al. Chem. Eur. J. 26 (2020), 2765.

(2) M. Ceglarska et al., to be published.

Rotational magnetocaloric effect in Ni(en)(H₂O)₄·2H₂O

P. Danylchenko, R. Tarasenko, E. Čížmár, V. Tkáč, A. Feher,
A. Orendáčová, M. Orendáč

Institute of Physics, Faculty of Science, P.J. Šafárik University in Košice,
Košice, Slovakia

email: petro.danylchenko@student.upjs.sk

Recently, the topic of the rotational magnetocaloric effect (MCE) has come to the essential role in the field of magnetic cooling. The cooling of the sample is obtained by a simple rotation of the magnetocaloric material in a constant magnetic field from easy to hard magnetization axis. An enhanced MCE may be anticipated in systems characterized by large spin, e. g. in rare-earth based materials. However, the shortcomings such as high price of rare-earth based materials, give rise to the search for the alternative materials. Nowadays, the $S=1$ Ni(II)-based systems are regarded as perspective substitute of the traditional materials. The $S=1$ Ni(II)-based systems with dominant influence of crystal field can be ascribed within a model of a spin-1 paramagnet in crystal field with a spin Hamiltonian $H = DS_z^2 + E(S_x^2 - S_y^2)$, where D and E represent uniaxial and in-plane anisotropy parameters, respectively. Thus, the magnetocaloric properties can be tuned by the combination of anisotropy parameters.

One example of $S=1$ Ni(II)-based system is Ni(en)(H₂O)₄SO₄·2H₂O (en=ethylenediamine). The previous study established this system as a spin-1 paramagnet with nonmagnetic ground state introduced by the easy-plane anisotropy $D/k_B=11.6$ K with $E/D=0.1$ and negligible exchange interactions $J \approx 0$.⁽¹⁾ Specific heat measurements in a zero magnetic field taken on single crystal have shown the absence of any kind of phase transition to a magnetically ordered state down to 1.8 K.

In this work we realized the experimental study of the rotational magnetocaloric effect in single crystal Ni(en)(H₂O)₄SO₄·2H₂O. The MCE evaluation of the studied system have been carried out by isothermal magnetization curves measurements in temperatures above 2 K and in magnetic fields up to 7 T in a commercial Quantum Design SQUID magnetometer. The experimental observations are completed with ab initio calculations of the anisotropy parameters.

The ab initio calculations yielded crystal field parameters $D/k_B=11.5$ K, $E/D=0.07$ with an average g -factor $g=2.22$. Large rotational MCE has been found around 3 K, where $-\Delta S_M \approx 17$ J K⁻¹kg⁻¹ for magnetic field 7 T. The large rotation MCE indicated that the Ni(en)(H₂O)₄SO₄·2H₂O single crystal could be a promising candidate for practical magnetic refrigeration.

Acknowledgments: This work was supported by the Slovak Research and Development Agency Project No.APVV-18-0197.

⁽¹⁾ R. Tarasenko et al. *Acta Phys. Pol. A* 113 (2008), 481.

Formation of crosslinked functional Poly (4-vinylpyridine)-CoBr₂ in both static and dynamic conditions

J. Chudzik, P. Dąbczyński, J. Rysz, A. M. Majcher-Fitas

Faculty of Physics, Astronomy and Applied Computer Science,
Jagiellonian University, Krakow, Poland

email: juliachudzik@doctoral.uj.edu.pl

Both static and dynamic formation of thin functional magnetic films of polymers crosslinked with single ion magnet complexes was thoroughly investigated. This approach is novel compared to the usual deposition of SIMs from crystalline form. The investigated material has promising potential applications and is easy to process since it is formed on the surface of thin spin coated polymer (Poly(4-vinylpyridine)) film after dipping it into CoBr₂ solution.⁽¹⁾ What is more, the studied material showed astonishing qualities in organic field-effect transistor-like geometries with proven conduction increase by four orders of magnitude.⁽²⁾

In order to think about applications, it was necessary to characterize fully the process of the complex formation and its dependence both on the concentration of the cobalt salt solution and on the time of immersion. We proved that the geometry of the wrinkled topology⁽³⁾ formed by the layer is directly related to the cobalt concentration on the surface. Both in the static and kinetic experiment a double process was observed, only the second of which coincides with the appearance of the wrinkles, which can be clearly seen in Fig. 1, which shows changes in the surface concentration of cobalt depending on concentration of CoBr₂ solution in which samples were immersed for 24 hours, inset shows the two breakthrough mechanism according to which wrinkled topography is formed in dynamic process. Presented data are supplemented by corresponding Atomic Force Microscopy (AFM) images.

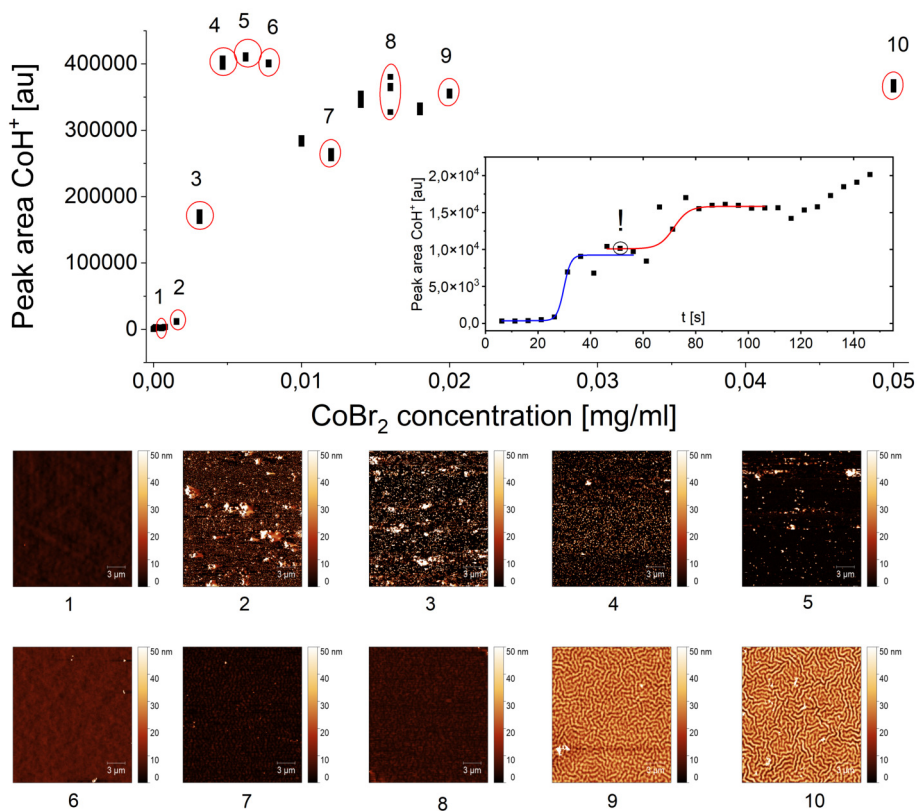


Figure 1. Secondary Ion Mass Spectrometry (SIMS) CoH⁺ peak area as a function of Cobalt salt concentration (inset: as a function of immersion time). AFM topography images of marked samples.

- (1) A. M. Majcher et al. Chem. Sci. 9 (2018), 7277.
- (2) P. Dabczynski et al. Appl. Mater. Today 21 (2020), 100880.
- (3) M. A. Biot. Proc. R. Soc. London 242 (1957), 444 – 454.

Dendrites formation on poly(methylmetacrylate) surface reactively sputtered with cesium ion beam

P. Dąbczyński,¹ B. R. Jany,¹ F. Krok,¹ M. Marzec,² A. Bernasik,^{2,3}
M. Gala,¹ U. Breuer,⁴ A. Budkowski,¹ J. Rysz¹

¹Faculty of Physics, Astronomy and Applied Computer Science, Jagiellonian University, Krakow, Poland

²Academic Centre for Materials and Nanotechnology, AGH University of Science and Technology, Krakow, Poland

³Faculty of Physics and Applied Computer Science, AGH University of Science and Technology, Krakow, Poland

⁴Zentralinstitut für Analytik ZEA-3, Forschungszentrum Jülich, Jülich, Germany

email: pawel.dabczynski@uj.edu.pl

The development plays an important role when low-energy projectiles are used to modify the surface or analyze properties of various materials. It can be a feature that allows one to create complex structures on the sputtered surface. It can also be a factor that limits depth resolution in ion-based depth profiling methods. In this work, we have studied the evolution of microdendrites on poly(methyl methacrylate) sputtered with a Cs 1 keV ion beam. Detailed analysis of the topography of sputtered surface shows a set of pillars with islands of densely packed pillars, which eventually evolve to fully formed dendrites. The development of the dendrites depends on the Cs fluence dose and temperature of the sample. Analysis of the sputtered surface by physicochemical methods (ToF SIMS, XPS, SEM EDX) shows that the mechanism responsible for the formation of the observed microstructures is reactive ion sputtering. It originates from the chemical reaction between the target material and primary projectile and is combined with mass transport induced by ion sputtering. Therefore, it is an example of an effect emerging only by a combination of ion sputtering and a chemical reaction. As a reference, an Xe 1 keV ion beam was used. The difference between such chosen beams in energy and momentum transfer should be marginal, due to Cs and Xe similar masses. Therefore, differences in the ion sputtering process for a given matrix originate from the chemical interaction. As we show on the PMMA surface sputtered with xenon there are no visible micro dendrites, and sputter induced topography development is considerably different from that in case of cesium ion beam. The gained knowledge about reactive ion sputtering can help in the design of complex surface microstructures and avoiding effects that limit depth resolution in ion-based depth profiling experiments.

Acknowledgments: This research was financed by the Polish National Science Centre under the auspices of the MINIATURA 4 project 2020/04/X/ST5/01847.

Magnetism and transport studies of thin iron films deposited on anodized titanium oxides

J. Chojenka, A. Zarzycki, M. Perzanowski, M. Marszałek

Institute of Nuclear Physics Polish Academy of Sciences, Kraków, Poland

email: juliusz.chojenka@ifj.edu.pl

Magnetic nanostructures, because of their extremely small size, possess properties that are often quantitatively and qualitatively different from the parent bulk material. In particular, the nanostructured magnetic systems received significant attention due to the rapid development of nanopatterning technologies which allow the creation of a system with tunable size and shape of the structures by various lithography methods such as solid-state dewetting or electrochemical anodization. One of the most efficient and costless processes is the anodization of transition metals, which permits for the control of dimensions of the nanostructures, such as the diameter and height of the pores/tubes, by changing reaction parameters like the anodization voltage, electrolyte composition, temperature, and time.

The nanopatterned magnetic structures are greatly affected by the preparation conditions including the used substrate. In particular, the magnetic films deposited on an array of nanopores exhibit different properties compared to the continuous analog. It is related to the impact of the surface morphology resulting from artificially made defects. The introduction of the morphology modifications leads to the change of the magnetoresistance properties, magnetization reversal processes, permeability, coercivity, and the intrinsic anisotropy of the film. There are only a few studies that focus on the physical properties of magnetic thin films on anodized titanium oxide because the most investigated properties of titanium oxide concern biocompatibility. However, the interesting effects for TiO_2 come also from their conducting properties. For example, the bulk anatase and rutile are the semiconductors for which the oxygen vacancies and titanium interstitials or titanium vacancies behave either as n- or p-type dopants. Furthermore, the Ti or O vacancies can induce a weak ferromagnetic signal. We decided to use anodized titanium oxides as the substrates for deposition of the iron thin films and create nanopatterned metal/semiconductor/metal junctions.

In this study, the junctions consist of a ferromagnetic thin iron layer of 50 nm thickness thermally deposited on anodized titanium oxide (ATiO). Fabrication of the ATiO layer was carried out in electrolyte containing ammonium fluoride (NH_4F) at constant voltages of 5 V, 15 V, and 60 V. To protect the iron from oxidation and ensure good electric contact a layer of gold was deposited on top of the junctions. The XRD measurements reveal the polycrystalline structure of junctions consists of a variety of titanium oxides. The reflectivity spectroscopy studies affirmed the semiconducting nature of the titanium oxide layer with a band gap of 2.3 eV.

Magnetic hysteresis curves showed a significant increase in the coercivity for nanopatterned samples, and the enhancement depends on the pore sizes with the maximum amplification of 4. The magnetization curves demonstrated a two-step magnetization reversal process. The exchange coupling strength between the soft and hard phases which were identified as oxidized iron and the iron layer, respectively, was analyzed for the sample made at 15 V using recoil curves. The experiment showed the existence of weak exchange coupling between magnetic phases. ZFC-FC measurements indicated the presence of a spin-glass-like disordered state below 50 K, explained by the formation of iron oxide at the titanium oxide-iron interface with short-range magnetic order. The magnetoresistance properties of the junctions displayed dual character with positive values at room temperature and negative values at 5 K for all samples.

Acknowledgments: The support from the NCN grant 2015/19/D/ST3/01843 is acknowledged.

Bilayers and double-shell nanotubes of Prussian blue and its Cr analog — the synthesis and magnetic properties

W. Sas, M. Fitta

Institute of Nuclear Physics Polish Academy of Sciences, Kraków, Poland

email: wojciech.sas@ifj.edu.pl

The concept of creating magnetic molecular materials relies on merging different magnetic ions into organic or inorganic molecules, which can combine several attractive properties: low density, the high magnetic moment per volume unit, or the sensitivity to external stimuli, including temperature and pressure, thus making them multifunctional materials. The systems composed of several magnetic phases are promising to investigate in terms of designing materials with a particular behavior at given external conditions. Prussian blue analogs (PBAs) are among the most studied molecular compounds. They are relatively easy to synthesize and can be obtained in many different forms (e.g., films, nanoparticles, or nanotubes).

This work presents the synthesis and physicochemical characterization of bilayers and nanotubes composed of Prussian blue, $\text{Fe}_4[\text{Fe}(\text{CN})_6]_3$ ($\text{Fe}^{\text{III}}\text{Fe}^{\text{II}}$) and its Cr analog, $\text{Fe}_3[\text{Cr}(\text{CN})_6]_2$ ($\text{Fe}^{\text{II}}\text{Cr}^{\text{III}}$). Both types of samples were synthesized by electrochemical deposition using different substrates. The films were grown on PET foil covered with ITO, while the nanotubes were manufactured inside the porous polycarbonate (PCTE) membranes covered with a thin film of gold. The two-step growth process is described in detail.

The morphology of the samples was examined by electron microscopy (SEM), while the energy-dispersive X-ray spectroscopy (EDS) was used to determine the mutual composition of magnetic ions. The magnetic measurements reveal the presence of two distinct magnetic phases associated with $\text{Fe}^{\text{III}}\text{Fe}^{\text{II}}$ and $\text{Fe}^{\text{II}}\text{Cr}^{\text{III}}$ components. Additionally, the magnetization curves were fitted to the mathematical model, which enables a deconvolution into separate hysteresis loops (Fig. 1).

Acknowledgments: W. S. acknowledges the Polish National Science Centre (Grant PRELUDIUM 16: UMO-2018/31/N/ST5/03300) for financial support.

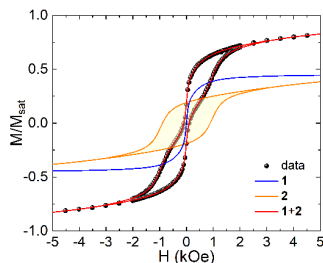


Figure 1. The magnetization curve of $\text{Fe}^{\text{II}}\text{Cr}^{\text{II}}/\text{Fe}^{\text{III}}\text{Fe}^{\text{II}}$ nanotubes deconvoluted into separate magnetic phases: 1: $\text{Fe}^{\text{III}}\text{Fe}^{\text{II}}$, 2: $\text{Fe}^{\text{II}}\text{Cr}^{\text{III}}$.

UV-light activated (Gd,Y)VO₄:Eu³⁺ nanoparticles as nano radio enhancers

S. Yefimova,¹ P. Maksimchuk,¹ V. K. Klochkov,¹ V. Seminko,¹
O. Ivankov,² O. Tomchuk²

¹Institute for Scintillation Materials NAS of Ukraine, Kharkiv, Ukraine

²Taras Shevchenko National University of Kyiv, Kyiv, Ukraine

email: ephimovasveta@gmail.com

Radiation therapy (RT) has become one of the first lines treatment modalities in oncology. Unfortunately, cancerous cells could be resistant to RT that requires enhanced doses of irradiation. However, high doses of radiation, in their turn, inevitably damage healthy cells and tissues located near the treatment area that limits exposed radiation doses. Recently, a new strategy in RT for cancer treatment based on the application of nanoparticles (NPs) containing high-*Z* elements and possessing high X-ray absorption has been proposed.^(1,2)

Here we report on strong X-ray induced hydroxyl radical ($\cdot\text{OH}$) generation in aqueous solutions containing UV-light activated (Gd,Y)VO₄:Eu³⁺ nanoparticles. (Gd,Y)VO₄:Eu³⁺ NPs were synthesized by the colloidal route and characterized using TEM, XRD, XPS, SANS/SAXS methods. The effect of NPs UV-light pre-treatment on their redox properties has been analyzed. The concentration of ($\cdot\text{OH}$) radicals formed in aqueous solutions were detected by the optical spectroscopy method using specific sensor coumarin.

Obtained experimental data have revealed that a preliminary treatment of (Gd,Y)VO₄:Eu³⁺ NPs with UV light is the effective tool to change drastically their redox properties. (Gd,Y)VO₄:Eu³⁺ NPs, which were UV-light pre-treated (L-GdYVO), exhibit strong $\cdot\text{OH}$ generation during X-ray exposure, whereas the same NPs, which were kept in the darkness before the experiment (D-GdYVO), show radioprotective action. The mechanism of D-GdYVO radioprotective action ($\cdot\text{OH}$ scavenging) is ascribed to the presence in the crystal lattice of (Gd,Y)VO₄:Eu³⁺ NPs of a large amount of V⁴⁺ and V³⁺ ions. Electrons stored in vanadium ions participate in neutralization of $\cdot\text{OH}$ formed at both water radiolysis and water splitting via reaction with the h^+ -mediated reaction. The mechanism of X-ray induced $\cdot\text{OH}$ generation in L-GdYVO is more complicated and three processes could be separated: (i) direct OH generation with the participation of thermalized holes (h^+) formed in NPs at X-ray irradiation, (ii) X-ray facilitated jumps of h^+ formed in the valence band at UV light pre-treatment and trapped in local levels formed by RSP, and (iii) formation of hydrogen peroxide (H₂O₂) via photo-induced electrons interaction with oxygen molecules and its further radiolysis under X-ray exposure.

Thus, depending on pre-treatment condition, we can change oppositely the redox properties of (Gd,Y)VO₄:Eu³⁺ NPs that makes this nanomaterials unique theranostic agents for RT enhancement allowing the problem of RT resistant hypoxic tumour to be overcome.

Acknowledgments: This research was supported by National Research Foundation of Ukraine for Leading and Young Scientists Research Support, Grant No. 2020.02/0052. The authors thank the Armed Forces of Ukraine for the opportunity to continue our research work.

⁽¹⁾ A. D. Paro et al. *Methods Mol. Biol.* 1530 (2017), 391.

⁽²⁾ N. Scher et al. *Biotechnol. Rep.* 28 (2020), e00548.

Luminescent ceria nanoparticles with controlled ROS scavenging activity

V. Seminko,¹ P. Maksimchuk,¹ G. Grygorova,¹ O. Ivankov,²
O. Tomchuk,² S. Yefimova¹

¹Institute for Scintillation Materials NAS of Ukraine, Kharkiv, Ukraine

²Taras Shevchenko National University of Kyiv, Kyiv, Ukraine

email: seminko@ukr.net

Reactive oxygen species (ROS) such as hydrogen peroxide (H_2O_2), superoxide anions (O_2^-) and hydroxyl radicals ($\cdot\text{OH}$) permanently formed inside the living cells possess strong destructive effect on the DNA and lipid membranes. Ceria (CeO_{2-x}) nanoparticles are widely investigated nowadays due to their effective ROS scavenging properties governed by easy oxidation and reduction of cerium ion on the nanoparticle surface. Depending on the balance between Ce^{3+} and Ce^{4+} ions CeO_2 nanoparticles can show either antioxidant or prooxidant properties. However, at present there is no consensus understanding on the origin of its unique redox features. Redox activity of nanoceria is generally attributed to high content of reactive sites, namely, oxygen vacancies and Ce^{3+} ions on its surface.

In order to reveal the role of different types of the surface defects in the formation of redox activity of ceria and ceria-based nanocrystals, we have obtained ceria nanoparticles of different sizes and doped by rare-earth (Re^{3+}) ions ($\text{Re}=\text{Y}$, Eu , Tb). The NPs were characterized using the methods of small-angle X-ray and neutron scattering, transmission electron microscopy, X-ray diffraction and X-ray photoelectron spectroscopy. We have used the methods of optical spectroscopy for studying the processes of nanoceria interaction with different types of ROS. The combination of the methods of optical absorption spectroscopy (allowing determining the change in ROS content) and luminescence spectroscopy (tracing the change of Ce^{3+} content using 5d-4f luminescence) opens the possibility to unveil the dynamics and mechanisms of nanoceria-ROS interaction. Both pro- and antioxidant action of nanoceria was revealed and the ways to switch the type of redox activity were proposed.

Generally, our results have shown that the dynamics of nanoceria-ROS interaction is determined by the subtle interplay of the concentration of Ce^{3+} and Re^{3+} ions in nanoceria lattice, ROS concentration in colloidal solution, pH and presence of UV-radiation. The ability to control and vary the type of redox activity of nanoceria provides the way to obtain redox-active NPs with pre-determined anti-/prooxidant properties for biological applications.

Acknowledgments: This research was supported by National Research Foundation of Ukraine for Leading and Young Scientists Research Support, Grant No. 2020.02/0052.

Investigation of electronic and magnetic properties of copper pyrophosphat

S. Pastukh, P. Piekarz

Institute of Nuclear Physics Polish Academy of Science, Kraków, Poland

email: svtlana.pastukh@ifj.edu.pl

In our study, we apply the density functional theory to in-depth study of the structural and electronic properties of the $\text{Cu}_2\text{P}_2\text{O}_7$ crystal. All calculations were performed with the Vienna Ab initio Simulation Package (VASP) within the general gradient approximation (GGA). The obtained results were compared with the experimental measurements of nanocrystalline copper pyrophosphates.

The electronic density of state (DOS) obtained within the GGA shows the incorrect metallic state in agreement with the previous LDA studies.⁽¹⁾ In the $\text{Cu}_2\text{P}_2\text{O}_7$ crystal, the gap opens due to the local Coulomb interaction U , indicating that the insulating ground state is of the Mott type. The total and partial electron DOS was calculated with the GGA+ U approach. The lowest total energy was found for the antiferromagnetic arrangement of magnetic moments on copper atoms, in agreement with the experimental observation.⁽¹⁾ The magnetic moment on Cu ion increases from $0.55 \mu_B$ to $0.84 \mu_B$ with the value of $U=9$ eV.⁽²⁾ The electronic structure shows the insulating state with the gap $E_g=2.6$ eV, which opens between the occupied states with both spin components and the empty spin-down 3d states in the upper Hubbard band.⁽²⁾ The lattice parameters and atomic positions obtained with the van der Waals correction agree very well with the experimental data.⁽²⁾

⁽¹⁾ O. Janson et al. Phys. Rev. B 83 (2011), 094435.

⁽²⁾ S. Pastukh et al. Nanotechnology 32 (2021), 415701.

The effect of solvent on oxidation behavior of copper during laser irradiation of suspension, a reactive bond molecular dynamics study

M. S. Shakeri,¹ Z. Swiatkowska-Warkocka,¹ T. Itina²

¹Institute of Nuclear Physics Polish Academy of Science, Kraków, Poland

²Laboratory of Hubert Curien, University of Jean Monnet, Saint-Etienne, France

email: ms.shakeri@ifj.edu.pl

Pulsed laser irradiation of suspension (PLIS) is a promising method for synthesis of multicomponent powders, i.e. composite materials and heterojunctions.⁽¹⁾ The process initiates with making a stable suspension following by laser irradiation. One of the advantages of this method is the production of completely spherical particles which are of great interest in high-tech applications. Beside the advantages of this method, there is an obstacle which restricts the usage of this method including the mechanism of phase formation. Laser irradiation increases the temperature of the suspension containing nano-powders; by the way, the exact temperature could not be easily determined due to the fastness and the excessive increasing of temperature during irradiation.⁽²⁾ Kinetics and thermodynamics rules play an important role in bond breaking and bond formation during laser irradiation of suspension. Hence, reactive bond molecular dynamics (RBMD) is considered as a suitable method for studying the atomic interactions in high temperatures and better understanding of PLIS. RBMD uses the conventional Newton's law to study the dynamic of a system, but, it is also contains bond orders for determination of bond breaking/formation procedure.⁽³⁾

In the present investigation, the effect of different kinds of solvent on oxidation behavior of copper has been evaluated using RBMD during PLIS. To determine the exact temperature of spheres, heating-cooling model has been utilized. The NVT simulations have been done for copper slabs exerted inside solvent molecule pack. Ethanol, ethyl acetate, toluene and acetone have been considered as the main solvents. Results of the investigation show that the solvent molecules firstly absorb on the copper surface. The oxidation behavior of copper is completely affected by the kind of solvent because each solvent decomposes to different species which play the role of oxidation or reduction agents. The top reactions, their network and timeline of oxidation process have also been reported.

Acknowledgments: This work was supported by the Polish National Science Center Program No. 2018/31/B/ST8/03043.

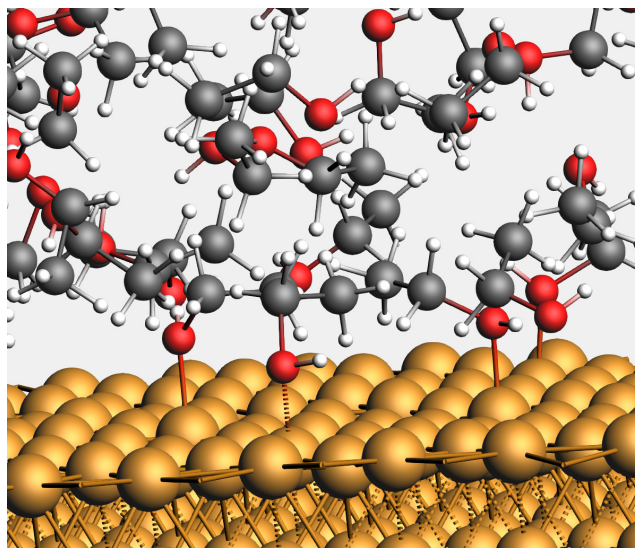


Figure 1. Absorption of ethanol molecules on Cu surface during the initiation of MD process.

- (1) S. Sakaki et al. *Chem. Phys. Chem.* 18 (2017), 1101 – 1107.
- (2) M. Dontgen et al. *J. Chem. Theory Comput.* 11 (2015), 2517 – 2524.
- (3) W. Zhu et al. *J. Phys. Chem. C* 124 (2020), 12512 – 12520.

Fluctuation (noise) spectroscopy as a tool to study the dynamics of multi-scale systems in condensed matter

J. Müller, T. Thomas, M. Mitschek, T. Thyzel, Y. Agarmani, M. Kopp, M. Al Mamoori, C. Garg, B. Hartmann, M. Pohlit

Institute of Physics, Goethe-University Frankfurt, Frankfurt (Main), Germany

email: j.mueller@physik.uni-frankfurt.de

Fluctuations (or noise) are inevitably present in any physical measurement, yet mostly aimed to be suppressed in order to increase the accuracy of the experiment. However, the fluctuations of a system (e.g. in the conductance of a sample) are related to a particular (here: current-current) correlation function and therefore provide valuable insights into the microscopic kinetics of the charge carriers, an energy-resolved information that is lost when considering only mean values.⁽¹⁾

In this talk, we will give a basic and general introduction into fluctuation processes in nature and condensed-matter systems and how to understand $1/f$ -type noise which is ubiquitous in nature and observed in almost all condensed matter systems. $1/f$ noise is a true multiscale phenomenon since it describes the accumulative effect of "somethings happening sometimes" on all time scales. More rigorously: each logarithmic interval in frequency contributes the same noise power. Since $1/f$ noise scales inversely with the volume of a system and therefore becomes a serious obstacle for the long-time stability of miniaturized electronic and magnetic devices.

We will (i) show that understanding the origin of the fluctuations in devices, as e.g. micro-Hall sensors, allows to improve their sensitivity enabling measurements of individual magnetic nanoparticles.⁽²⁾ We will then (ii) give several examples where fluctuation spectroscopy helps to delineate the low-frequency dynamics of charge carriers in strongly-correlated molecular (organic) conductors and intermetallic systems.⁽³⁾ There, we study the fluctuations of the conductance or resistance of a sample coupled to electric, magnetic or structural degrees of freedom and discuss the switching of nanoscale dielectric^(4,5) and ferromagnetic clusters^(3,6) related to the rich physics of various kinds of metal-insulator transitions.

Acknowledgments: This work has been performed in collaboration with Takahiko Sasaki, Satoshi Iguchi and Kenichiro Hashimoto from the Institute for Materials Research, Tohoku University, Japan, Hiroshi Yamamoto from the Institute for Molecular Science, Okazaki, Japan, John Schlueter from Argonne National Lab, USA, Thomas Hicken and Tom Lancaster from Durham University, UK. Work is funded by the Deutsche Forschungsgemeinschaft.

- (1) J. Müller, ChemPhysChem 12 (2011), 1222; J. Müller and T. Thomas, Crystals 8 (2018), 166.
- (2) J. Müller et al. Phys. Rev. Lett. 96 (2006), 186601; M. Al Mamoori et al. Materials 11 (2018), 289.
- (3) B. Hartmann et al. Phys. Rev. Lett. 114 (2015), 216403; P. Das et al. Phys. Rev. B 86 (2012), 184425.
- (4) J. Müller et al. Phys. Rev. B 102 (2020), 100103(R).
- (5) T. Thomas et al. Phys. Rev. B 105 (2022), L041114; T. Thomas et al. Phys. Rev. B 105 (2022), 205111.
- (6) M. Mitschek et al. Phys. Rev. B 105 (2022), 064404.

Magnetism in $\text{RMn}_{1-x}\text{Fe}_x\text{O}_3$ orthorhombically distorted perovskite compounds

M. Mihalik, M. Zentková, M. Mihalik

Institute of Experimental Physics SAS, Košice, Slovak Republic

email: matmihalik@saske.sk

The $\text{RMn}_{1-x}\text{Fe}_x\text{O}_3$ compounds belong to family of ABO_3 -type (A: s-, or f-cation; B: d-cation) orthorhombically distorted perovskite structure oxides. These compounds are subject of long-lasting interest in last decades and this demand continues in the present. The interesting phenomena for the basic research are for example multiferroicity,⁽¹⁾ magnetoelectricity,⁽²⁾ complex magnetic structures⁽³⁾ and other physical phenomena. From the application point of view, these systems can be used as cathodes for solid oxide fuel cells, gas sensors, materials for magnetic cooling, or hyperthermia.⁽⁴⁾

In the speech we will focus on the complete construction of magnetic phase diagrams of $\text{PrMn}_{1-x}\text{Fe}_x\text{O}_3$ (Fig. 1) light rare-earth and $\text{TbMn}_{1-x}\text{Fe}_x\text{O}_3$ heavy rare-earth compound as well as the several systems where the complete magnetic phase diagram is not known yet like $\text{NdMn}_{1-x}\text{Fe}_x\text{O}_3$ compound and other. As one can see (Fig. 1 and 2), these materials exhibit very rich magnetic phase diagram with several commensurate (canted) antiferromagnetic structures for light rare-earth (Fig. 1) and also incommensurate magnetic structures for Mn-rich region and heavy rare earth (see Fig. 2 and ref. (1)) which allows the multiferroicity in these compounds.⁽²⁾ In all cases, the Fe substitution on the manganese site is possible for the whole concentration range and it increases the magnetic ordering temperature T_{ord} . T_{ord} typically reaches the room temperature for Mn:Fe concentration around 40:60 which has an application potential on the field of hyperthermia and other applications.

Acknowledgments: This research project has been supported, in part, by the European Commission under the 7th Framework Programme through the "Research Infrastructure" action of the "Capacities" Programme, NMI3-II Grant No. 283883 and VEGA Project No. 2/0011/22.

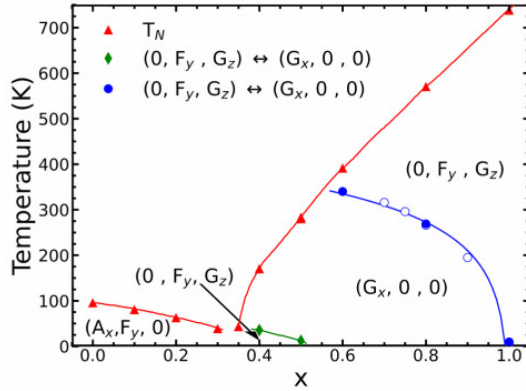


Figure 1. The magnetic phase diagram of $\text{PrMn}_{1-x}\text{Fe}_x\text{O}_3$ substitutional compound.

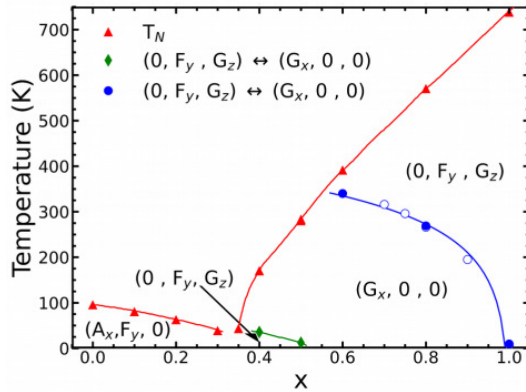


Figure 2. The magnetic phase diagram of $\text{TbMn}_{1-x}\text{Fe}_x\text{O}_3$ substitutional compound.⁽⁵⁾

- (1) T. Kimura et al. Nature 426 (2013), 55.
- (2) C. Lu et al. Sci. Rep. 6 (2016), 20175.
- (3) D. N. Argyriou et al. Phys. Rev. B 75 (2007), 020101(R).
- (4) M. Zentková et al. Act. Phys. Pol. A 137 (2020), 900.
- (5) M. Mihalik jr. et al. Phys. B 506 (2017), 163.

Thermodynamic properties around the metal-insulator spin phase boundary in the dimer-Mott organic compounds

Y. Nakazawa,¹ E. Yesil,¹ S. Imajo,² S. Yamashita,¹ H. Akutsu¹

¹Dept. of Chemistry & Research Centre for Thermal and Entropic Science, Osaka University, Toyonaka/Osaka, Japan

²Institute for Solid State Physics, the University of Tokyo, Kashiwa/Chiba, Japan

email: nakazawa@chem.sci.osaka-u.ac.jp

In this presentation, we discuss quantum mechanical features of molecule-based compounds studied by thermodynamic measurements using micro single crystals weighing in orders of 102 mg. The compounds we measured in this work are charge transfer complexes with chemical formula of κ -(BEDT-TTF)₂X, β' -Y[Pd(dmit)₂]₂ (X: counter anions, Y: counter cations) where BEDT-TTF denotes bis(ethylenedithio)tetrathiafulvalene and dmit is 1,3-dithiole-2-thione-4,5-dithiolate. These compounds are known as dimer-Mott system in which Mott insulating future are competed with metallic/superconductive properties and some other magnetic ground states. We present the heat capacity data of the spin-liquid (SL) systems such as κ -(BEDT-TTF)₂Cu₂(CN)₃, β' -EtMe₃Sb[Pd(dmit)₂]₂ and their alloying system in which gradually changes of their ground states from SL to AF, CO, and Fermi liquid ones by chemical pressure. Although we discuss that the SL state exists as a distinct phase and thermodynamic feature of SL resembles well with that of the Electronic Fermi liquid states, the alloying of the molecules induces continuous electronic changes across several types of boundaries shown in Fig. 1. By comparing the low temperature thermodynamic data, we discussed how the SL states changes to the other ground state in the dimer-Mott phase diagram.^(1,2) We especillay focus on the genuine Mott transition due to the openig/disapperance of charge gap by keeping frustrated structures with BEDT-TTF and BEDT-STF substitution.

We further discuss a change in thermodynamic feature induced by a doping of hole carriers into the spin liquid state.⁽³⁾ This is related to the exotic mechanisms of the electron correlation induced superconductivity predicted for two-dimensional triangle lattices. The hole doped state was found to show quite anomalous enhancement of the electronic heat capacity in κ -(BEDT-TTF)₄Hg_{2.89}Br₈ and κ -(BEDT-TTF)₄Hg_{2.78}Cl₈. The former compound shows a superconductivity with keeping spin liquid like feature in its magnetic properties. Although they have rather large residual electronic heat capacity coefficient γ^* , the normal state electronic heat capacity obtained by breaking the superconductivity gives rather large mass probably due to the strong electron correlations.⁽⁴⁾ The γ term of κ -(BEDT-TTF)₄Hg_{2.78}Cl₈ is also large probably the highest class among organic conductors and superconductors.

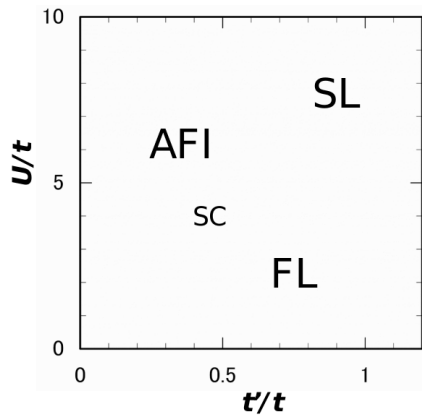


Figure 1. The phase diagram of dimer-Mott compounds. U is the on-site Coulomb on dimer-site and t' and t denote transfer integrals between the dimers in the k -type arrangement.

- (1) S. Imajo et al. Phys Rev B. 105 (2022), 125130.
- (2) E. Yesil et al. J. Phys. Soc. Jpn. 89 (2020), 073701.
- (3) A. Naito et al. Phys. Rev. B 71 (2005), 054514 – 054518.
- (4) S. Imajo et al. Phys. Rev. Res. 3 (2021), 033026.

Limit shape phase transitions: a merger of arctic circles

J. Pallister,¹ A. Abanov,² D. Gangardt¹

¹School of Physics and Astronomy, University of Birmingham, Edgbaston, Birmingham, UK

²Department of Physics and Astronomy and Simons Center for Geometry and Physics, Stony Brook, NY, USA

We consider a free fermion formulation of a statistical model exhibiting a limit shape phenomenon. The model is shown to have a phase transition that can be visualized as the merger of two liquid regions — arctic circles.⁽¹⁾ We show that the merging arctic circles provide a space-time resolved picture of the phase transition in lattice QCD known as Gross-Witten-Wadia transition.⁽²⁾ The latter is a continuous phase transition of the third order.

We argue that this transition is universal and is not spoiled by interactions if parity and time-reversal symmetries are preserved. We refer to this universal transition as the Merger Transition.⁽³⁾

⁽¹⁾ W. Jockusch, et al. arXiv:math/9801068 (1998).

⁽²⁾ D. J. Gross et al. Phys. Rev. D 21 (1980), 446.

⁽³⁾ J. Pallister et al., (submitted).

The hole doped perovskite manganites $\text{La}_{0.80}\text{Ag}_{0.15}\text{MnO}_3$ for bioapplications

M. Kovalik,¹ M. Zentková,¹ M. Mihalik,¹ M. Mihalik jr.,¹ M. Perovic,²
M. Boskovic,² R. Pelka³

¹Institute of Experimental Physics, Slovak Academy of Sciences, Košice, Slovakia

²The Vinca Institute, Belgrade, Serbia

³Institute of Nuclear Physics PAN, Krakow, Poland

email: zentkova@saske.sk

Current nanomaterials for use in biomedicine are based mainly on iron oxides as well known and described magnetic nanostructures. Advantage of manganese oxides for use in hyperthermia is fine tunable Curie temperature (T_C) in the whole therapeutic range. Specific T_C of material is related to the degree of hole doping of A^{3+} ion in perovskite lattice, ionic radius of dopant, Mn-O bond and length and angle, ratio of mixed valence state, presence of oxygen vacancies and structural phase transition from orthorhombic ($Pnma$) space group to rhombohedral ($R3c$). These properties can be directly influenced by character of synthesis route, temperature of annealing and ambient atmosphere. Our samples were prepared by wet route — glycine/nitrate — one step solution combustion synthesis and additionally processed via annealing 48 hour at 800°C in tube furnace with continuous flow of oxygen atmosphere.⁽¹⁾ Samples were additionally stabilized electrostatically and sterically in water suspension. Prepared magnetic nanoparticles were stabilized by dextrane in magnetic colloids. Samples were characterized by X-ray diffraction and magnetic measurements.

The value of critical temperature of transition into magnetically ordered state the Curie temperature was tuneable by heat treatment. Measurement of heat release was performed on 5 g/ml of bare powder in distilled water immobilized using 2% agar gel using multiple fields and frequencies.

Heat dissipation is strongly field dependent. During heat absorption measurement was therapeutic temperature range achieved at frequency 577 kHz at field amplitude 0.03 T (23.873 kA/m). Agar gel fixed nanoparticles prefer heat dissipation by Néel relaxation. Maximal temperature obtained by measurement of agar immobilized bare powder was 43.5°C (316.65 K) correspondent with $T_C^{\text{ZFC}}=320.20$ K and $T_C^{\text{FC}}=318.18$ K at field 0.01 T.

Acknowledgments: This research project has been supported by VEGA Project No. 2/0011/22.

⁽¹⁾ M. B. Bellakki et al. Mat. Re. Bu. 45 (1998), 1742.

Surface origin of Laser Induced White Light emission

M. Chaika, R. Tomala, W. Stręk

Institute of Low Temperature and Structure Research Polish Academy of Science, Wroclaw, Poland

email: m.chaika@intibs.pl

Since its discovery in 2009 by Tanner and co-workers, laser-induced white emission (LIWE) has been the subject of numerous reports in the past decade. LIWE was generated under a focused laser beam above a threshold in a vacuum ambient and is characterized by a high exponent of the power dependence characteristic for multi-photon absorption, long rise and decay times and a relatively low temperature of the light emitting sample. These characteristics, including broadband light emission and pressure dependence may lead to the conclusions that LIWE is caused by thermal heating, which isn't the case. This is evidenced by the fact the most of the studied materials have low thermal conductivity, which contributes to the accumulation of thermal energy. Therefore, the effect of temperature on LIWE is currently under discussion.

The purpose of this work is to study the effect of temperature on the LIWE characteristics. For this, a Cr-doped YAG transparent ceramics was synthesized by solid-state reaction sintering in vacuum at 1750°C. LIWE was investigated under vacuum (10^{-5} Pa) excited by focused laser beam ($\lambda_{\text{exc}}=1064$ nm, $P=3.4$ W, $D=0.175$ mm).

We have found that transparent Cr:YAG ceramics is able to generate bright LIWE at excitation power above a certain threshold. LIWE covers whole visible and near infrared region between 28000 cm^{-1} (350 nm) and 10000 cm^{-1} (1000 nm) (Fig. 1). It was shown that LIWE can be generated only at the surface of the samples. Due to the fact that the sample is transparent, the laser beam penetrated the entire volume of the sample, but white light was emitted only from the surface. It's impressive that the white emission was detected at the output of the laser beam from samples volume. This is surprising since the power of the laser beam decreased towards the exit due to absorption by Cr^{4+} as well as Cr^{3+} ions. The interaction of the laser beam with the surface leads to ionization with simultaneous emission of photons and free photoelectrons. The ionization process occurs due to the process of multiphoton absorption in a $\text{Cr}^{3+}/\text{Cr}^{4+}$ mixed valence pair with the ejection of electrons and subsequent recombination, leading to the transfer of electron with the emission of photons.

This work was supported by Polish National Science Centre, grant: PRELUDIUM-18 2019/35/N/ST3/01018.

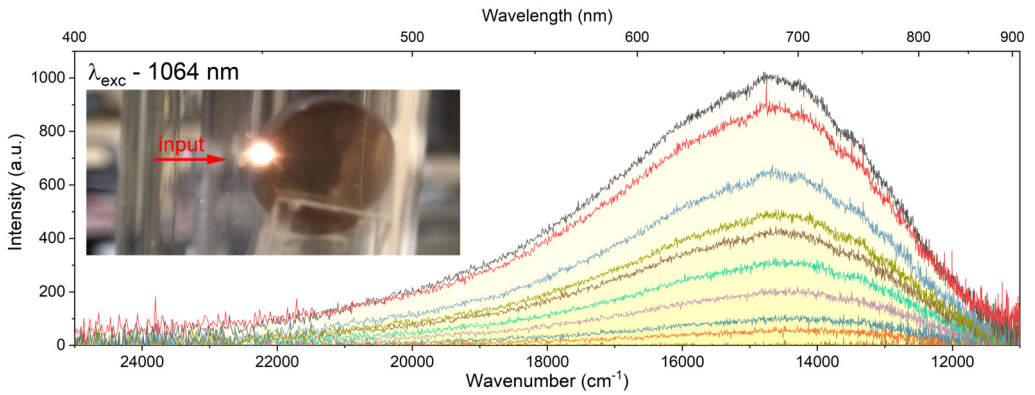


Figure 1. Emission spectra of transparent Cr⁴⁺:YAG ceramics in vacuum under $\lambda_{exc}=1064 \text{ nm}$.

3D liquid crystal structures determined by surface alignment

I. Nys, B. Berteloot, M. Stebryte, S. Liu, X. Xue, J. Beeckman,
K. Neyts

Liquid Crystals and Photonics, ELIS Department, Ghent University,
Ghent, Belgium

email: Kristiaan.neyts@ugent.be

Nematic Liquid Crystals (LC) are a class of soft matter that easily responds to external influences that have found their way in many display applications. Thanks to the liquid nature, the material can self-organize with a high degree of freedom. The surfaces of the volume in which the LC is contained play an essential role in the 3D structure that is formed in the volume.

In nematic LC, the molecules prefer to orient their long axes parallel to each other, with the average molecular orientation called the director. Spatial variations of the director correspond to elastic deformations and this leads to elastic energy. The LC director can relax to reduce the elastic energy until a stable equilibrium state is formed.

There are different methods to define the alignment at the surfaces. The most common one is mechanical rubbing, leading to the same preferred direction over the entire surface of a substrate. Recently new methods have been developed to realize variable preferred orientation: alignment by structured topography⁽¹⁾ and alignment by illumination of a photosensitive layer with polarized light, also called photoalignment. In this presentation both approaches will be discussed. Patterned photoalignment can be obtained by interference between two coherent laser beams,^(2,3) or by projecting the light reflected from the pixels of a spatial light modulator onto the substrate.⁽⁴⁾

Two-dimensional alignment patterns at the top and bottom surfaces of a LC device can lead to complex three-dimensional structures, when the elastic energy in the LC is minimized. Figure 1 illustrates a number of patterns: periodic patterns obtained after interference photoalignment and circular patterns obtained by photoalignment with the spatial light modulator. Even if the preferred alignment is parallel to the substrate at the top and bottom surfaces, an out of plane orientation can result in the bulk of the LC. The configuration corresponding to minimal elastic energy and the corresponding transmission images can be simulated numerically (also illustrated in Figure 1), to verify the assumptions that have been made.

In the presentation we will illustrate experimental results and numerical simulations for different boundary conditions. Using chiral liquid crystal with photonic band gap in the visible light, this approach can be used to obtain reflectors with optical functionality for use in augmented reality devices.⁽⁵⁾

Acknowledgments: This work is sponsored by the FWO project (Flemish Fund for Scientific Research) with grant number FWOOPR2021008601.

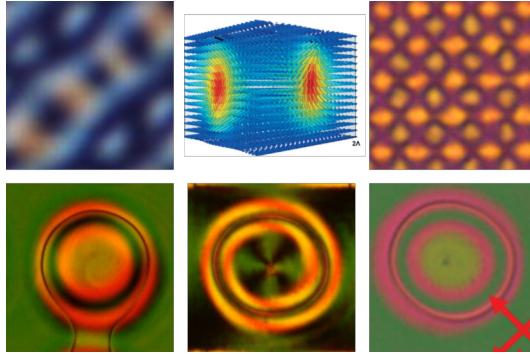


Figure 1. Five polarization microscope images of liquid crystal structures and one image of a unit cell of a 3D simulations. Top row: periodic gratings. Bottom row: circular liquid crystal structures.

- (1) I. Nys, et al. *Adv. Opt. Mater.* (2018), 1800070.
- (2) I. Nys et al. *Soft Matter* 11 (2015), 7802 – 8.
- (3) S. Liu et al. *Adv. Opt. Mater.* accepted.
- (4) B. Berteloot et al. *Soft Matter* 16 (2020), 4999 – 5008.
- (5) I. Nys et al. *Adv. Opt. Mater.* 7 (2019), 1901364.

Slow dynamics facilitates equilibration of liquids and glasses

S. S. Napolitano, Z. Song, C. Rodríguez-Tinoco, A. Mathew

Laboratory of Polymer and Soft Matter Dynamics, Experimental Soft Matter and Thermal Physics (EST), Université libre de Bruxelles, Brussels, Belgium

The rate at which a nonequilibrium system decreases its free energy is commonly ascribed to molecular relaxation processes, arising from spontaneous rearrangements at the microscopic scale. While equilibration of liquids usually requires density fluctuations at timescales quickly diverging upon cooling — known as the α -, structural (segmental) modes-, growing experimental evidence indicates the presence of different alternative pathways of weaker temperature dependence. Such equilibration processes exhibit a temperature-invariant activation energy on the order of 100 kJ mol^{-1} . Based on a large series of molecular dynamics and equilibration experiments, we identified the underlying molecular process responsible for this class of Arrhenius equilibration mechanisms with a slow mode (SAP), universally present in the liquid dynamics.⁽¹⁾ While in bulk samples the SAP can be masked by conductivity and electrode polarization, measurements in thin films permitted us to directly access the relaxation spectra of these slow modes.

Within experimental uncertainties, the SAP can be associated to the spectral response of a molecular mechanism with a single relaxation time, corresponding to a simple exponential decay in the time domain. By analyzing polymer chains of different molecular weight ($43 - 6000 \text{ kg mol}^{-1}$) and films of different thickness ($7 \text{ nm} - 100 \text{ nm}$), we verified that this process is present also in bulk melts and that the activation energy and the characteristic molecular time of the SAP are not affected by either the macromolecular or the sample size. This feature permitted us to discriminate between possible classes of relaxation mechanisms and discard diffusion-limited, nucleation-driven processes and polymer specific (Rouse) modes whose characteristic time would, instead, increase change with film thickness and molecular weight. Furthermore, as the position of the SAP peaks is invariant with sample size even in those cases where the α -process shifts upon confinement, we conclude the slow Arrhenius processes is related to a genuine molecular mechanism, totally decoupled from segmental motion in proximity of the glass transition.

The SAP, which we show is intimately connected to high temperature flow, can efficiently drive melts and glasses towards more stable, less energetic states. Our results show that measurements of liquid dynamics can be used to predict the equilibration rate in the glassy state.

Finally, we emphasize that our discussion does not invoke the macromolecular nature of polymers -SAPs have been observed, both via dielectric and mechanical spectroscopy, in small molecules- and we anticipate that the intimate relationship between equilibration and SAP holds independently on the chemical nature of the nonequilibrium system.

⁽¹⁾ Z. Song et al. *Sci. Adv.* 8 (2022), eabm7154.

Intermolecular association in co-amorphous systems and their relaxation to co-crystals

J. F. C. Silva,¹ M. T. S. Rosado,¹ P. S. Pereira,² M. R. Silva,²
E. Fantechi,³ L. Chelazzi,³ S. Ciattini,³ M. E. S. Eusébio¹

¹CQC-IMS, Centro de Química-Institute of Molecular Sciences,
Departamento de Química, Faculdade de Ciências e Tecnologia,
Universidade de Coimbra, Coimbra, Portugal

²Centro de Física da Universidade de Coimbra, CFisUC, Departamento
de Física, Universidade de Coimbra, Coimbra, Portugal
Centro di Cristallografia Strutturale (CRIST), Università degli Studi di
Firenze, Firenze, Italy

email: joana.silva@qui.uc.pt

To overcome water solubility issues of oral formulation of drugs, various amorphization techniques have been proposed.^(1,2) However, the thermodynamical metastability of amorphous phases makes them prone to relaxation into crystalline states. Co-amorphization has recently emerged as a successful technique to kinetically stabilize amorphous drug systems, combining APIs with small co-former molecules.^(3,4)

This work aims to design and study co-amorphous systems of nateglinide,⁽⁵⁾ an oral hypoglycemic agent used to treat type II diabetes mellitus with very low aqueous solubility (BCS class II), and a set of pyridinecarboxamides as co-formers, synthesized by melt quenching or mechanochemistry. The thermal behavior and the intermolecular association of the obtained materials were investigated by DSC and FTIR spectroscopy, respectively. Structural changes in the co-amorphous systems were monitored by variable temperature X-ray powder diffraction. Relaxations from co-amorphous to co-crystal were observed under different conditions.

The local intermolecular interactions responsible for the intimate drug-co-former association were studied by several electronic structure techniques based in the DFT calculations on dimers that could be fundamental units in the multicomponent solids. They included Non-Covalent Interactions (NCI), Natural Bond Orbitals (NBO), Atoms in Molecules (AIM) and Electrostatic Potential (ESP).

Acknowledgments: Joana F. C. Silva thanks to FCT- Fundação para a Ciência e a Tecnologia for scholar grant SFRH/BD/146809/2019. CQC-IMS is funded by national funds through FCT — Fundação para a Ciência e a Tecnologia, I.P., under the project UIDB/00313/2020.

- (1) Q. Shi et al. *AAPS PharmSciTech*, 23 (2021), 15.
- (2) K. T. Savjani et al. *ISRN Pharmaceutics* 1 (2012).
- (3) Q. Shi et al. *Acta Pharmacol, Sin B* 9 (2019), 19.
- (4) Y. Hatanaka et al. *JDDST* 65 (2021).
- (5) C. J. Halas et al. *AJHP* 58 (2001), 1200.

Neutrons to study multiscale phenomena in energy materials

M. Johnson

Institut Laue Langevin, Grenoble, France

email: johnson@ill.eu

Neutron techniques cover many orders of magnitude in time and length scales, which can be extended even further by combining real and reciprocal, time and space techniques — neutrons are therefore perfectly suited to studying multiscale phenomena.

In the critical context of climate change, it is essential to design and study new energy materials and devices. This talk will focus on the use of neutron diffraction, small angle scattering, reflectometry and imaging, as well as quasi and inelastic scattering to study battery, fuel cell and thermoelectric materials. The examples will include operando experiments and complementary atomistic simulations which give detailed understanding of materials. New instrumentation at ILL will be presented as the basis for the next generation of experiments in energy materials.

Atomic dynamics in condensed matter studied by neutron scattering with crystal spectrometers

A. Ivanov

Institut Laue-Langevin, Grenoble, France

email: aivanov@ill.fr

The crystal neutron spectrometers actually routinely use two-dimensionally focussing monochromators and analysers with variable and remotely controlled curvatures. The brightness of a measured (Q) pixel may be increased with these high-precision mechanical devices by a factor of more than 100. Several multi-analyser (multi-pixel) schemes have been proposed and designed. A particular place is taken by instruments with very large focusing crystal surfaces that permit registration of scattered neutrons in considerable solid angle of the order of several Steradian. High performance of such instruments in terms of registered neutron intensity and energy resolution allows advanced studies of atomic dynamics in polycrystalline materials. We present several examples of recently collected data with the IN1-Lagrange spectrometer at the ILL high-flux reactor. The accent is given to complex materials containing hydrogen characterised by broad spectrum of proton vibrations in the energy range up to several hundred milli-electronVolt.

Cluster structure and cluster-cluster interaction in nanodiamond aqueous sols by small-angle scattering

O. Tomchuk,^{1,2} L. Bulavin,² N. Mchedlov-Petrosyan³

¹Institute of Nuclear Physics of PAS, Kraków, Poland

²Taras Shevchenko National University of Kyiv, Kyiv, Ukraine

³V. N. Karazin Kharkiv National University, Kharkiv, Ukraine

email: oleksandr.tomchuk@ifj.edu.pl

The targeted design of nanomaterials demands a fundamental comprehension of the relationships between structure and properties. That should be based on a detailed analysis of molecular and supramolecular interactions. Diamond nanoparticles produced by the detonation-based synthesis from oxygen-imbalanced explosives appeared to be especially proper objects for applied areas because of low cost and mass production.

The structure and interaction of nanodiamond fractal clusters were studied by small-angle X-ray and neutron scattering including contrast variation.⁽¹⁾ The density of nanodiamonds, the aggregation number, and the ratio of aggregated/non-aggregated particles were determined. The analysis of the structure-factor made it possible to obtain the effective potential of cluster-cluster interaction. Branched fractal colloids behave to a certain extent like hard spheres, but the effective correlation length decreases with increasing concentration up to the sol-gel transition.

The proposed approach for analyzing cluster-cluster correlations can be used in wider class of liquid systems with nano-sized non-compact inclusions.

Acknowledgments: The support from the Ministry of Education and Science of Ukraine through the project 20BF051-01 of the Taras Shevchenko National University of Kyiv is acknowledged by OT and LB.

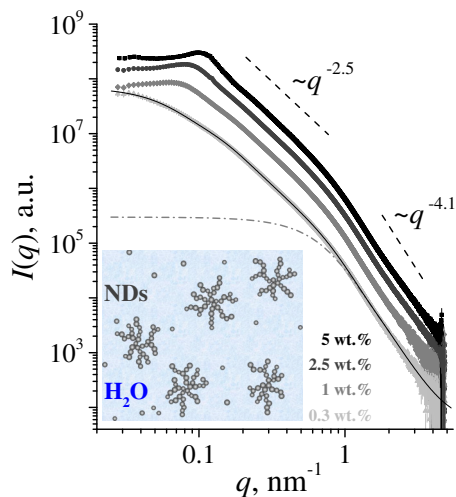


Figure 1. SAXS curves from ND aqueous sols at different concentrations. Model solid line corresponds to two-level unified exponential/power-law approximation for the lowest curve without structure-factor effect. Dashed lines denote the power-law behaviors for the cluster level (small q -values) and particle level (large q -values). Contribution from individual ND particles to the scattering is shown by dash-dotted line.

⁽¹⁾ O. Tomchuk et al. J. Mol. Liq. 354. (2022), 118816.

Structural studies of surfactant-polymer associations in bulk and at interfaces

O. P. Artykulnyi,^{1,2} V. I. Petrenko,^{3,4} O. I. Ivankov,⁵ L. A. Bulavin²

¹Institute for Environment Geochemistry of NAS of Ukraine, Kyiv, Ukraine

²Taras Shevchenko National University of Kyiv, Kyiv, Ukraine

³BCMaterials, Basque Center for Materials, Applications, and Nanostructures, 48940 Leioa, Spain

⁴Ikerbasque, Basque Foundation for Science, Bilbao, Spain

⁵Institute for Safety Problems of Nuclear Power Plants of NAS of Ukraine, Chornobyl, Ukraine

email: artykulnyi@gmail.com

The surfactant-polymer association complexes of anionic surfactant dodecylbenzene sulfonate acid (DBSA) and neutral polymer polyethylene glycol (PEG) were studied in the bulk of solution by small-angle neutron scattering (SANS)^(1,2) and at the surface of polymer brush system by neutron reflectometry.⁽³⁾ The influence of polymer binding effect on the surfactant micelle structure clearly can be seen from SANS curves (Fig. 1a), scattering intensity of DBSA 3 vol.% micellar solution significantly changes after the addition of 3 vol.% PEG in solution, and cannot be represented by the sum of the scattering intensities of the polymer and micelles separately.⁽¹⁾

Polymer brush system of PEG ($M_w=20$ kDa) was synthesized on a silica substrate using the "grafting to" method. Structural changes in the PEG polymer brush caused by the interaction with DBSA micelles were observed by neutron liquid cell reflectometry using a substrate with a titanium carrier layer for enhancing reflectivity signal (Fig. 1b).⁽³⁾ The effect is shown to be related to the formation of molecular polymer-micelle associates, which was previously studied by small-angle neutron scattering in a wide range of surfactant concentrations at various molecular weights of the polymer.⁽¹⁾ The structure of DBSA complexes in the dense medium of the PEG polymer brush under study remains unexplored and requires further investigations including the neutron reflectometry method.

Acknowledgments to the staff of the Frank Laboratory of Neutron Physics of the Joint Institute for Nuclear Research Dr. Mikhail Avdeev and Dr. Igor Gapon.

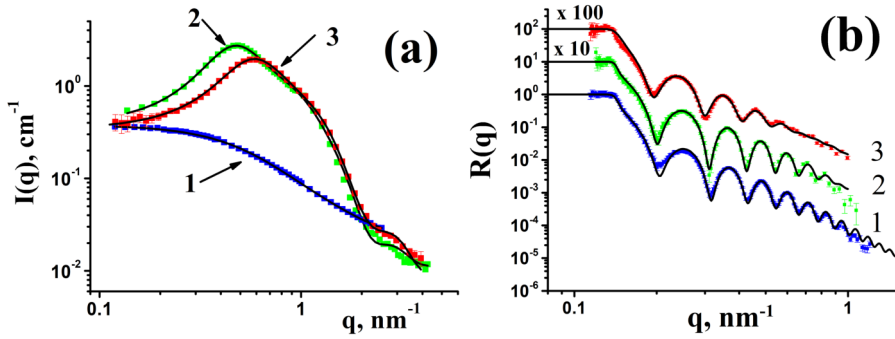


Figure 1. SANS data (a): scattering on PEG 20 kDa solution with 3 vol.% concentration (1), scattering on DBSA 3 vol.% solution (2), scattering on DBSA 3 vol.% + PEG 3 vol.% mixture solution (3); neutron reflectometry data (b): Si/Ti/SiO₂ substrate in the liquid cell (1), PEG polymer brush system at the substrate surface in the liquid cell (2), injection of 0.2 vol.% solution of DBSA in the liquid cell (3).

(1) O. P. Artykulnyi et al. *J. Mol. Liq.* 308 (2020), 113045.

(2) O. P. Artykulnyi et al. *J. Mol. Liq.* 276 (2019), 806.

(3) O. P. Artykulnyi et al. *Nucl. Phys. At. Energy* 22 (2021), 149.

Functional lipid pairs as building blocks of phase-separated membranes

D. Soloviov^{1,2}

¹Faculty of Physics, Adam Mickiewicz University, Poznan, Poland

²Institute for safety problems of nuclear power plants NAS of Ukraine, Chernobyl, Ukraine

email: DimkaupmL@gmail.com

The collective vibrations of molecules in two-component lipid membranes of dipalmitoylphosphatidylcholine-cholesterol (DPPC-Chol) were investigated using high resolution inelastic X-ray scattering technique. It was investigated the influence of cholesterol concentration on the characteristics of phonon modes, which exist in a two-component system. It has been experimentally proved for the first time, the existence of an optical phonon mode in binary lipid system — out of phase vibrations of coupled DPPC and Chol molecules. It has been found that the optical phonon mode in the lipid membrane has a gap, which may be explained by the presence of lipid complexes with approx. 1 nm size, which consist of several pairs of lipid and cholesterol molecules. The appearance of lipid complexes has a threshold character as a function of the Chol. The lifetime of such lipid pairs is determined by the diffusion rate of the molecules in the membrane. The observation of lipid pairs provides a spatial (subnanometer) and temporal (subnanosecond) window into the lipid-lipid interactions in complex mixtures of saturated/unsaturated lipids and cholesterol.

Based on experimental results, we proposed the model of the phase separation in multicomponent lipid membranes.⁽¹⁾

Acknowledgments: Mikhail Zhernenkov and Yong Cai (NSLS-2, Brookhaven National Laboratory), Dima Bolmatov (University of Tennessee/Oak Ridge National Laboratory).

⁽¹⁾ D. Soloviov et al. PNAS 117(9) (2020), 4749.

Lattice dynamics of thin europium oxide films: from the ferromagnetic semiconductor EuO to the high- k dielectric Eu₂O₃

S. Stankov,^{1,2} D. G. Merkel,^{3,4} J. Kalt,¹ J. Göttlicher,¹ J. Łażewski,⁵
M. Sternik,⁵ P. T. Jochym,⁵ P. Piekarczyk,⁵ T. Baumbach,^{1,2}
A. I. Chumakov,⁶ R. Rüffer⁶

¹Institute for Photon Science and Synchrotron Radiation, Karlsruhe Institute of Technology, Eggenstein-Leopoldshafen, Germany

²Laboratory for Applications of Synchrotron Radiation, Karlsruhe Institute of Technology, Karlsruhe, Germany

³Institute for Particle and Nuclear Physics, Wigner Research Centre for Physics, Hungarian Academy of Sciences, Budapest, Hungary

⁴Centre for Energy Research, Budapest, Hungary

⁵Institute of Nuclear Physics, Polish Academy of Sciences, Kraków, Poland

⁶ESRF — The European Synchrotron, Grenoble, France

email: Svetoslav.Stankov@kit.edu

Thin oxide films of the rare earth element europium (EuO, Eu₂O₃ and Eu₃O₄) constitute an attractive family of materials for spintronic, nanoelectronic and magneto-optic applications, as well as for a fundamental research. A comprehensive understanding of the properties of these materials requires a detailed knowledge of the lattice dynamics, namely phonon dispersions and phonon density of states (PDOS), in particular, due to the recently discovered giant spin-phonon coupling in bulk EuO.⁽¹⁾

In this talk, I will introduce a successful approach for a systematic study of the lattice dynamics of thin and ultrathin films, namely a combination of nuclear inelastic scattering of synchrotron radiation and first-principles theory. Examples of research on strain-control of the spin-phonon coupling in thin EuO films (Fig. 1)⁽²⁾ and phonon confinement and interface lattice dynamics in ultrathin Eu₂O₃ (Fig. 2)^(3,4) films will be presented and discussed.

We acknowledge ESRF-The European Synchrotron for provision of synchrotron radiation facilities, the National Isotope Development Center at Oak Ridge National Lab, which is sponsored by the U.S. DOE Basic Energy Sciences, for providing the 151Eu source material. S. S. acknowledges the financial support by the Helmholtz Association (VH-NG-625) and BMBF (05K16VK4). P. P. acknowledges the financial support by the National Science Centre (NCN) within the project no. 2017/25/B/ST3/02586 and the access to the ESRF financed by the Polish Ministry of Science and High Education (DIR/WK/2016/19).

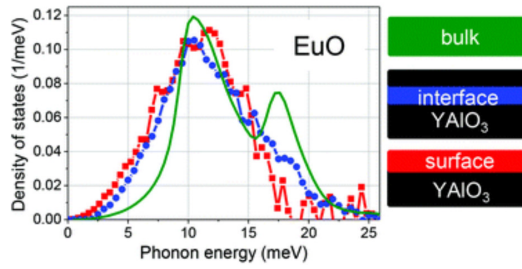


Figure 1. Eu-partial PDOS of EuO bulk crystal, interface and surface layer.⁽²⁾

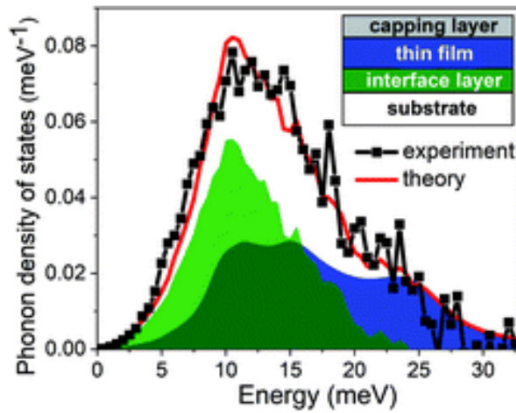


Figure 2. Eu-partial PDOS of thin Eu_2O_3 film.⁽⁴⁾

⁽¹⁾ R. Pradip et al. Phys. Rev. Lett. 116 (2016), 185501.

⁽²⁾ R. Pradip et al. Nanoscale 11 (2019), 10968.

⁽³⁾ J. Łażewski et al. Inorg. Chem. 60 (2021), 9571.

⁽⁴⁾ S. Stankov et al. Nanoscale Adv. 4 (2022), 19.

Modeling of ultrafast magnetization decrease in cobalt multilayer system under soft X-ray radiation

K. J. Kapcia,^{1,2} V. Tkachenko,^{3,4} F. Capotondi,⁵ A. Lichtenstein,^{4,6}
S. Molodtsov,⁴ L. Mueller,⁷ A. Philippi-Kobs,⁷ P. Piekarz,³ B. Ziaja^{1,3}

¹Center for Free-Electron Laser Science CFEL, Deutsches Elektronen-Synchrotron DESY, Hamburg, Germany

²Institute of Spintronics and Quantum Information, Faculty of Physics, Adam Mickiewicz University in Poznań, Poznań, Poland

³Institute of Nuclear Physics, Polish Academy of Sciences, Kraków, Poland

⁴European XFEL GmbH, Schenefeld, Germany

⁵Elettra-Sincrotrone Trieste S.C.p.A, Basovizza, Italy

⁶University of Hamburg, Hamburg, Germany

⁷Deutsches Elektronen-Synchrotron DESY, Hamburg, Germany

email: konrad.kapcia@cfel.de

We investigated the role of electronic excitation, relaxation and transport processes in X-ray induced ultrafast demagnetization of magnetic multilayer systems. In what follows, we report on the results obtained with the newly developed modeling tool, XSPIN, which enables nanoscopic description of electronic processes occurring in X-ray irradiated ferromagnetic materials.^(1,2) With this tool, we have studied the specific response of Co/Pt multilayer system irradiated by an ultrafast XUV pulse at the *M*-edge of Co (photon energy about 60 eV). It was previously studied experimentally at the FERMI free-electron-laser facility, using the magnetic small-angle X-ray scattering technique.⁽³⁾ The XSPIN simulations show that the magnetic scattering signal from cobalt decreases — on the femtosecond timescales considered — due to electronic excitation, relaxation and transport processes both in the cobalt and in the platinum layers. The signal decrease scales with the increasing fluence of incoming radiation, following the trend observed in the experimental data. Confirmation of the predominant role of electronic processes for X-ray induced demagnetization in the regime below the structural damage threshold, achieved with our theoretical study, is a step towards quantitative control and manipulation of X-ray induced magnetic processes on femtosecond timescales.

K. J. K. thanks the Polish National Agency for Academic Exchange for funding in the frame of the Bekker programme (PPN/BEK/2020/1/00184). K. J. K acknowledges also the CFEL-DESY theory group for the hospitality during his six month research stay in Hamburg in 2019 – 2020 financed by National Science Centre (Poland) under program SONATINA 1 no. 2017/24/C/ST3/00276. L. M. and A. P. K. acknowledge funding by the Deutsche Forschungsgemeinschaft (DFG, German Research Foundation) — SFB-925 — project 170620586.

- (¹) K. J. Kapcia et al. arXiv:2202.13845 [cond-mat.mtrl-sci] (2022).
- (²) N. Medvedev et al. 4Open Vol. 1 (2018), 3.
- (³) A. Philippi-Kobs et al. DOI: <https://doi.org/10.21203/rs.3.rs-955056/v1> (2021).

Mechanical properties and pore size distribution in athermal porous glasses

S. Niyogi, B. S. Gupta

Vellore Institute of Technology, Vellore, Tamil Nadu, India

email: sucharita.niyogi@vit.ac.in

Porous glass is a specific type of glassy material that includes pores usually in the size range between nanometers to micrometers.⁽¹⁾ They have attracted substantial interest in the field of research and industry due to their diverse applications starting from biomedical implants: such as drug delivery and tissue engineering, energy storage and conversion technique, functional applications in the process of heat conduction, and civil infrastructure including wear resistance tools.⁽²⁾ We have studied the mechanical properties and pore structure in a three-dimensional molecular dynamics model of porous glass under athermal quasistatic shear.⁽³⁾ The vitreous samples have been prepared by rapid thermal quench from a high-temperature molten state. The pore structures have formed via solid-gas phase separation. The quiescent samples have exhibited a wide range of pore topography, from inter-connected pore networks to randomly distributed compact pores depending on the material density. We have found the shear modulus strongly depends on the density and porosity. Under mechanical loading, the pore structure rearranges which has been reflected in the pore size distribution function.⁽⁴⁾ Our results have shown that with increase in strain the distribution widens as the adjacent pores coalesce and form larger pores.⁽⁵⁾ We also have proposed a universal scaling law for the pore size distribution function which offers excellent data collapse for highly porous materials in the undeformed case.⁽⁶⁾ From the data scaling, we have identified a critical density that can be attributed to the transition point from a porous-type to bulk-type material. The validity of the scaling law under finite deformation has been also analyzed.

Acknowledgments: We acknowledge Science and Engineering Research Board (SERB), Department of Science and Technology (DST), Government of India (no. SRG/2019/001923) for financial support.

⁽¹⁾ X.-Y. Yang et al. *Chem. Soc. Rev.* 46 (2017), 481.

⁽²⁾ B. Sarac et al. *Acta Mater.* 77 (2014), 411.

⁽³⁾ W. Kob, H. C. Andersen. *Phys. Rev. E: Stat. Phys.* 51 (1995), 4626.

⁽⁴⁾ N. V. Priezjev, M. A. Makeev. *Phys. Rev. E.* 96 (2017), 053004.

⁽⁵⁾ J. Kovacik. *J. Mater. Sci. Lett.* 20 (2001), 1953.

⁽⁶⁾ K. K. Phani, S. K. Niyogi. *J. Mater. Sci.* 22 (1987), 257.

Computer simulations of mesophases formed by bent-shaped molecules with excluded-volume type interactions

P. Kubala,¹ W. Tomczyk,^{1,2} M. Cieřła¹

¹Institute of Theoretical Physics, Kraków, Poland

²Jerzy Haber Institute of Catalysis and Surface Chemistry, Kraków, Poland

email: wojciech.tomczyk@ikifp.edu.pl

The recent decade brought exciting discoveries in the realm of liquid crystals.⁽¹⁻⁵⁾ Many novel phases were reported, among which is the twist-bend nematic (N_{TB}). The distinctive feature of this mesophase is that it forms due to the spontaneous mirror symmetry breaking in a system of non-chiral bent-shaped molecules. The corollary of this phenomenon is an emergence of a heliconical (1D modulated) structure of nanoscale pitch with a ground-state exhibiting a degenerate sign of chirality (ambidextrous chirality). This has implications far beyond the field of soft matter, hence no wonder N_{TB} attracted worldwide interest, which pushed it to the forefront of hot topics in liquid crystal research.⁽⁶⁾

Using Monte Carlo and Molecular Dynamics simulations we have numerically studied a liquid composed of non-chiral, bent-shaped molecules built of eleven tangent spheres. The system is known to spontaneously break mirror symmetry, as it forms a macroscopically chiral, twist-bend nematic phase.⁽⁷⁾ Interestingly, quite similar systems to the aforementioned one, were shown to exhibit a multitude of unique liquid crystalline phases.⁽⁸⁾ We have investigated a full phase diagram (Fig. 1) and observed several phases characterized by the orientational and/or translational ordering of molecules.⁽⁹⁾ Apart from nematic (N), smectic A (SmA), and twist-bend nematic phase, we have identified the antiferroelectric smectic A phase (SmAP_A). For large densities and a high degree of molecule's structural bend, another smectic phase emerged (SmX), where the polarization vector rotates within a single smectic layer.

Acknowledgments: P. K. and M. C. acknowledge the support of the Ministry of Science and Higher Education (Poland) grant no. 0108/DIA/2020/49. W. T. was funded by the statutory activity of the Jerzy Haber Institute of Catalysis and Surface Chemistry, Polish Academy of Sciences. Numerical simulations were carried out with the support of the Interdisciplinary Center for Mathematical and Computational Modeling (ICM) at the University of Warsaw under grant no. GB76-1.

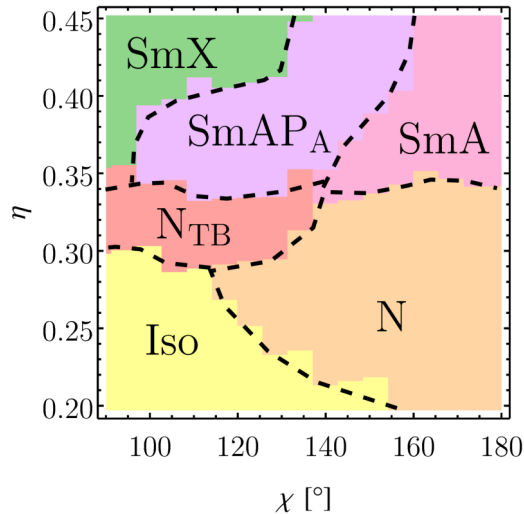


Figure 1. Phase diagram of bent-shaped molecules as a function of packing fraction (η) and bend angle (χ), displaying: isotropic phase (Iso), nematic (N), twist-bend nematic (N_{TB}), non-polar smectic A (SmA), antiferroelectric smectic A ($SmAP_A$) and unidentified polar smectic (SmX). Black dashed lines were drawn arbitrarily in order to visually differentiate between the respective phases' stability regimes.

- (1) V. Borshch et al. Nat. Commun. 4 (2013), 2635.
- (2) D. Chen et al. Proc. Natl. Acad. Sci. U. S. A. 110 (2013), 15931.
- (3) C. Meyer et al. Sci. Adv. 6 (2020), eabb8212.
- (4) C. Fernandez-Rico et al. Science 369 (2020), 950.
- (5) N. Sebastián et al. arXiv: 2205.00193 [cond-mat.soft] (2022).
- (6) A. Jakli et al. Phys. Rev. X 90 (2018), 045004.
- (7) C. Greco, A. Ferrarini. Phys. Rev. Lett. 115 (2015), 147801.
- (8) M. Chiappini, M. Dijkstra. Nat. Commun. 12 (2021), 2157.
- (9) P. Kubala et al. arXiv: 2112.14607 [cond-mat.soft] (2021).

Prussian blue type nano-objects: new opportunities for old materials

J. Larionova, Y. Guari, S. Sene, G. Félix, J. Long

Institute Charles Gerhardt Montpellier (ICGM), CNRS/University of Montpellier/ENSCM, Montpellier, France

email: joulia.larionova@umontpellier.fr

Prussian blue type nanoparticles are exciting nano-objects that combine the advantages of molecule-based materials and nanochemistry (see Figure below). They are made by transition metal ions or lanthanides assembled through cyano-bridged ligand into nano-sized architectures of the general formula $A_xM_y[M'(CN)_6]_z$ (where A is a monovalent cation, M and M' are bivalent or trivalent transition metal ions or lanthanides). These nano-objects attracted a great deal of interest during the last ten years due to their specific molecule-based nature that is different compared to other inorganic nanoparticles and which brings to them many advantages presented in Fig. 1. This lecture will provide a brief critical look on the recent advancement in this field of research focusing on the design of multifunctional Prussian blue type nano-objects and their nanocomposites promising as nanoprobes for imaging, as therapeutic agents for photothermal therapy or as nanomedicine for theragnostic.⁽¹⁻⁷⁾ A focus is also done on the synthesis of multifunctional nanoheterostructures containing Prussian blue as one of components.^(3,5)

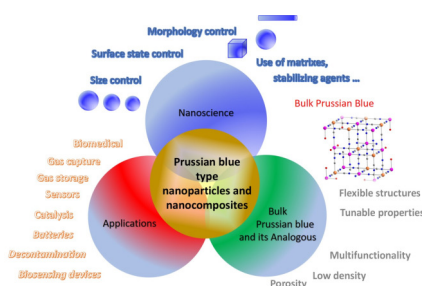


Figure 1. Advantages of Prussian blue nanoparticles situated at the cross-section between bulk molecule-based materials and nanoscience as well as their main applications.

- (1) Y. Guari, J. Larionova, Prussian Blue-Type Nanoparticles and Nanocomposites: Synthesis, Devices, and Applications. Ed. Jenny Stanford Publishing (2019), ISBN 9789814800051.
- (2) J. Long et al. Dalton Trans. 45 (2016), 17581.
- (3) G. Maurin-Pasturel et al. Angew. Chem. 53 (2014), 3872.
- (4) E. Mamontova et al. Nanoscale 11 (2019), 7097.
- (5) E. Mamontova et al. Inorg. Chem. Front. 8 (2021), 2248.
- (6) E. Mamontova et al. Inorg. Chem. 59 (2020), 4567.
- (7) M. Cahu et al. J. Mat. Chem. B 9 (2021), 9670.

Scattering from magnetic monopoles and antiferromagnetic domain manipulation in a frustrated pyrochlore iridate

M. J. Pearce,^{1,2} K. Götze,^{1,3} A. Szabó,^{2,4,5} T. S. Sikkenk,^{4,6} M. R. Lees,¹
A. T. Boothroyd,² D. Prabhakaran,² C. Castelnovo,⁴, P. A. Goddard¹

¹Department of Physics, University of Warwick, Coventry, UK

²Department of Physics, University of Oxford, Clarendon Laboratory, Oxford, UK

³Deutsches Elektronen-Synchrotron (DESY), Hamburg, Germany

⁴TCM Group, Cavendish Laboratory, University of Cambridge, Cambridge, UK

⁵ISIS Facility, Rutherford Appleton Laboratory, Didcot, UK

⁶Institute for Theoretical Physics and Center for Extreme Matter and Emergent Phenomena, Utrecht University, Utrecht, The Netherlands

email: p.goddard@warwick.ac.uk

Magnetically frustrated systems provide fertile ground for complex behaviour, including unconventional ground states with emergent symmetries, topological properties, and exotic excitations. A canonical example is the emergence of magnetic-charge-carrying quasiparticles in spin-ice compounds.⁽¹⁻³⁾

Despite extensive work, a reliable experimental indicator of the density of these magnetic monopoles is yet to be found. Using measurements on single crystals of $\text{Ho}_2\text{Ir}_2\text{O}_7$ combined with dipolar Monte Carlo simulations, we show that the isothermal magnetoresistance is highly sensitive to the monopole density. Moreover, we uncover an unexpected and strong coupling between the monopoles on the holmium sublattice and the antiferromagnetically ordered domains of iridium ions.⁽⁴⁾

These results pave the way towards a quantitative experimental measure of monopole density and demonstrate the ability to control antiferromagnetic domain walls using a uniform external magnetic field, a key goal in the design of next-generation spintronic devices.

Acknowledgments: This project has received funding from the European Research Council (ERC) under the European Union's Horizon 2020 research and innovation program (Grant Agreement No. 681260). We acknowledge support from the Engineering and Physical Sciences Research Council (EPSRC) under the following grant numbers: EP/N509796/1, EP/P034616/1, EP/M007065/1, EP/T028580/1, EP/N034872/1 and EP/J017124/.

⁽¹⁾ M. J. Harris et al. Phys. Rev. Lett. 79 (1997), 2554.

⁽²⁾ S. T. Bramwell et al. Science 294 (2001), 1495.

⁽³⁾ C. Castelnovo et al. Nature 451 (2008), 42.

⁽⁴⁾ M. J. Pearce et al. Nat. Commun. 13 (2022), 444.

Porous Ti/TiO_x/Fe magnetic junction and its magnetotransport properties

A. Zarzycki, J. Chojenka, M. Perzanowski, M. Marszałek

Institute of Nuclear Physics Polish Academy of Sciences, Krakow, Poland

email: arkadiusz.zarzycki@ifj.edu.pl

Junctions based on metal oxides show considerable attention resulting from their interesting electrical, optical or magnetic properties. Here we present the magnetic, electrical and magnetotransport properties of the Ti/TiO_x/Fe thin film magnetic junction. The studies were performed in a temperature range of 5 – 300 K, and magnetic fields between -50 kOe and +50 kOe. The obtained results were compared with morphological and structural properties.

The Ti/TiO_x/Fe junction was prepared in a few steps. First, a thin Ti layer was deposited on Si substrate. Next, a top part of the titanium layer was oxidized with an anodization process. Finally, the oxide layer was covered with a 50 nm thick iron layer. The as-prepared junction was heated to 750 K.

Magnetic studies showed ferromagnetic properties of the junction with a strong in-plane magnetic anisotropy. Detailed analysis revealed the presence of two magnetic phases: one corresponding to the iron layer and the other assigned to a small amount of iron oxide formed at the TiO_x/Fe interface. The strong diffusion and atomic mixing at the top TiO_x/Fe interface were confirmed with XRD and depth profile analyses.

The electrical transport properties showed strong non-linear and temperature dependent current-voltage characteristics. Schottky diode behaviour was observed for both Ti/TiO_x and TiO_x/Fe interfaces. The most intriguing observation was found for Ti/TiO_x barrier where an ohmic dependence at room temperature changed into Schottky diode characteristics below 250 K. The change of the transport properties around 250 K was also found in the resistance vs. temperature measurements as a small increase in resistance. Additionally, at 25 K a transition to the insulating state was found. Because of the nonlinear I - V characteristics, the $R(T)$ dependence showed sensitivity to voltage magnitude, voltage bias, and to the magnetic field. The magnetoresistance for all studied temperatures showed positive values of a few percent while being responsive to the applied voltage, its magnitude and polarization. This unusual magnetoresistance behaviour gives possibilities to tune magnetotransport properties.

This work was partially supported by the Polish National Science Centre with a grant 2015/19/D/ST3/01843.

Search for dependency between Verwey and Curie temperatures in magnetite monocrystals doped with Mn, Zn, Al and Ti

M. A. Gala,¹ K. Podgórska,¹ A. Kozłowski,¹ W. Tabiś,^{1,2}

¹AGH University of Science and Technology, Faculty of Physics and Applied Computer Science, Kraków, Poland

²Institute of Solid State Physics, TU Wien, Vienna, Austria

Magnetite ($\text{Fe}^{\text{II}}\text{Fe}^{\text{III}}_2\text{O}_4$, usually Fe_3O_4) is a natural magnetic mineral, well-known for centuries since it was used by sailors for geo-localization. It is ferrimagnetic at ambient conditions and can be found both as a mineral in inanimate and in animate nature, e.g., in teeth of invertebrates, chitons. Also, some birds accumulate magnetite crystallites in their beaks and as a part of their neural system, thus obtaining natural global positioning. Due to its chemical simplicity (just two elements: oxygen and iron) and abundant spectacular properties, magnetite started to play a role as a test ground for new experimental and theoretical approaches. Nevertheless, many properties of magnetite are still not fully understood, e.g., a link between the metal-insulator phase transition at $T_V \approx 125$ K (so called Verwey transition, VT)⁽¹⁾ and magnetic ordering temperature $T_C \approx 858$ K.

According to the Verwey model, tetrahedral A positions in the high- T spinel cubic lattice are occupied by Fe^{3+} ions while the octahedral B iron cations have a mean valence of 2.5+, what may be interpreted as one electron oscillating between the B sites. At T below T_V , the structure changes to monoclinic Cc , with this electron stabilizing on several B sites that form cigarlike structures, dubbed trimerons, with Fe^{2+} and Fe^{3+} ions of fractional valences.^(2,3) Since the same 3d Fe electrons are engaged in VT and convey magnetic interactions, a change of magnetic properties was expected, but only a 0.1% change of magnetization, yet 2 orders of magnitude rise of magnetic anisotropy were found. The problem of linking the VT and Curie point is now coming back due to recent studies. It was first shown⁽⁴⁾ that within the first unit cell substantial local structural distortions exist, other than those typical for $Fd-3m$ cubic, and these distortions persist up to T_C , matching T dependence of magnetization. It was suggested⁽⁴⁾ that structural and electronic fluctuations responsible for the Verwey transition and magnetic order are coupled and that VT is a direct result of the long-range magnetic order. Other studies, however, showed that lattice dynamics in magnetite is very well described by DFT⁽⁵⁾, but mainly in Cc phase which suggested that trimeron-phonon coupling is extended above T_V . Finally, core-level X-ray spectroscopy and electrical conductivity measurements combined with theory,⁽⁶⁾ showed charge reordering at the B sublattice, starting from 330 K, and terminating at T_C (see also Fig. 1).

All these results seek for further T_C vs. T_V correlation studies and our preliminary results for magnetite's properties investigated at both low and high temperatures and concerned with this issue will be presented in my talk. I will compare resistivity and magnetic moment data with AC susceptibility results both around T_V and T_C trying to prove correlation between them plausibly exists.

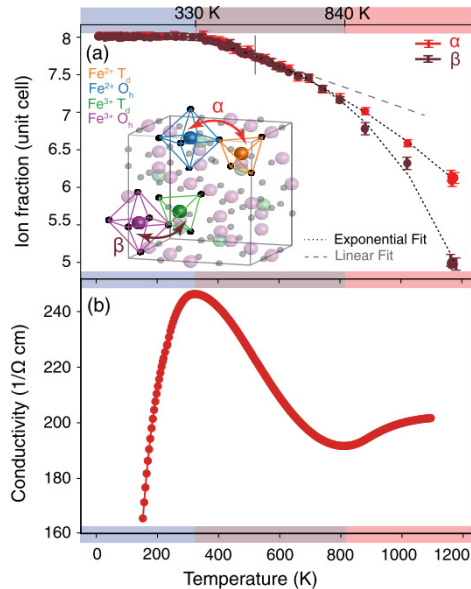


Figure 1. The charge redistribution between A and B Fe atoms (a) in stoichiometric magnetite is reflected in its electrical conductivity measurement (b) as a function of temperature.

- (1) E. J. W. Verwey. *Nature* 144 (1939), 327.
- (2) M. S. Senn et. al. *Nature* 481 (2012), 173.
- (3) R. Řezníček et al. *Phys. Rev. B* 91 (2015), 125134.
- (4) G. Perversi et al. *Nat. Comm.* 10 (2019), 2857.
- (5) P. Piekarz et al. *Phys. Rev. B* 103 (2021), 104303.
- (6) H. Elnaggar et al. *Phys. Rev. Lett.* 127(18) (2021), 186402.

Evolution of the Hall-coefficient, dc-resistivity and Fermi-surface in cuprates

B. Klebel-Knobloch,¹ W. Tabiś,^{1,2} O. S. Barišić,³ N. Barišić^{1,4}

¹TU Wien, Vienna, Austria

²AGH University of Science and Technology, Krakow, Poland

³Institute of Physics, Zagreb, Croatia

⁴University of Zagreb, Zagreb, Croatia

email: benjamin.klebel@tuwien.ac.at

Cuprates exhibit a number of unusual properties, including the highest superconducting transition temperatures at ambient pressures known today. Despite tremendous research efforts, there is no consensus regarding the understanding of these compounds, except in two limits: at zero doping (parent compounds) and in the highly overdoped regime. The parent compounds are charge-transfer insulators, while at high doping levels they behave as a Fermi liquid with itinerant carriers.

Only recently it has been revealed that the itinerant charges preserve their Fermi-liquid nature across the phase diagram, without a change of the scattering rate and effective mass.⁽¹⁾ Consequently, the complexity of cuprates is due to a gradual (de)localization of exactly one hole per CuO_2 unit.^(1,2) Such an evolution implies the opening of a partial gap at the Fermi surface, not its reconstruction.

Here we show that the transport coefficients correspond to the ungapped parts of the Fermi surface, which are directly observed by photoemission spectroscopy. We use tight-binding parametrisations of measured ARPES spectra of $\text{HgBa}_2\text{CuO}_{4+\delta}$,^(3,4) $\text{Tl}_2\text{Ba}_2\text{CuO}_{6+\delta}$ ^(5,6) and $\text{La}_{2-x}\text{Sr}_x\text{CuO}_4$ ⁽⁷⁾ (LSCO) to calculate the Hall-coefficient and dc-resistivity, where we consider only those parts of the Fermi surface which are not gapped. We find an excellent agreement between our model and measured values. This is particularly interesting in the case of LSCO which exhibits a complex evolution of the Fermi surface topology. Namely, LSCO undergoes a Lifshitz transition thereby strongly altering the Hall-response, an effect which is fully captured by our approach.

Acknowledgments: The work at TU Wien was supported by the European Research Council (ERC Consolidator Grant No. 725521). NB acknowledges the support of project CeNIKS (Grant No. KK.01.1.1.02.0013) and Croatian-Swiss Research Program (project No. IZHRZ0_180652), while OSB acknowledges the support of the QuantiXLie Center of Excellence (Grant KK.01.1.1.01.0004).

- (1) N. Barišić et al. *New J. Phys.* 21 (2019), 113007.
- (2) D. Pelc et al. *Sci. Adv.* 5 (2019), eaau4538.
- (3) T. Das. *Phys. Rev. B* 86 (2012), 054518.
- (4) I. Vishik et al. *Phys. Rev. B* 89 (2014), 195141.
- (5) M. Platé et al. *Phys. Rev. Lett.* 95 (2005), 077001.
- (6) D. C. Peets, et al. *New J. Phys.* 2 (2007), 28.
- (7) T. Yoshida et al. *J. Phys.: Condens. Matter* 19 (2007), 125209.

Liquid crystals: smart molecular systems

E. Chrzumnicka,¹ J. Stachera,¹ T. Martyński,¹ J. Myśliwiec,²
A. Szukalska²

¹Faculty of Materials Engineering and Technical Physics, Poznan University of Technology, Poznan, Poland

²Faculty of Chemistry, Wroclaw University of Science and Technology, Wroclaw, Poland

email: ewa.chrzumnicka@put.poznan.pl

Liquid crystal (LC) is a intermediate phase of matter possessing both the mobility of liquids and the long-range molecular ordering of crystal. Due to the unique combination of properties, LC has been widely used to create Smart Materials also known Functional Materials, that optically report information about their environment, such as changes in electric field (Smart-Phone Displays), temperature (Medical Thermography). Research in many scientific centers seeks to understand how the unique characteristics of LC mediate intermolecular/interparticle/interfacial phenomena and leverage the knowledge to design New Class of Smart Materials that will enable applications in a variety of fields (modern photonics and nanotechnology). Most liquid crystalline materials commonly utilized in the industry are composed of rod-like molecules; however, banana or disc-shaped molecules are also known to form liquid crystalline phases. Due to the liquid-like behavior, LCs can be easily functionalized by the addition of dye molecules.⁽¹⁾ Thus, they can gain additional desired properties. Here are discussed how the LC phases can influence the design of laser devices⁽²⁾ and how use the liquid crystalline columnar phases to the study of electronic and magnetic phenomena in semiordered media.⁽³⁾

Acknowledgments: This work was supported by the research project of the Polish Ministry of Education and Science 0511/SBAD/2251.

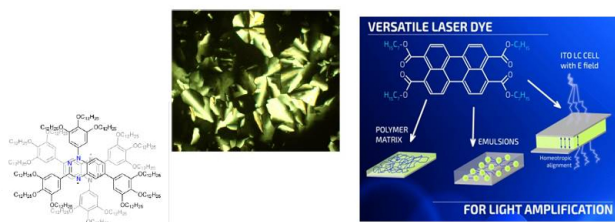


Figure 1. Optical textures of a Col_h phase obtained upon cooling in $4 \mu\text{m}$ cell and proposed molecular arrangement in the columnar phase for paramagnetic disc-like molecules (left)⁽³⁾; Perylene-Based Chromophore as a Versatile Dye for Light Amplification (right).⁽²⁾

- (1) E. Chrzumnicka et al. *Mol. Cryst .Liq. Cryst.* 1 (2011), 541.
- (2) A. Szukalska et al. *Materials* 15 (2022), 980.
- (3) M. Jasiński et al. *J. Am. Chem. Soc.* 138 (2016), 9421.

Multiple mechanisms for equilibrium recovery in glasses

D. Cangialosi^{1,2}

¹Centro de Física de Materiales (CFM/CSIC), San Sebastian, Spain

²Donostia International Physics Center (DIPC), San Sebastian, Spain

email: daniele.cangialosi@ehu.eus

Approach to equilibrium, so-called physical aging, in glasses is generally described as triggered the main α relaxation. As a result, the evolution of the thermodynamic state below but close to the glass transition temperature T_g , exhibits monotonous decay towards equilibrium. In this contribution, I will show that, once physical aging is carried out significantly below T_g and for prolonged time, glasses of different nature, including polymers, metallic glasses and low molecular weight glass formers, approach equilibrium via at least two steps.⁽¹⁾ The slower equilibration step exhibits large activation energy and, therefore, is associated to the α relaxation. In contrast, fast equilibration mechanisms, responsible for the initial steps of glass equilibration, are mildly activated and, therefore, their action survives way below T_g . Finally, I will show how fast equilibration mechanisms can be exploited in glasses with large amount of free interface to access energy states low enough to identify the transformation from standard to ideal glass,^(2,3) theorized long ago.

⁽¹⁾ D. Cangialosi et al. Phys. Rev. Lett. 111 (2013), 095701.

⁽²⁾ D. Cangialosi et al. Phys. Chem. Chem. Phys 19 (2017), 961.

⁽³⁾ X. Monnier et al. Phys. Rev. Lett. 126 (2021), 118004.

Insight into complex crystallization mechanisms of chiral smectogenic liquid crystal

A. Drzewicz,¹ M. Jasiurkowska-Delaporte,¹ E. Juszyńska-Gałązka,^{1,2}
A. Deptuch,¹ M. Gałązka,¹ W. Zajęc,¹ P.Kula³

¹Institute of Nuclear Physics Polish Academy of Sciences, Krakow,
Poland

²Osaka University, Osaka, Japan

³Military University of Technology, Warszawa, Poland

email: anna.drzewicz@ifj.edu.pl

A systematic study of liquid crystals exhibiting the chiral smectic phases with ferro- and antiferroelectric properties is still highly desired for the use in display technology. The in-depth understanding of the complex melt- and cold crystallization phenomena may be useful in the field of creating a new generation of liquid crystal displays, where glass-forming materials are more suitable as components of usable mixtures than easily crystallizing compounds. In this work we report the phase situation and the kinetics of cold crystallization process of the 3F5HPhH7 compound under isothermal and non-isothermal conditions as well as the kinetics of isothermal melt crystallization, using complementary methods, e.g. differential scanning calorimetry (DSC), broadband dielectric spectroscopy (BDS) and Fourier transform infrared spectroscopy (FTIR). This compound belongs to a family of $3FmX_1PhX_2r$ compounds (where 3F is the C_3F_7- group, m is the number of methylene groups in the non-chiral terminal chain, $m=2-7$, X_1 and X_2 are hydrogen or fluorine atoms in the phenyl ring, and r is the length of alkyl chain connected with the asymmetric carbon atom, $r=4-9$). Besides two enantiotropic chiral smectic phases (SmC^* and SmC_A^*), the compound under study also forms the hexatic smectic SmX_A^* phase and two crystal phases (Cr1 and Cr2). The sample crystallizes upon slow cooling, while the SmX_A^* phase undergoes a glass transition during fast cooling.⁽¹⁾ Upon subsequent heating, cold crystallization is observed. In contrast to the compounds which are the subject of several papers,^(2,3) the 3F5HPhH7 liquid crystal exhibits isothermal cold crystallization as a two-route process, well described in terms of the modified Avrami model.⁽⁴⁾ The determined dependences of $\ln(\tau_{cr})$ vs. $10^{-3} T_{rc}^{-1}$ for both crystallization processes confirm that the cold crystallization depends primarily on diffusion rates, while the melt crystallization is limited by the formation of nuclei. The results obtained for isothermal cold- and melt crystallization kinetics studied by DSC, BDS and FTIR methods are consistent with each other.

Acknowledgments: Anna Drzewicz acknowledges the National Science Centre (Grant MINIATURA 5: UMO-2021/05/X/ST3/00888) for financial support.

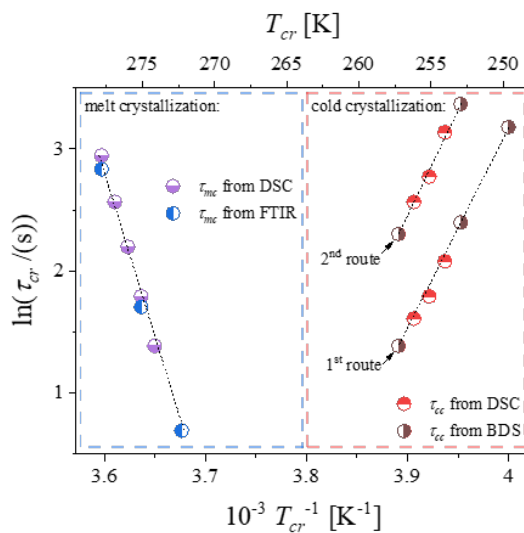


Figure 1. The temperature dependence of the relaxation times determined from the DSC, FTIR and BDS measurements for both crystallization processes of the 3F5HPhH7 compound.

- (1) A. Drzewicz et al. Phys. Chem. Chem. Phys. 24 (2022), 4595.
- (2) A. Drzewicz et al., Phys. Chem. Chem. Phys. 23 (2021), 8673.
- (3) A. Deptuch et al. Mater. Res. Bull. 150 (2022), 111756.
- (4) A. Drzewicz et al. CrystEngComm 24 (2022), 3074.

Influence of stereoregularity on the glass transition dynamics under high-pressure conditions and geometrical nanoconfinement

K. Chat,^{1,2} W. Tu,^{1,2} A. B. Unni,^{1,2} K. Adrjanowicz^{1,2}

¹Institute of Physics, University of Silesia, Chorzow, Poland

²Center for Education and Interdisciplinary Research (SMCEBI), Chorzow, Poland

email: kchat@us.edu.pl

Understanding how the molecular order influences the properties of soft matter in confined geometry can be essential to producing materials with desirable behavior and functions. Measurements under elevated pressure provide information on the sensitivity of the glass-transition dynamics to density changes, which can be helpful to better understand or even predict the confinement effect. In this talk, we would like to discuss the effects of high pressure and geometrical nanoconfinement on segmental dynamics of isotactic and syndiotactic PMMA. We have found that the segmental relaxation of the syndiotactic PMMA is less modified by compression compared to isotactic stereoisomers. Based on that, it can be predicted that the isotactic PMMA is more sensitive to density fluctuations induced by the geometrical nanoconfinement compared to the syndiotactic stereoisomer. The influence of tacticity on the segmental dynamics of isotactic and syndiotactic PMMA thin films was also investigated. Apart from the differences in sensitivity to density/pressure changes, stereoregularity also affects the interactions of the polymer with the substrate seen in the amount of irreversibly adsorbed chains.

Influence of nanoclusters concentration on low-temperature properties of As-S system

P. Baloh,¹ V. Tkáč,¹ M. Orendáč,¹ A. Orendáčová,¹ E. Gažo,²
R. Holomb,^{3,4} V. Mitsa,³ A. Feher¹

¹P. J. Šafárik University in Košice, Košice, Slovakia

²Institute of Experimental Physics, SAS, Košice, Slovakia

³Uzhhorod National University, Uzhhorod, Ukraine

⁴Wigner Research Centre for Physics, Budapest, Hungary

email: pavlo.baloh@student.upjs.sk

Low-temperature (LT) properties of amorphous materials have been under research for over 50 years.⁽¹⁾ Numerous works indicate behavior that differs from the single crystals. Unexpected properties in reduced specific heat (C_p/T^3) and thermal conductivity ($k(T)$) are known as universal and "anomalous" at LT (<50 K). The specific heat in this temperature range reveals a broad maximum commonly accepted as the Boson peak (BP) (Fig. a). At the same time, thermal conductivity is characterized by a sequence of $k(T)$ temperature dependencies. In the case of As₂S₃ (Fig. b), the $k(T)$ starts with a quadratic ($k(T) \propto T^2$) dependence at the lowest temperatures (<5 K), followed by the constant dependence (plateau region 5 – 15 K), which continues into a linear temperature dependence.

Both properties could be analyzed within the Soft-Potential Model (SPM).⁽²⁾ The model theoretically describes the temperature area below BP and an onset of the plateau (<5 K), which helps in the determination of the essential characteristic parameters. In addition, by combining the SPM with the recent nanocluster approximation,⁽³⁾ we applied a more detailed approach to analyzing the LT properties of disordered solids. It is possible to estimate the contribution from the individual nanoclusters to the $k(T)$ based on the information about various types of nanoclusters located in the As-S system obtained from the DFT calculations and Raman spectroscopy. It is achieved by theoretically calculating the SPM parameters from the macroscopic parameters of the nanoclusters of As₂S₃.

Our study was performed on binary chalcogenide glasses of As_xS_{100-x} composition with $x=20, 28.6, 40, 45$ and 50 . The system revealed a tendency to vanish the plateau region in $k(T)$ with the increasing concentration of arsenic (see As₄₅S₅₅ in Fig. b). We correlate this behavior to the decreasing concentration of S₈ ring nanoclusters. Our analysis reveals the importance of knowledge of the microstructure of glasses to determine the LT properties of $k(T)$.

Acknowledgments: This work was supported by the Slovak Research and Development Agency Projects numbers APVV-18-0197 and APVV-SK-BY-RD-19-0008.

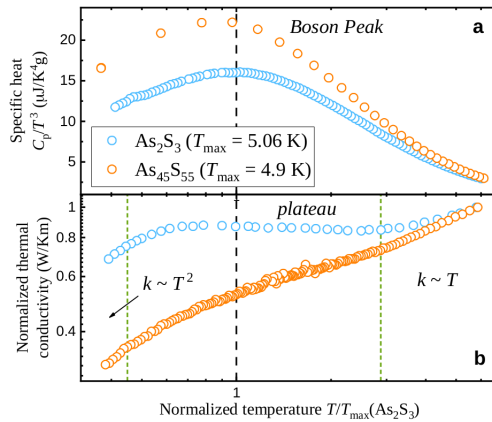


Figure 1. Temperature dependence of (a) reduced specific heat and (b) thermal conductivity of As_2S_3 (blue circles) and $\text{As}_{45}\text{S}_{55}$ (orange circles) between 2 – 30 K.

- (1) R. C. Zeller, R. O. Pohl, Phys. Rev. B 4 (1971), 2029.
- (2) M. A. Ramos, U. Buchenau, Phys. Rev. B 55 (1997), 5749.
- (3) R. Holomb, et al. Appl. Nanosci. 9 (2019), 975.

The state of water adsorbed on a MOF: an NMR study

S. Pizzanelli,¹ F. Martini,² L. Calucci,¹ L. G. Gordeeva,³ A. Freni,¹
S. Monti,¹ G. Barcaro,¹ C. Forte¹

¹CNR-ICCOM, Institute of Chemistry of OrganoMetallic Compounds,
Pisa, Italy

²University of Pisa, Chemistry Department, Pisa, Italy

³Boreskov Institute of Catalysis, Novosibirsk, Russia

⁴CNR-IPCF, Institute for Chemical and Physical Processes, Pisa, Italy

email: silvia.pizzanelli@pi.iccom.cnr.it

Metal Organic Frameworks (MOFs) are attractive materials because of their high potential for applications in diverse fields, such as gas separation and storage, energy storage, catalysis, pollutant adsorption, and thermal energy conversion. Distinctive features of these versatile materials are an extraordinarily large porosity and surface area, and unique adsorption properties.

Recently, use of Cr-MIL-101 for freshwater production in coastal areas by adsorption of moisture from the atmosphere was proposed.⁽¹⁾ Water is involved in many of the applications using Cr-MIL-101, but an understanding of its adsorption at a molecular level is still lacking. In this MOF, the inorganic building unit consists of a Cr₃O cluster, where two out of three Cr³⁺ ions exhibit an accessible coordinatively unsaturated site (CUS) (Fig. 1).⁽²⁾ Previous studies suggest that the formation of coordinative bonds between the CUS and water is responsible for the observed strong adsorption affinity.⁽³⁾

In this study, we investigated Cr-MIL-101 at different hydration levels and temperatures using solid state Nuclear Magnetic Resonance, and in particular ¹H Magic Angle Spinning, and Fast Field Cycling relaxometry to gain insight into the (i) water binding sites; (ii) distribution of water in the porous structure vs. hydration level; (iii) confined water dynamics; (iv) exchangeability of water bound to CUS with free water.

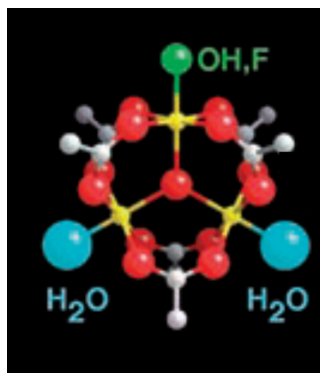


Figure 1. A chromium trimer in MIL-101, where water molecules bound to Cr^{3+} CUS sites are depicted. Chromium atoms yellow, carbon atoms pale gray, oxygen atoms red.

- (1) H. Zhao et al. *Microporous Mesoporous Mater.* 297 (2020), 110044.
- (2) Y. K. Hwang et al. *Angew. Chem., Int. Ed. Engl.* 47 (2008), 4144.
- (3) T. Wittmann et al. *J. Am. Chem. Soc.* 140 (2018), 2135.

Lead Halide Perovskites for energy applications: structural complexity and dynamics revealed by solid state NMR

E. Carignani,^{1,2} N. Landi,³ S. Borsacchi,^{1,2} L. Calucci,^{1,2} M. Geppi^{2,3}

¹Institute for the Chemistry of OrganoMetallic Compounds, National Research Council, CNR-ICCOM, Pisa, Italy

²Center for Instrument Sharing, University of Pisa (CISUP), Pisa, Italy

³Department of Chemistry and Industrial Chemistry, University of Pisa, Pisa, Italy

email: elisa.carignani@pi.iccom.cnr.it

Lead Halide Perovskites (LHPs), of general formula $APbX_3$ ($A=MA^+$, FA^+ , Cs^+ ; $X = I, Br, Cl$), have emerged as very promising classes of materials for applications in optoelectronic devices, such as solar cells, LEDs and lasers. The impressive interest aroused by LHPs is due to their remarkable optoelectronic properties (large absorption coefficients over the visible spectrum, long charge carrier diffusion lengths), with easy preparation, abundant constituent elements and broad compositional tunability.⁽¹⁾ Among the successful approaches devised to improve performances and stability of LHPs, the mixing of different cations and/or different halides gave very interesting results: mixed ion perovskites showed higher Power Conversion Efficiency (PCE) in solar cells, and higher moisture stability with respect to pure perovskites. Another strategy to improve the moisture stability consists in the use of 2D Ruddlesden-Popper (RP) phases. These structures are prepared by adding a large organic mono ammonium cation, L^+ , the 3D structure of corner-sharing octahedra (ABX_3) is disrupted and a structure with a bilayer of spacer cations between metal halide sheets is formed ($L_2A_{n-1}B_nX_{3n+1}$). 2D perovskites are more stable with respect to their 3D analogues but are generally give lower PCE.

The structural characterization and atomic-scale understanding of these materials is often challenging and the investigation of structure-properties relationship requires the combination of different methods. In these perspectives, Solid-State Nuclear Magnetic Resonance (SSNMR) stands out as characterization technique for LHPs for its ability to study ion dynamics, compositional variations and ion incorporation, chemical interactions, and degradation mechanisms.⁽²⁾

In this work, the potentialities of SSNMR are presented and discussed through the application to a multiple-cation lead mixed-halide perovskite $Cs_{0.05}FA_{0.81}MA_{0.14}PbI_{2.55}Br_{0.45}$, and 2D Ruddlesden-Popper (RP) phases containing ButylAmmonium as spacer ($BA_2MA_{n-1}Pb_nI_{3n+1}$ with $n=1-4$, Fig. 1). In these two cases ^{207}Pb , 1H , and ^{13}C SSNMR, both under Magic Angle Spinning and static conditions were applied. Some structural and dynamic features of these systems have been compared with those of 3D pure $MAPbI_3$ and discussed in relation to very recent literature.⁽³⁾

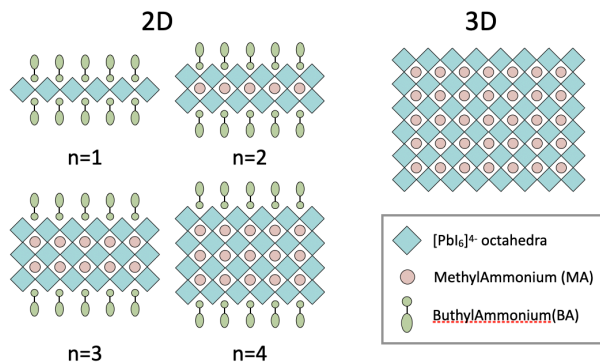


Figure 1. Schematic structure of 2D RP perovskites $\text{BA}_2\text{MA}_{n-1}\text{Pb}_n\text{I}_{3n+1}$ for $n=1-4$, and of the corresponding 3D perovskites MAPbI.

- (1) J. Y. Kim et al. *Chem. Rev.* 120 (2020), 7867.
- (2) W. M. J. Franssen, A. P. M. Kentgens, *Solid State Nucl. Magn. Reson.*, 100 (2019) 36 – 44; L. Piveteau et al. *J. Am. Chem. Soc.* 142 (2020), 19413 – 19437; D. J. Kubicki et al. *Nat Rev Chem* 5 (2021), 624 – 645.
- (3) J. Lee et al. *Chem. Mater.* 33 (2021), 370 – 377; M. A. A. Kazemi et al. *Energy Environ. Mater* (2022) DOI: 10.1002/eem2.12335.

Nanovolumes of soybean oil-based biopolymer matrices to the construction of biosensors for trace water pollutants

M. Goździuk,¹ B. Zgardzińska,¹ T. Kavetsky^{2,3}

¹Institute of Physics, Maria Curie-Skłodowska University, Lublin, Poland

²Drohobych Ivan Franko State Pedagogical University, Drohobych, Ukraine

³The John Paul II Catholic University of Lublin, Lublin, Poland

email: magdalena.gozdziuk@poczta.umcs.lublin.pl

The nanostructure of biopolymers matrices based on soybean oil to production of biosensors of trace pollutants was investigated using Positron Annihilation Lifetime Spectroscopy (PALS). The polymer matrices consist the following substances in various molar ratios: acrylated epoxidized soybean oil (AESO) as a base substance and additives: vanillin diacrylate (VDA) or vanillin dimethacrylate (VDM), which contains two methyl groups more than VDA. Some of the samples additionally contained triarylsulfonium hexafluorophosphate (PI).⁽¹⁾

Thermal studies were conducted in a wide range of temperature (120 K – 320 K) to determine the phase transitions in samples. The effect of the additive (VDM or VDA) and the molar ratio of the substance on the structure of biopolymer matrices at the nanoscale level was investigated.

The Tao-Eldrup model^(2,3) was used to calculate the sizes of free nanovolumes in the matrices. It has been shown that the chemical composition of the matrix has a crucial influence on the created nanostructure, which in turn determines the detection parameters of biosensors.⁽⁴⁾

Measurements of sorption/desorption process with the use of distilled water, NaCl solution and polluted water from a water reservoir allowed to investigate the sorption properties of the matrices in a liquid environment.⁽⁴⁻⁶⁾ Time constants for the sorption/desorption processes of distilled water, saline solution and polluted water into the matrix were estimated. The interaction of positrons with ions contained in the above liquids was found. Samples with the best sorption parameters were selected to further investigation. The analyzes make it possible to forecast the mechanism of the detection process in real working conditions of biosensors.

⁽¹⁾ M. Lebedevaite, J. Ostrauskaite. *Ind. Crops and Prod.* 161 (2021), 113210.

⁽²⁾ D. Lightbody et al. *Chem. Phys. Lett.* 70(3) (1980), 487.

⁽³⁾ M. Eldrup et al. *Chem. Phys.* 63(1-2) (1981), 51.

⁽⁴⁾ M. Goździuk et al. *Acta Phys. Pol. A* 139(4) (2021), 432.

⁽⁵⁾ T. Kavetsky et al. *Eur. Polym. J.* 115 (2019), 391.

⁽⁶⁾ T. Kavetsky et al. *Acta Phys. Pol. A* 137(2) (2020), 246.

Influence of sulfur-curing conditions on the dynamics and crosslinking of rubber networks: a time-domain NMR study

F. Nardelli,¹ L. Calucci,^{2,3} E. Carignani,^{2,3} S. Borsacchi,^{2,3} M. Cettolin,⁴
M. Arimondi,⁴ L. Giannini,⁴ M. Geppi,^{1,3} F. Martini^{1,3}

¹Dipartimento di Chimica e Chimica Industriale, Università di Pisa, Pisa, Italy

²Istituto di Chimica dei Composti Organo Metallici, Consiglio Nazionale delle Ricerche, Pisa, Italy

³Centro per l'Integrazione della Strumentazione Scientifica dell'Università di Pisa (CISUP), Pisa, Italy

⁴Pirelli Tyre SpA, Milano, Italy

email: francesca.nardelli@dcci.unipi.it

Elastomers are polymeric materials extensively used for manufacturing a wide range of products for industrial applications, especially in the tire industry. These materials are obtained by vulcanization of one (or more) polydiene polymer(s) in the presence of sulfur and other additives (accelerators, activators, plasticizers, reinforcing fillers, etc.). During this process, chemical crosslinks are formed between the polymeric chains, which provide elasticity and durability to the final product. Furthermore, depending on the formulation and the vulcanization conditions, other mechanical properties required for industrial applications can be obtained. Importantly, such macroscopic properties are strongly related to the microscopic structure of the polymeric network.⁽¹⁾ Consequently, the investigation of microscopic and macroscopic properties giving access to information on the network structure in relation to the vulcanization conditions is fundamental for the optimization of processing and performance of elastomeric materials.

In this context, ¹H time-domain NMR (TD-NMR) represents a valuable tool to gain insights into the molecular dynamics of the polymeric chains. In fact, this technique allows to measure NMR observables (¹H T_1 and T_2 relaxation times and ¹H-¹H residual dipolar couplings (D_{res})), which depend on the modulation of ¹H-¹H dipolar couplings by segmental motions. These motions are quite fast in elastomers above glass transition temperature, but are anisotropic, resulting in residual ¹H-¹H dipolar interactions, which depend on the amount and distribution of topological constraints in the polymeric network.⁽²⁾

In this work, natural and isoprene rubbers vulcanized at different curing temperatures and different sulfur contents have been investigated by exploiting ¹H TD-NMR techniques, including ¹H multiple-quantum experiments for the measurements of D_{res} , Carr-Purcell-Meiboom-Gill pulse sequence for the evaluation of ¹H T_2 relaxation times, and field cycling NMR relaxometry for the measurements of ¹H T_1 relaxation times on a wide range of Larmor frequencies (10 kHz – 35 MHz).

The NMR observables were compared with the crosslink density or macroscopic properties of the material that depend on this quantity, obtained using routinely employed methods in industrial analyses, allowing to gain insight into the effects of the formulation and the vulcanization conditions on the structure and dynamics of the polymeric networks.⁽³⁾

Acknowledgments: The authors would like to acknowledge CISUP (Center for Instrument Sharing-University of Pisa) for the use of the Bruker Avance Neo 500 solid-state NMR spectrometer and the contribution of the COST Action CA15209 (Eurelax: European Network on NMR Relaxometry).

⁽¹⁾ S. P. O. Danielsen et al. *Chem. Rev.* 121 (2021), 5092.

⁽²⁾ K. Saalwächter. *Rubber Chem. Technol.* 85 (2012), 350.

⁽³⁾ F. Nardelli et al. *Polymers* 14 (2022), 767.

Water electrolysis for hydrogen production — focus on high-temperature steam electrolysis using solid oxide cells

A. Leon

European Institute for Energy Research (EIFER), Karlsruhe, Germany

email: aline.leon@eifer.org

The climate target settled worldwide for 2050 requires that our current energy system based on fossil fuels is gradually replaced by renewable energy.⁽¹⁾ In this frame, hydrogen is foreseen to play a key role for decarbonizing not only all sectors including power generation, industry, transports and buildings but also to store the excess solar and wind energy.⁽²⁾ Such a widespread implementation requires a deployment of related technologies in larger scale based on the peculiar properties of hydrogen.

Within the energy transition, hydrogen demand is estimated to increase by 10-fold.⁽²⁾ As such, multiple resources have to be envisaged based on carbon or without carbon like water. To split the water molecule into hydrogen and oxygen, different processes can be envisaged like electrolysis, thermolysis and photo-electrolysis. As concern water electrolysis, three technologies are available namely proton exchange membrane electrolysis (PEMEL), alkaline electrolysis (AEL) and high-temperature steam electrolysis (HTEL).⁽³⁾ Currently for the three technologies, one needs to decrease the cost by increasing the capacity (scaling-up to GW system), by industrializing the manufacturing process and by reducing the degradation rate below 1%/1000 h over long-term operation of the system. This presentation will focus on high-temperature steam electrolysis (HTEL) as it is an attractive technology whenever waste heat is available. The HTEL process is based on oxide ion conduction with ceramic based materials. The performance, durability and flexibility will be shown when scaling-up from single cell⁽⁴⁾ to short-stack (10 cells), stack (30 cells) and module (90 cells).⁽⁵⁾ Long-term operation of cell (above 20 000 hours) and stack (above 4500 hours) as well as ON/OFF switching profiles (above 10 000 cycles) will be shown and discussed in terms of degradation rate. It will be shown that tracing the source of degradation requires a multi modal approach with classical and advanced imaging, scattering and spectroscopy techniques down to nanoscale. As so, 2D nano X-ray fluorescence maps of the cells will be presented and how it helped to highlight the active as well as the detrimental layers to the electrochemical reaction.⁽⁶⁾ Finally, the combination of long-term operation data with in-situ impedance spectroscopy and complementary characterization techniques will be discussed to provide new insight to design and develop novel materials with long term stability.

- (1) <https://www.europarl.europa.eu/legislative-train/theme-a-european-green-deal>
- (2) <https://hydrogencouncil.com/wp-content/uploads/2017/11/Hydrogen-scaling-up-Hydrogen-Council.pdf>, November 2017.
- (3) A. Brisse et al. High temperature steam electrolysis in Hydrogen production by water electrolysis edited by T. Smolinka & J. Garche (2021), Chapter 7.
- (4) J. Schefold et al. International Journal of Hydrogen Energy 45 (2020), 5143.
- (5) A. Léon et al. J. Power Sources 510 (2021), 230346.
- (6) J. Villanova et al. J. Power Sources 421 (2019), 100.

Self-assembly in deep eutectic solvents: from surfactant aggregation to protein folding

A. Sanchez-Fernandez,^{1,2,4} K. J. Edler,³ A. J. Jackson^{4,5}

¹Centro Singular de Investigación en Química Biolóxica e Materiais Moleculares (CIQUS), Universidade de Santiago de Compostela, Santiago de Compostela, Spain

²Food Technology, Engineering and Nutrition, Lund University, Lund, Sweden

³Department of Chemistry, University of Bath, Bath, UK

⁴European Spallation Source, Lund, Sweden

⁵Department of Physical Chemistry, Lund University, Lund, Sweden

email: andrew.jackson@ess.eu

In recent years many studies into green solvents have been undertaken and deep eutectic solvents (DES) have emerged as environmentally friendly alternatives in many fields, such as separation processes, metal processing, biocatalysis and electrochemistry.⁽¹⁾ DES are solvents obtained through the complexation of organic compounds, where the interaction between the precursors promotes a depression in the melting point that allows the mixture to remain liquid at room temperature. Moreover, through different combinations of precursors the physicochemical properties of the solvent can be tuned for particular applications.

Research into DES has dramatically increased in volume and variety, especially in the last few years, as the advantages of DES in multiple processes becomes clear. Our recent studies have been focused on the ability of DES to sustain self-assembly of amphiphilic molecules. Such alternatives bring the possibility to develop new, sustainable alternatives for surfactant templating, drug delivery and preservation of bioactive molecules.

Here we will explore the behaviour of amphiphilic molecules of different complexity in DES: surfactants, phospholipids and proteins.^(2,3) Our results provide a novel approach for aggregate manipulation in the absence of water through specific and non-specific ion interactions.⁽⁴⁻⁷⁾ Small-angle neutron and X-ray scattering, in combination with other techniques, have been used to explore the bulk behaviour of these systems, showing that these preserve their activity in DES. Aiming to understand the fundamentals of amphiphile behaviour in these solvents, we will present details of self-assembly with varied physicochemical properties of the solvent, amphiphile characteristics and the effects of ion-ion interaction.

- (1) E. L. Smith et al. *Chem. Rev.* 114 (2014), 11060.
- (2) T. Arnold et al. *Langmuir* 31 (2015), 12894.
- (3) A. Sanchez-Fernandez et al. *Phys. Chem. Chem. Phys. B* (2017), 8667.
- (4) A. Sanchez-Fernandez et al. *Phys. Chem. Chem. Phys.* 18 (2016), 33240.
- (5) A. Sanchez-Fernandez et al. *Langmuir* 33 (2017), 14304.
- (6) A. Sanchez-Fernandez et al. *Journal of Colloid and Interface Science* 581 (2021), 292.
- (7) A. Sanchez-Fernandez et al. *JACS* 143 (2021), 14158.

Dependence of structural and optical properties on the type of phase structure in the luminescent $\text{BiVO}_4:\text{Tm}^{3+}$

K. Lenczewska, D. Szymański, D. Hreniak

Institute of Low Temperature and Structural Research, Polish Academy of Sciences, Wrocław, Poland

email: k.lenczewska@intibs.pl

The relation between structural properties two types of phase structure of $\text{BiVO}_4:\text{Tm}^{3+}$ and the synthesis parameters and also their optical properties, such as the energy gap and luminescent properties was investigated. Microwave-assisted hydrothermal method was used to synthesize single phase sub-microcrystalline $\text{BiVO}_4:\text{Tm}^{3+}$ powders with two polymorphic crystal structures — tetragonal zircon-type phase ($I4_1/amd$) or monoclinic fergusonite-type phase ($I2/b$).

A results of correlation between the type of phase structure and optical properties in $\text{BiVO}_4:\text{Tm}^{3+}$ are shown in Fig. 1. It was observed that the crystal structure and the decreasing the crystallites size changes the bandgap value for $\text{BiVO}_4:\text{Tm}^{3+}$. The observed significant red shift in the position of the absorption edge for the monoclinic fergusonite-type phase relative to the tetragonal zircon-type phase manifests itself in a different color of the samples, i.e. light yellow powder for the tetragonal phase and intense yellow for the monoclinic phase. The NIR luminescence of Tm^{3+} ions analyzed for both structural phases of the samples with the smallest crystallites sizes showed that the emission intensity is higher for the monoclinic phase than for the tetragonal phase.⁽¹⁾

Apart from that, the $\text{BiVO}_4:\text{Tm}^{3+}$ could have the potential use as a material to improve the performance of photovoltaic cells in order to increase their protection and lifetime due to the strong absorption of solar radiation in the UV-Vis range by the BiVO_4 host and for enhancement of effective optical conversion efficiency in hydrogenated amorphous and nano-crystalline silicon solar cells, which can effectively absorb the Tm^{3+} ions emission in the NIR range.

Acknowledgments: The work was created as a result of the research project No. 2018/31/N/ST5/01551 financed from the funds of the National Science Centre.

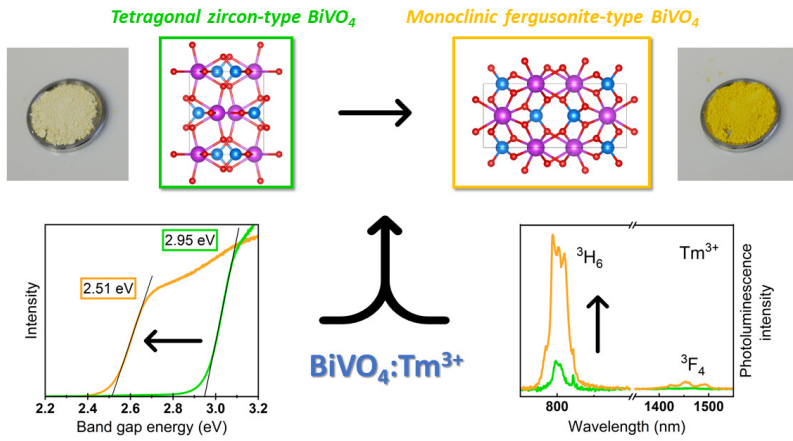


Figure 1.

⁽¹⁾ K. Lenczewska et al. Materials Research Bulletin (2022), in review.

Magnetization reversal mechanism in exchange-biased spring-like thin-film composite

M. Perzanowski, A. Zarzycki, J. Gregor-Pawlowski, M. Marszalek

Institute of Nuclear Physics Polish Academy of Sciences, Krakow, Poland

email: marcin.perzanowski@ifj.edu.pl

Development of modern spintronic devices requires materials exhibiting specific magnetic effect. One of them is exchange bias effect which is a phenomenon occurring at the interface between a ferromagnet (FM) and an antiferromagnet (AFM). It appears after cooling such a FM/AFM system in the external magnetic field below the Néel temperature of the AFM, giving rise to the magnetic hysteresis loop shift along the field axis. The possible technological application of the exchange bias effect has been studied in the context of its implementation in sensors, biomedicine, and magnetic read heads and spintronic devices.

In this work, we present studies on the cooling field influence on the magnetization reversal mechanism for the exchange biased system where the CoO antiferromagnetic layer is sandwiched between two [Co/Pd] ferromagnetic multilayers with different coercivities. The layered structure [Co/Pd_x]₇/CoO/[Co/Pd_y]₇ allowed us to combine two magnetic effects in one study — exchange bias and magnetic exchange spring, to find how they affect the reversal process. Such type of FM/AFM/FM composite that we study here is similar to the hard-soft exchange spring materials which can be applied in high density magnetic recording devices.

We find that the magnetization switching process and the magnitude and the sign of the exchange bias field are different depending on the magnetic state of both the ferromagnetic and the antiferromagnetic films induced by cooling the system in various external magnetic fields. The studies of the magnetic hysteresis loops obtained under different conditions are supported by the First Order Reversal Curve (FORC) measurements. The FORC investigations were carried out for both ascending and descending branches of the hysteresis loop which is especially significant for the exchange biased systems with bias loop shift from zero position.

Crystal structures and magnetic studies of two-types of Ni-W octacyanide bimetal assemblies

S. Akagi,¹ J. Wang,¹ K. Imoto,² S. Ohkoshi,² H. Tokoro¹

¹Department of Materials Science, Faculty of Pure and Applied Science, University of Tsukuba, Ibaraki, Japan

²Department of Chemistry, School of Science, The University of Tokyo, Tokyo, Japan

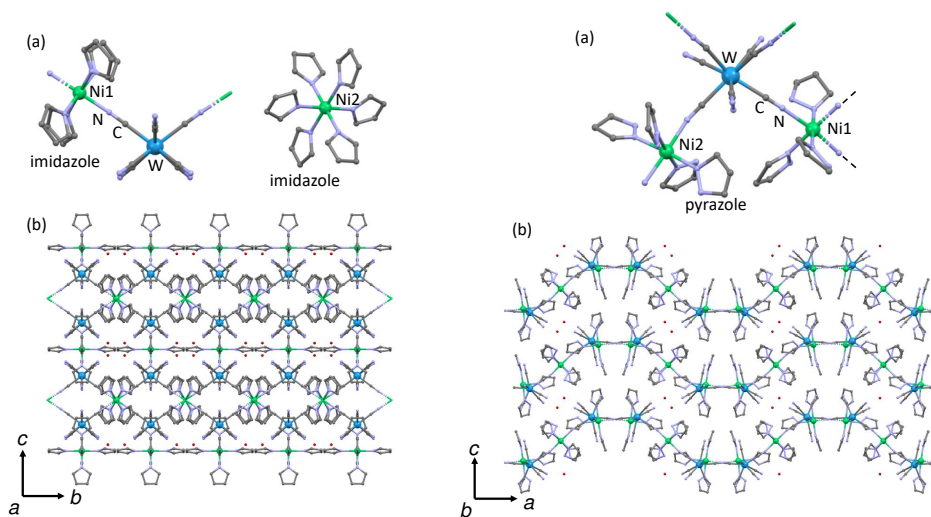
email: s2120313@s.tsukuba.ac.jp (S. Akagi),

tokoro@ims.tsukuba.ac.jp (H. Tokoro)

Introduction Cyano-bridged bimetal assemblies are particular molecule-based magnets that can exhibit various magnetic functionalities such as photomagnetism, magnetization-induced second harmonic generation phenomena, gas-sensitive magnetic properties and so on.⁽¹⁾ In this work, we synthesized cyano-bridged Ni-W bimetal assemblies, $[\text{Ni}^{\text{II}}(\text{imidazole})_6]\{[\text{Ni}^{\text{II}}(\text{imidazole})_4][\text{W}^{\text{V}}(\text{CN})_8]\}_2 \cdot 5\text{H}_2\text{O}$ (1) and $[\text{Ni}^{\text{II}}(\text{pyrazole})_4]\{[\text{Ni}^{\text{II}}(\text{pyrazole})_3][\text{W}^{\text{V}}(\text{CN})_8]\}_2 \cdot 2\text{H}_2\text{O}$ (2), where Ni and W are selected as magnetic centers. Their crystal structures and magnetic properties are reported.

Experiment Single crystals of 1 were prepared by slow diffusion of $\text{NiCl}_2 \cdot 6\text{H}_2\text{O}$ and imidazole aqueous solution into $\text{Cs}_3[\text{W}(\text{CN})_8] \cdot 2\text{H}_2\text{O}$ aqueous solution at room temperature for two weeks. Single crystals of 2 were prepared by mixing aqueous solution of $\text{NiCl}_2 \cdot 6\text{H}_2\text{O}$, $\text{Cs}_3[\text{W}(\text{CN})_8] \cdot 2\text{H}_2\text{O}$ and pyrazole at room temperature. Valence state were evaluated by IR spectrometer (JASCO FT/IR-4700). Crystal structures were determined by Single-crystal X-ray structural analysis (Rigaku R-axis rapid). Magnetic properties were measured by SQUID magnetometer (Quantum Design MPMS)

Results IR spectrum of 1 showed the CN stretching modes due to $\text{W}^{\text{V}}\text{-CN-Ni}^{\text{II}}$ at 2194, 2174, 2146, and 2134 cm^{-1} . Single crystal X-ray structural analysis indicated that 1 is monoclinic structure ($C2/m$). 1 consists of one-dimensional (1D) anionic $\{[\text{Ni}^{\text{II}}(\text{imidazole})_4][\text{W}^{\text{V}}(\text{CN})_8]\}$ — chains and isolated counter cations $[\text{Ni}^{\text{II}}(\text{imidazole})_6]^{2+}$ as shown Fig . Magnetic property of 1 showed a paramagnetic behavior with an antiferromagnetic interaction between $\text{W}^{\text{V}}(S=1/2)$ and $\text{Ni}^{\text{II}}(S=1)$. IR spectrum of 2 showed the CN stretching modes due to $\text{W}^{\text{V}}\text{-CN-Ni}^{\text{II}}$ at 2207, 2168, 2155, 2145, and 2127 cm^{-1} . Single crystal X-ray structural analysis indicated that 2 is orthorhombic structure ($Pbcn$). 2 consists of two-dimensional (2D) layered structure of cyano-bridged Ni-W framework. Magnetic properties of 2 exhibited spontaneous magnetization below 20 K and spin-flip transition at 300 Oe.



⁽¹⁾ S. Ohkoshi et al. Nat. Chem. 12 (2020), 338.

Kinetics of the thermal decomposition of thermally reduced graphene oxide (TRGO)

M. S. Barabashko,¹ R. M. Basnukaeva,¹ M. Drozd,² A. V. Dolbin,¹
N. A. Vinnikov¹

¹B. Verkin Institute for Low Temperature Physics and Engineering of the National Academy of Sciences of Ukraine, Kharkiv, Ukraine

²Institute for Low Temperatures and Structure Research Polish Academy of Sciences, Wrocław, Poland

email: msbarabashko@gmail.com

The thermal stability and the kinetics of thermal decomposition of the thermally reduced graphene oxide (TRGO) have been studied. Modified Hummers method was used for obtaining the initial graphite oxide (GO) from graphite powders.^(1,2) The thermal exfoliation of the graphene oxide powder has been performed in the vacuum conditions when heated with the temperature rate of 5 – 7 degrees per minute to a temperature of 300°C for obtain the TRGO. The samples of TRGO were treated by a pulsed high-frequency discharge in a hydrogen atmosphere before measurements. Pulsed high-frequency discharge in a hydrogen atmosphere of TRGO lead for partial graphene hydrogenation (chemical addition of atomic hydrogen) that leads to structural changes in the carbon planes and the formation of C-H sp³ bonds. The TGA measurements of TRGO samples for study the mass loss have been carried from room to 1000°C in a nitrogen atmosphere with a nitrogen flow and different heating rates. The Kissinger's multiple heating rate method has been used to determine activation energy for decomposing substances. Activation energies have been compared with the energies of the activation of thermal defunctionalization of multi-walled carbon nanotubes (MWCNTs).⁽³⁾ Obtained experimental results are useful for practical application of TRGO, such as hydrogen energy and high temperature sintering of new promising composite materials with its additives.

Acknowledgments: We are grateful for the possibilities cooperate in the frame of the platform "International Polish-Ukrainian Scientific Laboratory of Hydrogen Technologies" IPU-SciLabHT and National Research Foundation of Ukraine (Grant No.197/02.2020) for partial support of our investigations.

⁽¹⁾ A. V. Dolbin et al. *Low Temperature Physics* 46(3) (2020), 293.

⁽²⁾ A. V. Dolbin et al. *Appl. Surf. Sci.* 361 (2016), 213.

⁽³⁾ S. A. Chernyak et al. *J. Phys. Chem. C* 120 (2016), 17465 – 17474.

Kinetics of cold crystallization of the chiral fluorinated smectogenic 3F5HPhH6 compound

A. Deptuch,¹ M. Jasiurkowska-Delaporte,¹ W. Zając,¹
E. Juszyńska-Gałązka,^{1,2} A. Drzewicz,¹ M. Urbańska³

¹Institute of Nuclear Physics Polish Academy of Sciences, Kraków, Poland

²Research Center for Thermal and Entropic Science, Graduate School of Science, Osaka University, Osaka, Japan

³Institute of Chemistry, Military University of Technology, Warszawa, Poland

email: aleksandra.deptuch@ifj.edu.pl

Phase transitions of mesogenic (S)-4'-[1-(methylheptylcarbonyl)biphenyl-4-yl 4-[5-(2,2,3,3,4,4,4-heptafluorobutoxy)pentyl-1-oxy]-benzoate, denoted as 3F5HPhH6, are investigated by differential scanning calorimetry (DSC), polarizing optical microscopy (POM) and broadband dielectric spectroscopy (BDS). Analysis of dielectric data is supported by DFT calculations.⁽¹⁾ 3F5HPhH6 has two enantiotropic smectic phases: SmC^{*}, SmC_A^{*}, and one monotropic (formed only on cooling) hexatic smectic phase SmX_A^{*}, which is either SmF_A^{*} or SmI_A^{*}. Identification of smectic phases is based on observed collective relaxation processes: Goldstone mode in SmC^{*} and P_L and P_H phasons in SmC_A^{*}. The SmC_A^{*}→SmX_A^{*} transition on cooling is confirmed by appearance of the third phason P_{hex} at frequency between P_L and P_H.

During slow cooling (2 K/min), 3F5HPhH6 crystallizes in the Cr2 phase, which changes to the Cr1 phase on subsequent heating. Both Cr2 and Cr1 are conformationally disordered (CONDIS) phases, as a weak relaxation process is detected in them and interpreted as rotations of the benzene ring and neighbor -COO- group.

During fast cooling (5 – 20 K/min), vitrification of the SmX_A^{*} phase is observed. The temperature dependence of the relaxation time of the α -process in SmC_A^{*} and SmX_A^{*} phases, after fitting with Vogel-Fulcher-Tammann formula, gives the fragility parameter $m_f=89$, which classifies 3F5HPhH6 as an intermediately fragile glassformer. In the high-frequency tail of α -process, there is a weaker, secondary β -process with Arrhenius dependence of relaxation time. On subsequent heating of the SmX_A^{*} glass, the glass softening followed by cold crystallization to the Cr2 phase occur. The Cr2→Cr1 transition is further observed.

The kinetics of cold crystallization is investigated by DSC for heating rates of 1 – 20 K/min. Analysis by Kissinger and Augis-Bennett methods shows that the activation energy of cold crystallization is higher for slow heating (1 – 5 K/min) than for fast heating (8 – 20 K/min). By application of Ozawa model, it is obtained that cold crystallization kinetics is controlled mainly by diffusion rate below 273 K and to similar extent by nucleation and diffusion above 273 K.

The Ozawa exponent $n_O \approx 3$ indicates that the growth of crystallites is either 2- or 3-dimensional. By using the isothermal approximation, the coupling coefficient between the characteristic time of cold crystallization and relaxation time of α -process is determined to be $\xi = 0.71$, indicating that up to 277 – 278 K cold crystallization is controlled mainly by diffusion. It is slightly higher border temperature than obtained by Ozawa method.

Acknowledgments: This research was supported in part by the PLGrid Computational Infrastructure.

⁽¹⁾ A. Deptuch et al. *Phys. Chem. Chem. Phys.* 23 (2021), 19795.

Synthesis of lambda-type trititanium pentoxide using a block copolymer

A. F. Fadilla,¹ Y. Araki,¹ H. Tokoro,^{1,2} S. Ohkoshi²

¹Department of Material Science, Faculty of Pure and Applied Sciences, University of Tsukuba, Tsukuba, Japan

²Department of Chemistry, School of Science, University of Tokyo, Tokyo, Japan

email: s2126033@s.tsukuba.ac.jp

Phase transition materials are an interesting field of study because of their fundamental approach and wide applications such as optical memory, heat storage, and sensors. Titanium oxides with various polymorphs offer the phase transition phenomenon between a semiconducting phase and a metallic phase. Among them, it has been reported that the metallic phase lambda type Ti_3O_5 nanoparticles show a reversible phase transition with the beta type of the semiconductor phase by various external stimuli: light, heat, pressure, and electrical field.⁽¹⁾ This material is expected to be applied as a heat storage material due to its heat storage properties.⁽²⁾ Because of the promising application and wide opportunity for development, it is important to develop a new synthesis method of $\lambda\text{-Ti}_3\text{O}_5$. In this study, we develop a new synthesis method for $\lambda\text{-Ti}_3\text{O}_5$ nanocrystal using a block copolymer.⁽³⁾

Elemental measurement by the X-ray fluorescence (XRF) suggests the sample's element content ratio (Ti:O=37.4:62.6) is almost the same value as the theoretical calculation (Ti:O=37.5:62.5). Rietveld analysis result of X-ray powder diffraction (XRPD) pattern and crystal structure (Fig. 1(a)) shows that the obtained sample is a single-phase $\lambda\text{-Ti}_3\text{O}_5$ (monoclinic system, $C2/m$; $a=9.8376(4)$ Å, $b=3.78435(14)$ Å, $c=9.6964(4)$ Å, $\beta=91.2279(10)^\circ$). TEM and SEM observations show the 450 ± 130 nm particles as an aggregate of square nanocrystals (22 ± 8 nm) with a flake-like morphology (Fig. 1(b)). Examination result shows that the ratio of phase transition from lambda type to the beta type increases by the applied pressure with the pressure threshold was 300 Mpa. In addition, when the sample to which pressure was applied was heated, the phase transition from the beta type to the lambda type occurred, and a reversible phase transition due to pressure and heat could be confirmed.

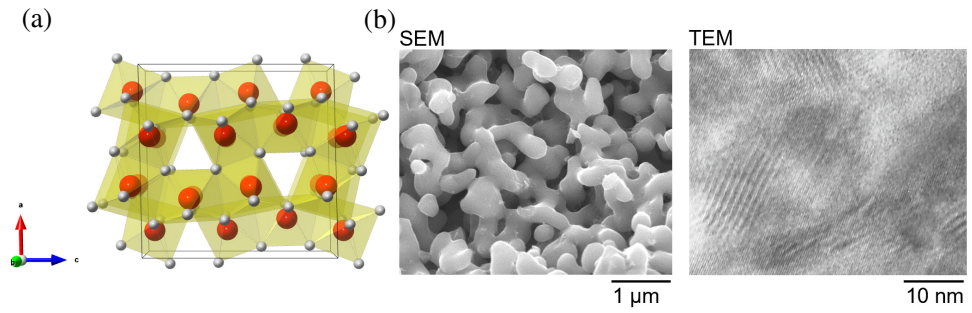


Figure 1. (a) Crystal structure, (b) SEM and TEM images of the sample.

- (1) S. Ohkoshi et al. *Nature Chem.* 2 (2010), 539.
- (2) H. Tokoro et al. *Nature Commun.* 6 (2015), 7037.
- (3) Y. Araki et al. *Mater. Today Energy.* 18 (2020), 100525.

Thermal conductivity of bulk and nanostructured materials in modern concepts framework

Y. V. Horbatenko, A. I. Krivchikov, O. O. Romantsova, O. A. Koroluyk

B. Verkin Institute for Low Temperature Physics and Engineering,
Kharkiv, Ukraine

email: horbatenko@ilt.kharkov.ua

Thermal conductivity investigation is an important area of condensed matter physics and material science: it stimulates the creation of new functional materials with specified properties. For ordered bulk crystals thermal conductivity curve $\kappa(T)$ shows a pronounced maximum, but for disordered crystals it's proportional to T^2 , after that it exhibits plateau which transforms to small growth of thermal conductivity when temperature increases.⁽¹⁾ Such behavior of $\kappa(T)$ also occurs in bulk and nanostructured materials, and also in complex materials, so called "superlattices".

Here we are presented procedure of analysis thermal conductivity data for different bulk (ordered) and nanostructured solids. It was shown our analysis provides universal analytical dependences to describe the thermal conductivity of any solid, so it confirms the assumption of unified theory of thermal transport that it can be describes as the sum of two contributions — particle-like propagation and wave-like tunneling according to unified theory of thermal transport.⁽²⁾

Acknowledgments: This work has received funding from the National Research Foundation of Ukraine (NRFU project No. 2020.02/0094).

⁽¹⁾ M. A. Ramos, U. Buchenau. Springer, Berlin, Heidelberg (1998), 527 – 569.

⁽²⁾ M. Simoncelli et al. Nature Physics 15 (2019), 809 – 813.

Multifunctional ordered mesoporous silica-based materials for nanotechnological applications

S. El Houbbadi, A. Fedorchuk, Ł. Laskowski

Institute of Nuclear Physics Polish Academy of Sciences, Krakow, Poland

email: sara.elhoubbadi@ifj.edu.pl, andrii.fedorchuk@ifj.edu.pl

Since its initial discovery, ordered mesoporous silica (OMS) has attracted the attention of various research groups that have begun to develop its synthesis, leading to several mesostructures. Among them, some of the most widely used are SBA-15, MCM-41, and KIT-6, which possess highly ordered and tailored mesoscale pores. OMS varieties differ from each other in specific surface area, pore structure, pore diameter, stability, synthesis medium, etc. Additionally, silica is biocompatible, non-toxic, and thermally and chemically stable.

Ordered mesoporous silica is of such great interest also because it can be functionalized by introducing various molecules into its mesostructure. After the functionalization of the silica surface, it can be treated as a deposited layer of a 2D solvent.⁽¹⁾ The surface of silica can be modified by functionalization in two different ways — by grafting or by co-condensation. Both methods provide a uniform dispersion of active functional units separated by passive functionalities, so-called spacers, on the silica surface. This approach gives a possibility to create surfaces with various concentrations of active functional units. Concisely this 2D-solid solvents concept is basically a material suitable to provide a feasible way to incorporate the desired functionalities (e.g. metal ions, molecules) by attaching them to the active groups on the silica surface.

The demand for supporting materials with versatile properties such as various pore structures, tuneable pore sizes, and large specific surface areas makes ordered mesoporous silica crucial in nanocomposites preparing processes. Silica mesostructure provides good mechanical properties and ensures space to introduce various molecules, which leads to the creation of new material in the form of nanocomposite that can exhibit unique properties not observed in separate components. Our research is devoted to use propyl-phosphonate or propyl-carboxylic groups functionalized SBA-15 and MCM-41 silica. The material with 2D hexagonal structure is prepared in the form of powder and thin films.

Since the thin film form is crucial from an applicative point of view, we prepare the materials using two methods to ensure two pore architectures (vertically and horizontally arranged mesopores). Silica nanocomposites containing active functional groups with attached metal ions such as copper or silver can find application in optoelectronics, catalysis, and also as bioactive coatings.^(2,3)

The materials prepared by our group were characterized by means of several methods such as XRD, TEM, SEM, EDS, isothermal sorption of nitrogen, and vibrational spectroscopy.

- (1) M. Laskowska et al. *International Journal of Molecular Sciences* 21 (2020), 8137.
- (2) M. Laskowska et al. *Naoscale* 9 (2017), 2123.
- (3) M. Laskowska et al. *Journal of Nanomaterials* (2017), 7698.

Mean squared displacement of molecules from lattice sites in the orientationally ordered phase of $^{15}\text{N}_2$

D. E. Hurova,¹ N. A. Aksenova,^{1,2} L. A. Alekseeva,¹ N. N. Galtsov¹

¹B. Verkin Institute for Low Temperature Physics and Engineering of NAS of Ukraine, Kharkiv, Ukraine

²Ukrainian State University of Railway Transport, Kharkiv, Ukraine

email: hurova@ilt.kharkov.ua

The last and most comprehensive review, in which the mean squared vibration amplitudes of various molecules are considered in detail, was published in 1968 by Sivin. In ref. (1), the characteristics of molecular vibrations are given, and both theoretical and experimental methods for their determination are considered in detail. Recently, the problem of correct processing of the molecular crystals structural data of has attracted increasing interest. In particular, the X-ray scattering by molecules in a wide temperature range of the solid phase existence.

This work is devoted to the determination of mean squared displacements of $^{15}\text{N}_2$ molecules in the entire region of an orientationally ordered solid phase existence. To calculate the mean squared displacements, we used the experimental structural data presented in ref. (2). The well-known Debye and Peresada models were used to analyze the temperature dependences of the mean squared displacements of $^{14}\text{N}_2$ molecules in the ordered phase of solid nitrogen.⁽³⁾

As a result of the research, the temperature dependences of the mean squared displacements of $^{15}\text{N}_2$ molecules in the ordered phase were obtained. We carried out a comparative analysis of the behavior of the mean squared displacements of $^{15}\text{N}_2$ molecules calculated using the Debye and Peresada models, as well as using the method proposed by Kogan in ref. (4).

(1) S. J. Cyvin. Elsevier (1968).

(2) I. N. Krupskii et al. Fiz. Niz. Temp. 6 (1980), 661.

(3) L. A. Alekseeva et al. Low Temp. Phys. 48 (2022), 113.

(4) V. S. Kogan, UFN LXXVIII 579 (1962).

Synthesis and investigation of cerium and boron and/or magnesium doped YAG and LuAG for high quality scintillators application

G. Inkrataitė, R. Skaudžius

Institute of Chemistry, Faculty of Chemistry and Geosciences, Vilnius University, Vilnius, Lithuania

email: greta.inkrataite@chgf.vu.lt

In order to convert high-energy radiation, such as gamma or X-rays, into a visible light, a certain type of material is needed. Such compounds are usually referred to as scintillators. Over the years many different candidates to fit the requirements were examined. However, compounds with garnet structure have attracted a particularly large amount of attention.⁽¹⁾ Cerium doped yttrium and lutetium aluminum garnets (YAG:Ce, LuAG:Ce), have high density, high thermal stability, a rather intensive emission/excitation and high quantum efficiency which are needed for a good scintillator. However, further optimization and improvement is still needed especially on the shortening of the decay time. One way to approach this problem is to alloy the aforementioned compounds with different elements, such as boron and magnesium.^(2,3)

In this work we describe the synthesized YAG and LuAG garnets that are doped with 0.5% cerium that are additionally doped with 5% of boron and/or 0.03% of magnesium. The initial powders of garnets were synthesized by sol-gel method. Ceramics were obtained using hydrostatic pressure. Boron and additional doping by magnesium are expected to improve required luminescent properties. Selected sol-gel method determines the homogeneity of compounds and low temperatures of synthesis. Samples were analyzed by X-ray diffraction analysis and scanning electron microscopies. Emission, excitation spectra and decay times have been investigated as well. The results clearly indicate the positive effect of the addition of boron on desired properties.

⁽¹⁾ I. P. Machado et al. *J. Alloys Compd.* 777 (2019), 638.

⁽²⁾ C. Foster et al. *J. Cryst. Growth.* 486 (2018), 126.

⁽³⁾ M. T. Lucchini et al. *J. Lumin.* 194 (2018), 1.

Influence of thermoactivate contribution on isochoric thermal conductivity of tetrafluorethane

A. Karachevtseva, V. Konstantinov, V. Sagan

B. Verkin ILTPE of NASU, Kharkiv, Ukraine

email: zvonaryova@ilt.kharko.ua

Over many years of research of molecular crystals, a huge amount of experimental data has been collected. However, there is still no unified theoretical model for describing the temperature dependences of the thermal conductivities of disordered systems. Recently, was published in ref. (1) general microscopic theory of heat conduction was presented:

$$\kappa(T) = \kappa_{\text{ph}} + \kappa_{\text{dif}} = A/T + B \quad (1)$$

where κ_{ph} is the heat transfer by phonons, κ_{dif} is diffuse contribution wich does not depend on temperature.

At high temperatures, the behavior of the isobaric and isochoric thermal conductivities of molecular crystals are different. Such behavior is explained by the appearance of a thermal activation mechanism. This contribution is associated with thermal activation of some intramolecular modes. In works ref. (2-4), this contribution was described using the Arrhenius equation

$$\kappa_{\text{TA}} = \kappa_0 \exp(-E/T) . \quad (2)$$

This expression contains two parameters. κ_0 is the pre-exponential factor and the activation energy E . These parameters are typical for the thermal activation process. This study is a continuation of the study of the thermal activation mechanism. This contribution leads to an increase in thermal conductivity with temperature in the orientationally disordered phases of molecular crystals.⁽⁵⁾

The object of the study was tetrafluoroethane (freon *F-134a*). Isochoric studies were carried out by the stationary method on a coaxial geometry setup.⁽⁶⁾ The samples were grown at pressures of 100 – 700 MPa. After growing, the samples were annealed for 5 – 6 hours. The purity of tetrafluoroethane (Sigma-Aldrich) was not lower than 99%.

The isochoric thermal conductivity of crystalline tetrafluoroethane was studied for samples with different molar volumes. Growth pressures were 700 MPa, 300 MPa and 150 MPa. It was found that the thermal conductivity increases with temperature in the orientationally disordered phase. The coefficients κ_0 and E were also calculated for all samples 100 MPa $\kappa_0=0.45$, 500 MPa $\kappa_0=0.46$, 700 MPa $\kappa_0=0.49$, $E=111.11$ K. It was found that the pre-exponential factor κ_0 depends on the density of the sample, while the activation energy is constant.

- (1) M. Simoncelli et al. *Nature Physics* 15 (2019), 809.
- (2) V. A. Konstantinov, A. Belmiloudi (Ed.) *InTech Open Access Publisher* (2011), 157.
- (3) Y. V. Horbatenko et al. *J. Phys. Chem. Solid.* 127 (2019), 151.
- (4) M. A. Strzhemechny et al. *Chem. Phys. Lett.* 647 (2016), 55.
- (5) V. A. Konstantinov et al. *Solid State Communications* 329 (2021), 114241.
- (6) V. A. Konstantinov et al. *Instr. Eksp. Tech.* 42 (1999), 133 – 135.

Synthesis of manganese whitlockite via dissolution-precipitation process

A. Kizalaite, H. Klipan, T. Murauskas, A. Zarkov

Institute of Chemistry, Vilnius University, Vilnius, Lithuania

email: agne.kizalaite@chgf.vu.lt

Magnesium whitlockite ($\text{Ca}_{18}\text{Mg}_2\text{H}_2(\text{PO}_4)_{14}$) is one of the major mineral components of the human body constituting to approximately 20 – 35 wt% of human hard tissue.⁽¹⁾ This compound is highly biocompatible and is known for its excellent osteogenic capability therefore a promising candidate for application in bone regeneration.⁽²⁾ Other ions instead of Mg can be used to further improve biological properties of the material. One of the promising candidates for this role is manganese. Mn ions play a role in bone metabolism, promote osteoblast proliferation and differentiation.⁽³⁾ Mn-doped calcium phosphates have been shown to promote cellular adhesion and induce both cartilage and subchondral bone regeneration.⁽⁴⁾

In the present work, pure-phase whitlockite powders containing Mn ions were successfully obtained and investigated. Calcium hydrogen phosphate dihydrate and manganese acetate tetrahydrate were used as starting materials to synthesize manganese whitlockite powders. Synthesis was performed via dissolution-precipitation process in a closed system at 75°C temperature for 3 h.

Synthesised compounds were characterized using X-ray diffraction (XRD), Fourier-transform infrared spectrometry (FTIR), Raman spectroscopy and X-ray photoelectron spectroscopy (XPS). Scanning electron microscopy (SEM) was used to characterize the morphology of the particles. Brunauer-Emmett-Teller (BET) method was utilized to investigate surface area of the particles. Rietveld analysis was employed for calculations of lattice parameters.

Acknowledgments: This research was funded by a grant WHITCERAM (No. S-LJB-22-1) from the Research Council of Lithuania.

(1) H. Cheng et al. *Acta Biomater.* 69 (2018), 342.

(2) H. L. Jang et al. *Adv. Healthc. Mater.* 5 (2015), 128.

(3) E. Boanini et al. *Cryst. Growth Des.* 21 (2021), 1689.

(4) M. E. Zilm et al. *Mater. Sci. Eng. C* 87 (2018), 112.

Structural investigation of ferrofluids by small-angle neutron scattering

A. V. Nagorny

Taras Shevchenko National University of Kyiv, Kyiv, Ukraine

email: avnagorny23@gmail.com

Current interest in colloidal systems containing magnetic and nonmagnetic nanoparticles (NPs), such as magnetic fluids, is due to an effective combination of properties and features at nanoscale affecting on their bulk state, which is useful in various industrial technologies and biomedical applications.⁽¹⁻³⁾ Thus, for example, the combination of fluidity and magnetism is important for biomedical applications.⁽⁴⁾ Colloidal nanoparticles (including magnetic NPs) intended for these purposes should have as narrow size distribution as possible, be chemically stable, non-toxic, and at the same time demonstrate superparamagnetic properties. For effective use, colloidal NPs ought to have controlled size and, as far as possible, be resistant to formation of large aggregates. Colloidal aggregation cannot be avoided completely in water-based magnetic fluids.^(5,6) The issue of aggregation becomes especially important in biorelevant solutions, which are naturally water-based.

The reason for aggregation in an aqueous medium is the dominance of the energy of interaction between particles over the energy of thermal motion in the medium that is especially pronounced for magnetic NPs. This work considers structural studies of aqueous magnetic fluids and aqueous dispersions with nonmagnetic nanoparticles basing par excellence on small-angle neutron scattering techniques as powerful tool in condensed matter science.

⁽¹⁾ V. Socoliuc et al. *Magnetochemistry* 6(1) (2020), 1 – 36.

⁽²⁾ T. Krasia-Christoforou et al. *Nanomaterials* 10(11) (2020), 1 – 67.

⁽³⁾ K. Siposova et al. *ACS Applied Bio Materials* 2(5) (2019), 1884 – 1896.

⁽⁴⁾ L. Vekas et al. *China Particuology* 5(1-2) (2007), 43 – 49.

⁽⁵⁾ A. V. Nagorny et al. *J. Mag. Mag. Mater.* 501 (2020), 166445.

⁽⁶⁾ A. V. Nagorny et al. *Journal of Molecular Liquids* 312 (2020), 113430.

Observation of surface magnetic domain on magnetic thin films of hexacyanochromium-chromium magnetic film

S. Nagashima,¹ Y. Yahagi,¹ S. Ohkoshi,² H. Tokoro¹

¹Department of Materials Science, Faculty of Pure and Applied Sciences, University of Tsukuba, Ibaraki, Japan

²Department of Chemistry, School of Science, The University of Tokyo, Tokyo, Japan

email: 2120349@s.tsukuba.ac.jp (S. Nagashima),
tokoro@ims.tsukuba.ac.jp (H. Tokoro)

Introduction Magnetic domains are important properties related to the recording magnetic media, and much research has been done so far. On the other hand, molecular magnetic materials have interesting characteristic to design magnetic functionality.⁽¹⁾ Up to date, the magnetic domain of the molecular magnetic material has not been reported. In this work, we focus on a hexacyanochromium-chromium (CrCr),⁽²⁾ which can be synthesized electrochemically as a thin film, and report on the detailed study of the surface magnetization state.

Experiment $\text{Cr}^{\text{II}}[\text{Cr}^{\text{III}}(\text{CN})_6]_{2/3} \cdot 5\text{H}_2\text{O}$ (CrCr) were prepared by electrochemical method, reducing aqueous solutions containing Cr^{III} and $\text{K}_3[\text{Cr}^{\text{III}}(\text{CN})_6]$. Characterization was performed using UV-vis spectrum, IR spectrum, SEM, and AFM. Magnetic property was measured by SQUID magnetometer. Magnetic domains were observed using a magnetic force microscopy (MFM).

Results CrCr was obtained as a transparent thin film sample on SiO_2 -coated glass. In the IR spectrum, a peak was observed at 2190 cm^{-1} . This peak can be assigned to the CN stretching mode of $\text{Cr}^{\text{II}}\text{-NC-Cr}^{\text{III}}$. By the SEM image, CrCr thin film had a smooth surface with a crystalline size of $0.61 \pm 0.12 \mu\text{m}$. The thickness of the film was $1.70 \pm 0.06 \mu\text{m}$. A similar surface condition was observed in the AFM image (Fig. 1b). The magnetization vs temperature curves of CrCr film shows a spontaneous magnetization below Curie temperature (T_C) of 246 K (Fig. 1a). This spontaneous magnetization was generated by ferrimagnetism in which the spins on Cr^{II} ($S=2$) and Cr^{III} ($S=3/2$) are arranged in antiparallel. In the observation of the magnetization state of CrCr by MFM, the magnetic domain was observed as a clear contrast at a temperature below T_C (Fig. 1c). The orange part of the MFM image is the area where the attractive force due to the magnetic force acts between the MFM probe and the sample. The black part is the area where the repulsive force works. It was observed that the distribution of magnetic domains was not related to the surface morphology of the film sample. It was also suggested that the size of the magnetic domain of spontaneous magnetization in CrCr is about $1 - 2 \mu\text{m}$.

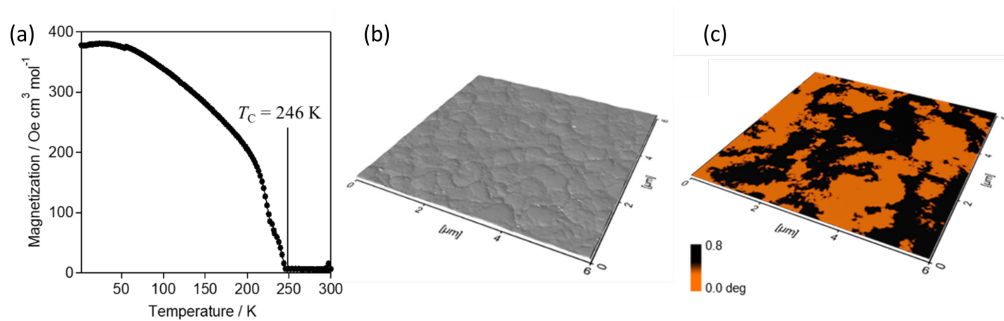


Figure 1. (a) Magnetization vs temperature curve of CrCr, (b) AFM image and (c) MFM image of CrCr at 153 K.

(1) S. Ohkoshi et al. Nature Chem. 12 (2020), 338.

(2) S. Ohkoshi et al. J. Am. Chem. Soc. 120 (1998), 5349.

Structure and magnetic properties of FeCo nanowires

A. Nykiel,^{1,2} A. Walcarius,² M. Kac¹

¹Institute of Nuclear Physic, Polish Academy of Science, Cracow, Poland

²Laboratory of Physical Chemistry and Microbiology for the Materials and the Environment (LCPME), Lorraine University, CNRS, Nancy, France

email: anna.nykiel@ifj.edu.pl

Nanowires are one-dimensional objects, which due to the shape anisotropy and dominant surface effects have different properties than their macroscopic counterparts. Especially fascinating, magnetic nanowires thanks to their magnetic, optical and electrical properties find many applications from biomedicine to customer electronics.⁽¹⁾

In this study, we focused on investigations of FeCo alloyed nanowires prepared by electrodeposition in polycarbonate membranes. The nanowires with a diameter of 50 nm and a length of 6 μm were deposited at different cathodic potentials (-1 V, -2 V vs. Ag/AgCl) and varied contents of Fe^{2+} and Co^{2+} ions in the electrolyte. Morphology and elemental composition were examined using a scanning electron microscope (SEM) equipped with an energy dispersive spectrometer (EDS). The structural and magnetic properties of nanowires were investigated based on X-ray diffraction (XRD) and superconducting quantum interference device (SQUID) measurements. Furthermore, using the Scherer equation, the crystallite size was determined.

The SEM images revealed densely packed arrays of continuous nanowires with a smooth surface and no trace of porosity, regardless of the applied potentials. Chemical analysis of nanowires showed an increase in cobalt content with increasing cathodic potential, and its decrease with increasing ion concentration in the electrolyte at a constant molar ratio (Co:Fe=2). For estimated Co concentration (51 – 66 at.%), according to the equilibrium phase diagram,⁽²⁾ FeCo alloys form the solid solution of Co and Fe with the cubic structure. The XRD studies indicated peaks at positions that moved towards higher angles compared to those characteristic of Fe bcc structure, which originated from the B_2 phase ($Pm-3m$). The diffractograms showed a slight variation in the peak intensities, which did not correlate with changes in the chemical composition. Simultaneously, the peak positions shifted towards lower angles (closer to the Fe peak position) as the Co content decreased. All samples showed a polycrystalline structure. Based on the structural peak broadening, the mean crystallite sizes were calculated. The results showed a non-monotonic relationship with the chemical composition.

The nanowires with a cobalt content of 66% had the largest crystallite size of 20 nm, while the smallest crystallites of about 10 nm were observed for the sample with 53% of cobalt. Magnetic studies indicated an easy axis of magnetization parallel to the nanowire axis. The increase in the cobalt content resulted in a coercivity increase by about 70%.

⁽¹⁾ J. A. Moreno et al. *IEEE Trans. Magn* 57 (2021), 1 – 17.

⁽²⁾ I. Ohnuma et al. *Acta Mater.* 50 (2002), 379 – 393.

Switchable composite materials based on polymers and chain-like molecular magnet

A. Pacanowska,¹ G. Wota,² W. Sas,¹ B. Nowicka,²
M. Jasiurkowska-Delaporte,¹ M. Fitta¹

¹Institute of Nuclear Physics, Polish Academy of Sciences, Cracow, Poland

²Faculty of Chemistry, Jagiellonian University, Cracow, Poland

email: aleksandra.pacanowska@ifj.edu.pl

The quest for novel materials offering different functionalities in one has been of increasing interest to researchers in the field of chemistry, physics, nanotechnology, and material engineering, especially with the focus on magnetic and electronic potential. The frameworks of different dimensionality composed of metal ions linked by organic ligands can exhibit a change in optical and magnetic properties in response to external stimuli with a change of the spin state of the metal centers called a spin crossover phenomena (SCO). Another group of materials shows a change in the oxidation state of the neighboring metal centers due to the transfer of an electron between them in a process called metal-to-metal charge transfer (MMCT). Bistability and responsiveness to external perturbations offered by those molecule-based materials make them promising candidates for the development of molecular switches and sensors. One of the ways to make them more processable materials, important for applications and integration into devices, is by embedding functional frameworks into polymer matrices. It is a straightforward approach, which can easily transform brittle crystals into flexible polymeric composites while maintaining the functionality of the molecular systems.

In our recent study, we have focused on the multi-responsive chain-like coordination compound $\{\text{NH}_4[\text{Ni}(\text{cyclam})][\text{Fe}(\text{CN})_6]\cdot 5\text{H}_2\text{O}\}_n$ (cyclam=1,4,7,11-tetraazacyclotetradecane), exhibits reversible thermal MMCT phase transition with bistability in the room temperature region.⁽¹⁾ The switching between the low temperature $\text{Ni}^{\text{III}}\text{-Fe}^{\text{II}}$ phase and the high temperature $\text{Ni}^{\text{II}}\text{-Fe}^{\text{III}}$ phase is abrupt and characterized by broad hysteresis (284 – 312 K). By employing a method called electrospinning we incorporated sub-micro and nanoparticles of the bistable material into fibers of poly(ϵ -lactone) (PCL) and poly(2-vinylpyridine-co-styrene) (P2VP-PS) (Fig. 1). The loading of particles in the obtained electrospun fibers was observed with the use of the dynamic vapor sorption (DVS) technique, due to the reversible change of water molecules in the coordination structure. Switchable properties are retained, which can be observed by optical observation, however, SQUID measurement revealed that the temperature range in which the bistability appears shifts to the lower temperature range in both polymeric matrices (Fig. 1).

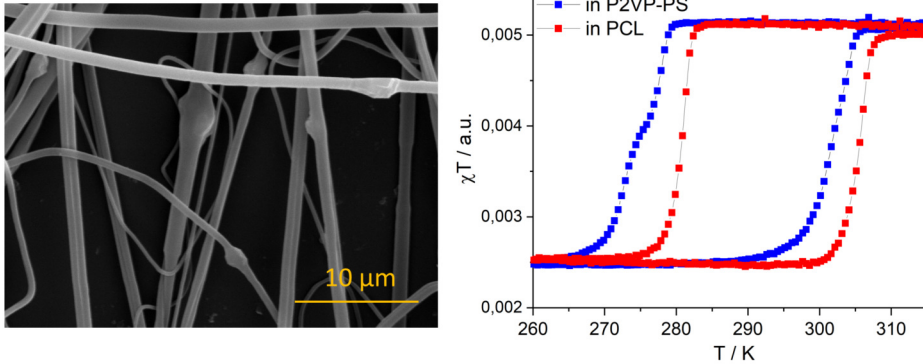


Figure 1. SEM image of electrospun fibers of P2VP-PS loaded with $\{\text{NH}_4[\text{Ni}(\text{cyclam})][\text{Fe}(\text{CN})_6] \cdot 5\text{H}_2\text{O}\}_n$ (left) and comparison of magnetic susceptibility measurement of electrospun fibers of PCL and P2VP-PS loaded with $\{\text{NH}_4[\text{Ni}(\text{cyclam})][\text{Fe}(\text{CN})_6] \cdot 5\text{H}_2\text{O}\}_n$ (right).

⁽¹⁾ M. Reczyński et al. *Angew. Chem. Int. Ed.* 60 (2021), 2330.

Investigation of crystal structure and doping driven phase transitions in $\text{Lu}_{(1-x)}\text{Sc}_x\text{FeO}_3$ system

A. Pakalniskis,¹ R. Skaudzius,¹ D. Karpinsky,² G. Niaura,³ S. Chen,^{4,5}
T. C.-K. Yang,^{4,5} A. Kareiva¹

¹Institute of Chemistry, Vilnius University, Vilnius, Lithuania

²Namangan Engineering-Construction Institute, Namangan, Uzbekistan

³Department of Organic Chemistry, Center for Physical Sciences and Technology, Vilnius, Lithuania

⁴Precision Analysis and Materials Research Center, National Taipei University of Technology, Taipei, Taiwan

⁵Department of Chemical Engineering and Biotechnology, National Taipei University of Technology, Taipei Taiwan

email: andrius.pakalniskis@chgf.vu.lt

The crystal structure and properties of compounds with perovskite structure (nominal chemical formula ABO_3) can be drastically modified by a chemical substitution in A- and/or B- perovskite sublattices. Introduction of elements with different ionic radii leads to a stabilization of structural distortions. The possibility to control physical properties via chemical doping is particularly important when concerning the formation of both electrical and magnetic orderings in the same compounds, which are commonly referred as multiferroics. These conditions are often contradictory, since magnetic ordering usually requires partially filled d orbitals and electrical ordering — empty d orbitals. However, nowadays different mechanisms allowing ferroelectricity have been determined that permit both types of orderings to coexist, which would allow for practical applications.⁽¹⁾

Recently, a new family of room temperature multiferroic compounds based on LuFeO_3 with hexagonal structure (space group $P63cm$) has been found. It has been discovered that LuFeO_3 in the hexagonal state has both ferroelectric and weak ferromagnetic ordering. Furthermore, it has been reported that the compound in orthorhombic phase (space group $Pnma$) is antiferromagnetic below 620 K, while being in hexagonal structure the magnetic transition shifts down to 440 K while also showing weak ferromagnetism, due to a canting of the magnetic moments towards the c -axis, with the polarization being retained up to 1050 K, at least in the case of thin films.^(2,3)

It should be noted, that the preparation of hexagonal compounds is quite difficult and the crystal structure can be modified either using the chemical substitution or via preparing the compounds in a form of thin films as the crystal lattice is unstable and tends to form an orthorhombic structure. Due to the unstable nature of the lattice and difficulty of preparation and characterization of the hexagonal variant of LuFeO_3 , the main available results have been performed on thin films.

However, when analyzing thin films, it is important to take into account the effect of strain and interface interactions as it can significantly affect chemical and physical properties.⁽⁴⁾

We provide a new route to prepare Sc doped LuFeO_3 polycrystalline compounds using aqueous sol-gel synthesis procedure. While also providing further clarification on the concentration ranges of the different structural phases present in the system and analyzed by means of SEM, EDX/EDS, X-ray diffraction technique, and Raman spectroscopy.

Acknowledgments: This project has received funding from the European Union's Horizon 2020 research and innovation programme under the Marie Skłodowska-Curie grant agreement No 778070 — TransFerr — H2020-MSCA-RISE-2017.

- (1) M. Kumar et al. *Mater. Lett.* 277 (2020), 128369.
- (2) W. Wang et al. *Phys. Rev. Lett.* 110 (2013), 237601.
- (3) S. Cao et al. *J. Phys. Condens. Matter* 28 (2016), 156001.
- (4) J. Luxová et al. *J. Therm. Anal. Calorim.* 138 (2019), 4303.

Influence of particles-solvent interactions on composite particles formation during pulsed laser irradiation in liquid process

O. Polit,¹ M. S. Shakeri,¹ B. Polakowska,¹ J. Gurgul,²
Z. Swiatkowska-Warkocka¹

¹Institute of Nuclear Physics Polish Academy of Sciences, Krakow, Poland

²Jerzy Haber Institute of Catalysis and Surface Chemistry Polish Academy of Sciences, Krakow, Poland

email: oliwia.polit@ifj.edu.pl

In the last decades, laser processing has become an important route for producing nano- and submicrometer particles. Pulsed laser ablation method uses a focusing laser beam which can bring high energy density on small areas on target which leads to explosive particles formation.⁽¹⁾ Using an unfocused laser beam for irradiation of nanoparticles dispersed in liquid results in a completely different formation of particles. These irradiated particles are melted and merged to form submicrometer spherical particles.^(2,3)

In this work we investigate experimentally and theoretically the physical and chemical processes involved in particles formation by laser irradiation of α -Fe₂O₃ raw nanoparticles dispersed in different organic solvents. Fig. 1(a) and (b) shows an exemplary SEM image of obtained composite particles and XRD results for three different solvents, respectively. In our research we focus on the role of solvent, interaction between irradiated particles and also interactions between particles and solvent molecules. Besides this we will show details on the influence of temperature and initial size of raw nanoparticles on the submicrometer particle formation process. We believe that exploring the interactions between irradiated material and solvent molecules and investigating the thermodynamic behavior of particles in various circumstances are necessary to design and produce materials with specific unique structures and desired physical properties.

This work was supported by the Polish National Science Centre Program No. 2018/31/B/ST8/03043.

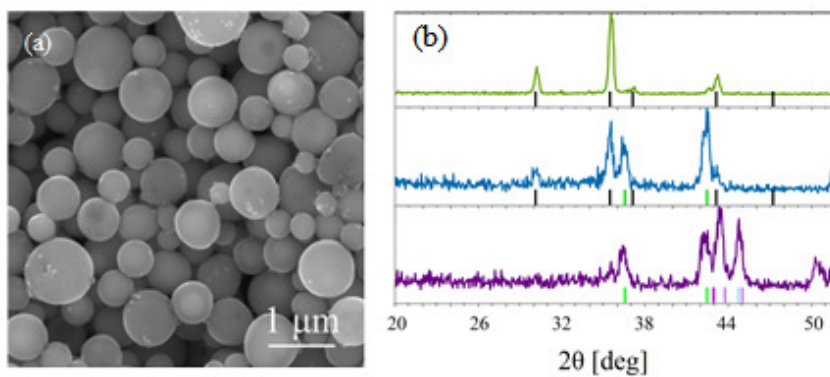


Figure 1. (a) SEM image of particles obtained during laser irradiation of $\alpha\text{-Fe}_2\text{O}_3$ in liquid, (b) XRD measurements of irradiated $\alpha\text{-Fe}_2\text{O}_3$ in three different solvents.

(¹) D. Zhang et al. *Chemical Reviews* 117 (2017), 3990.

(²) Y. Ishikawa et al. *Appl. Phys. A* 99 (2010), 797.

(³) Z. Swiatkowska-Warkocka et al. *J. Phys. Chem. C* 121 (2017), 8177.

Influence of finite size effects and surface interactions on the molecular and collective dynamics in confined liquid crystals

S. A. Rózański

Stanisław Staszic University of Applied Sciences in Piła, Piła, Poland

email: srozansk@asta-net.com.pl

Broadband dielectric spectroscopy (BDS) is an important method of studying the dielectric properties of soft matter, in particular the molecular and collective dynamics of liquid crystals (LCs) in dispersion systems and porous matrices.⁽¹⁾ Geometric restrictions and controlled disorder introduced into the LCs mesophases leads to a significant modification of their thermodynamic properties and relaxation dynamics. Based on the analysis of the dielectric spectra, the information is obtained about the relaxation time, broadening and asymmetry of the relaxation time distribution as well as the dielectric increment. This enables conclusions to be drawn about the influence of the surface and the finite size effects on the origin of the phase transition and modification of the relaxation processes.

In nematic liquid crystals (NLCs), the influence of interactions with the surface manifests itself significantly when placed, for example, in membranes with ordered cylindrical pores or with a very complex pore structure.⁽²⁾ In the case of cylindrical pores, by appropriate surfactant modification of their inner surfaces, it is possible to separate the processes related with molecular rotation around the short axis (δ -process, planar orientation on the pore surface) and the reorientation around the direction of the director (homeotropic orientation on the pore surface). The dynamics of both molecular processes is modified in relation to the bulk sample. Moreover, in dispersion systems with hydrophilic and hydrophobic aerosil, the dynamics of the δ -process is of the Arrhenius type, while the dynamics of the second process satisfy the Vogel-Fulcher-Tammann equation.

In the ferroelectric liquid crystals (FLCs), apart from molecular processes, there are two common collective processes, namely soft mode (SM) and Goldstone mode (GM). The SM is associated with the fluctuation of the tilt angle of the molecules, while the GM is associated with the fluctuation of the azimuthal angle of the molecules in the helical structure present in the FLC smectic phase (SmC*). An important parameter determining the FLC structure is the helical pitch, which is a characteristic length scale in relation to the length scale of the geometric constraints. The dynamics of the collective processes in porous membranes is significantly modified. BDS studies show that despite the lack of the GM activity in the given geometry of the experiment (electric field perpendicular to the spontaneous polarization and parallel to the pores), there is still a tilted smectic phase inside the cylindrical pores.⁽³⁾

Furthermore, in dispersion systems with aerosil, both the dynamics of the SM and GM changes. The SM becomes more broadened and its increment decreases significantly. On the other hand, the influence of aerosil on the dynamics of the GM is spectacular.⁽⁴⁾ In the SmA-SmC* phase transition temperature, the frequency degeneracy of the GM and SM is removed and the frequency gap increases with increasing aerosil concentration. As the concentration of aerosil increases, the dielectric increment of the GM decreases until the disappearance for a specific aerosil concentration. The main cause of the GM disappearance is related to the formation of a hydrogen bonded spatial structure inside the ferroelectric phase, which divides the FLC phase into domains whose dimensions are comparable or smaller with the helix pitch.

The aim of the work is to analyze the influence of finite size effects and interactions with the surfaces on the dynamics of molecular and collective processes in geometrically restricted LC.

- ⁽¹⁾ Z. Galewski, L. Sobczyk. Dielectric properties of liquid crystals (Eds.), Transworld Research Network, Trivandrum (2007).
- ⁽²⁾ S. A. Rózański et al. *Liq. Cryst.* 33 (2006), 833.
- ⁽³⁾ S. A. Rózański, J. Thoen. *Liq. Cryst.* 33 (2006), 1043.
- ⁽⁴⁾ S. A. Rózański, J. Thoen. *Liq. Cryst.* 32 (2005), 331.

Phase $V(T)$ transformations in freons of the ethane series under isochoric conditions

V. V. Sagan, V. A. Konstantinov, A. V. Karachevtseva

B.Verkin Institute for Low Temperature Physics and Engineering of the National Academy of Sciences of Ukraine, Kharkov, Ukraine

email: sagan@ilt.kharkov.ua

A phase diagram is a graphical representation of the equilibrium states of matter as a function of temperature, pressure, and volume. P - T diagrams are the most widely used, where pressure is plotted along the ordinate axis, and temperature is plotted along the abscissa axis. The regions of coexistence of two phases are bounded by curves, at any point of which the temperature and pressure allow the two phases to exist in equilibrium. In turn, V - T diagrams make it possible to visually observe the position of interphase boundaries in isochoric studies of thermal conductivity, heat capacity, dielectric properties, etc.

Freons — the technical name of a group of halogen-containing derivatives of saturated hydrocarbons (mainly methane and ethane) used as refrigerants, propellants, blowing agents, solvents. Solid freons of the ethane series, as a rule, have a wide range of phases that differ in the nature of translational and orientational ordering, and can also form conformers. Violation of the orientational order is possible for most of these compounds due to the relative weakness of the off-center interaction. High-temperature phases of freons of the ethane series usually have a cubic body-centered bcc lattice with two molecules per cell. As a rule, they are dynamically orientationally disordered, and the lifetime of molecular axes orientations along certain spatial diagonals of the cube becomes small as the melting temperature is approached. These phases are highly plastic, and their melting occurs at anomalously low enthalpy and entropy values.⁽¹⁾

In the present work, for the first time, the V - T phase diagrams of freons of the ethane series: 1,1-difluoroethane — R-152a ($\text{CH}_3\text{-CHF}_2$), 1,1,1,2-tetrafluoroethane — R-134a ($\text{CF}_3\text{-CH}_2\text{F}$) and hexafluoroethane — (C_2F_6)⁽²⁻⁴⁾ are constructed using both reference data, and our own experimental data obtained in the process of studying the isochoric thermal conductivity. All studies of thermal conductivity were carried out on the same setup, using the method of stationary heat flow in a cell of coaxial geometry. The setup, sample growth procedure, and measurements are described in more detail in ref. (5). In the case of a fixed volume, melting occurs in a certain temperature range, and the onset of melting shifts to higher temperatures. The temperature T_0 of the beginning of fulfillment in the experiment of the condition $V=\text{const.}$ and the temperature T_m of the beginning of melting of the samples were determined from the characteristic breaks in the heat conduction curve.

It was shown that the high-temperature phases of all freons considered here are dynamically orientationally disordered, and upon cooling, a transition into ordered phases occurs. The jumps of the molar volume during melting and the boundaries of the existence of dynamically orientationally disordered phases are determined. The V - T phase diagrams of fluorinated ethanes turned out to be of the same type, with the exception of ethane, which has three phases near melting point.

Acknowledgments: This work was supported by the National Research Foundation of Ukraine (Grant No.197/02.2020).

- (1) J. N. Serwood (ed.). The Plastically Crystalline State, (Orientationally-Disordered Crystals), John Wiley & Sons, (1979).
- (2) V. A. Konstantinov et al. Low Temperature Physics 32 (2006), 689.
- (3) V. A. Konstantinov et al. Low Temperature Physics 33 (2007), 1048.
- (4) V. A. Konstantinov et al. Solid State Comm. 329 (2021), 114241.
- (5) V. A. Konstantinov et al. Sov. Prib. Tekn. Eksp. 42 (1999), 145.

One-step metal-semiconductor phase transition observed in nanosize tetratitanium heptoxide

R. Seiki,¹ Y. Araki,¹ I. Nagata,¹ S. Ohkoshi,² H. Tokoro¹

¹Department of Material Science, Faculty of Pure and Applied Sciences, University of Tsukuba, Tsukuba, Japan

²Department of Chemistry, School of science, University of Tokyo, Tokyo, Japan

email: s2220343@s.tsukuba.ac.jp

Phase transition phenomena in solid state materials are attracting widespread attention from the points of view of fundamental sciences and practical applications. For example, spin-crossover, charge-transfer, and metal-semiconductor materials have been aggressively studied.^(1,2) Controlling the phase transition properties by changing the crystal size is an interesting topic. Here, we focus on the metal-semiconductor phase transition in Ti_4O_7 (tetratitanium heptoxide) by temperature change and report the anomalous phase transition observed in a nano-sized tetratitanium heptoxide.⁽²⁾

Tetratitanium heptoxide is widely known since showing a two-step phase transition from both of the charge-delocalized to charge-localized phase (high-temperature (HT) to intermediate-temperature (IT) phase) around 150 K and the charge-disordered to charge-ordered phase (IT to low-temperature (LT) phase) around 130 K. In this study, we synthesize a Ti_4O_7 nanocrystal by sintering TiO_2 nanoparticles in a hydrogen atmosphere. Then, a nano-sized Ti_4O_7 crystal shows a one-step phase transition behavior from a charge-delocalized to charge-localized phase because of suppression the transition from the charge-disordered phase to the charge-ordered phase. This anomalous phase transition can be understood by perturbation to the Gibbs free energy contributed by the surface energy. The present nanoscopic effect controlling cooperativity behavior of phase transition should contribute to expand advanced sensor and switching materials.

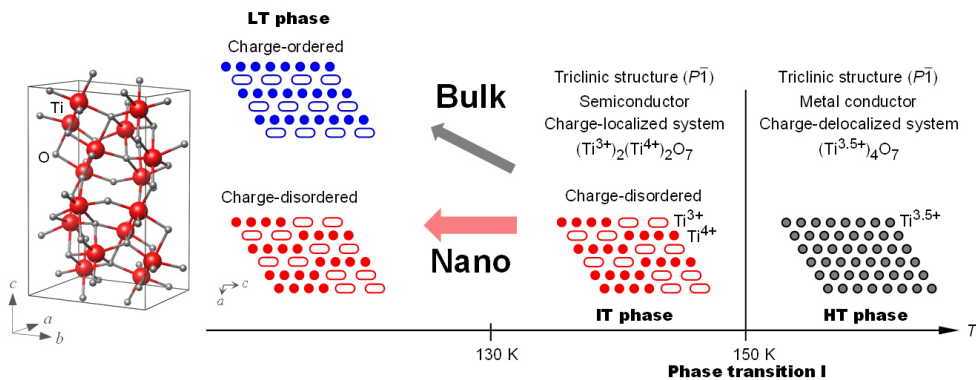


Figure 1. Crystal Structure (left) and schematic (right) of the two-step phase transition in a Ti_4O_7 conventional bulk crystal and the one-step phase transition in a nanocrystal Ti_4O_7 .

- (1) H. Tokoro et al. Nature Commun. 6 (2015), 7037.
- (2) H. Tokoro et al. Mater. Res. Lett. 8 (2020), 261.

Luminescent ceria nanoparticles with controlled ROS scavenging activity

V. Seminko,¹ P. Maksimchuk,¹ G. Grygorova,¹ O. Ivankov,²
O. Tomchuk,² S. Yefimova¹

¹Institute for Scintillation Materials NAS of Ukraine, Kharkiv, Ukraine

²Taras Shevchenko National University of Kyiv, Kyiv, Ukraine

email: seminko@ukr.net

Reactive oxygen species (ROS) such as hydrogen peroxide (H_2O_2), superoxide anions (O_2^-) and hydroxyl radicals ($\cdot\text{OH}$) permanently formed inside the living cells possess strong destructive effect on the DNA and lipid membranes. Ceria (CeO_{2-x}) nanoparticles are widely investigated nowadays due to their effective ROS scavenging properties governed by easy oxidation and reduction of cerium ion on the nanoparticle surface. Depending on the balance between Ce^{3+} and Ce^{4+} ions CeO_2 nanoparticles can show either antioxidant or prooxidant properties. However, at present there is no consensus understanding on the origin of its unique redox features. Redox activity of nanoceria is generally attributed to high content of reactive sites, namely, oxygen vacancies and Ce^{3+} ions on its surface.

In order to reveal the role of different types of the surface defects in the formation of redox activity of ceria and ceria-based nanocrystals, we have obtained ceria nanoparticles of different sizes and doped by rare-earth (Re^{3+}) ions ($\text{Re}=\text{Y}$, Eu , Tb). The NPs were characterized using the methods of small-angle X-ray and neutron scattering, transmission electron microscopy, X-ray diffraction and X-ray photoelectron spectroscopy. We have used the methods of optical spectroscopy for studying the processes of nanoceria interaction with different types of ROS. The combination of the methods of optical absorption spectroscopy (allowing determining the change in ROS content) and luminescence spectroscopy (tracing the change of Ce^{3+} content using 5d-4f luminescence) opens the possibility to unveil the dynamics and mechanisms of nanoceria-ROS interaction. Both pro- and antioxidant action of nanoceria was revealed and the ways to switch the type of redox activity were proposed.

Generally, our results have shown that the dynamics of nanoceria-ROS interaction is determined by the subtle interplay of the concentration of Ce^{3+} and Re^{3+} ions in nanoceria lattice, ROS concentration in colloidal solution, pH and presence of UV-radiation. The ability to control and vary the type of redox activity of nanoceria provides the way to obtain redox-active NPs with pre-determined anti-/prooxidant properties for biological applications.

Acknowledgments: This research was supported by National Research Foundation of Ukraine for Leading and Young Scientists Research Support, Grant No. 2020.02/0052.

Phase behaviors of liquid crystal 8CB under steady shear flow

T. Yamamoto, Y. Nagae, H. Suzuki

Department of Chemistry, Kindai University, Japan

email: koora00132357@gmail.com

Some fluid phases with partial orientational order, such as liquid crystalline phases, exhibit shear induced structures which are not observed without shear flow. A liquid crystalline compound 4-cyano-4'-n-octylbiphenyl (8CB) exhibits such shear induced structures and the transitions between those structures depend on the shear-rate and temperature.^(1,2)

The aim of this study is to reveal the thermodynamic of those structures. We developed a new differential scanning calorimeter (DSC) equipped with steady shear flow system constructed, and measured the DSC thermogram of 8CB under shear in the temperature range from 300 to 320 K and in the shear-rate range from 0 to 500 s⁻¹.

Fig. 1 shows the results obtained on the heating scans ($T \approx 0.4$ K min⁻¹). For non-sheared sample, two endothermic peaks were observed at 306.5 and 313.4 K, which correspond to the transition between the nematic (N) and the isotropic liquid (I) and the that between the smectic A (S_mA) and N, respectively. Both peaks were found to slightly shift to lower temperature with increasing shear-rate, indicating that the transitions are affected by the shear flow. A large and broad exothermic phenomenon was also observed below 306 K, which was attributed to the frictional heat, which became prominent in the highly viscous S_mA at high shear rate measurements.

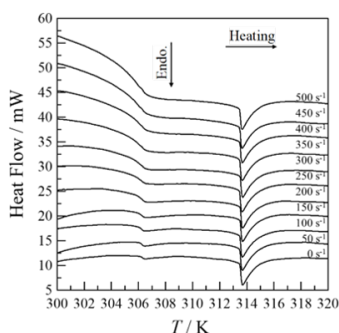


Fig. 1: DSC curves on heating measurement of liquid crystal 8CB in the shear rate range from 0 to 500 s⁻¹.

Figure 1. DSC curves on heating measurement of liquid crystal 8CB in the shear rate range from 0 to 500 s⁻¹.

(1) N. Negita, H. Kaneko. Phys. Rev. E 80 (2009), 011705.

(2) C. R. Safinya et al. Phys. Rev. Lett. 66 (1991), 15.

UV-light activated (Gd,Y)VO₄:Eu³⁺ nanoparticles as nano radio enhancers

S. Yefimova,¹ P. Maksimchuk,¹ V. K. Klochkov,¹ V. Seminko,¹
O. Ivankov,² O. Tomchuk²

¹Institute for Scintillation Materials NAS of Ukraine, Kharkiv, Ukraine

²Taras Shevchenko National University of Kyiv, Kyiv, Ukraine

email: ephimovasveta@gmail.com

Radiation therapy (RT) has become one of the first lines treatment modalities in oncology. Unfortunately, cancerous cells could be resistant to RT that requires enhanced doses of irradiation. However, high doses of radiation, in their turn, inevitably damage healthy cells and tissues located near the treatment area that limits exposed radiation doses. Recently, a new strategy in RT for cancer treatment based on the application of nanoparticles (NPs) containing high-*Z* elements and possessing high X-ray absorption has been proposed.^(1,2)

Here we report on strong X-ray induced hydroxyl radical ($\cdot\text{OH}$) generation in aqueous solutions containing UV-light activated (Gd,Y)VO₄:Eu³⁺ nanoparticles. (Gd,Y)VO₄:Eu³⁺ NPs were synthesized by the colloidal route and characterized using TEM, XRD, XPS, SANS/SAXS methods. The effect of NPs UV-light pre-treatment on their redox properties has been analyzed. The concentration of ($\cdot\text{OH}$) radicals formed in aqueous solutions were detected by the optical spectroscopy method using specific sensor coumarin.

Obtained experimental data have revealed that a preliminary treatment of (Gd,Y)VO₄:Eu³⁺ NPs with UV light is the effective tool to change drastically their redox properties. (Gd,Y)VO₄:Eu³⁺ NPs, which were UV-light pre-treated (L-GdYVO), exhibit strong $\cdot\text{OH}$ generation during X-ray exposure, whereas the same NPs, which were kept in the darkness before the experiment (D-GdYVO), show radioprotective action. The mechanism of D-GdYVO radioprotective action ($\cdot\text{OH}$ scavenging) is ascribed to the presence in the crystal lattice of (Gd,Y)VO₄:Eu³⁺ NPs of a large amount of V⁴⁺ and V³⁺ ions. Electrons stored in vanadium ions participate in neutralization of $\cdot\text{OH}$ formed at both water radiolysis and water splitting via reaction with the h^+ -mediated reaction. The mechanism of X-ray induced $\cdot\text{OH}$ generation in L-GdYVO is more complicated and three processes could be separated: (i) direct OH generation with the participation of thermalized holes (h^+) formed in NPs at X-ray irradiation, (ii) X-ray facilitated jumps of h^+ formed in the valence band at UV light pre-treatment and trapped in local levels formed by RSP, and (iii) formation of hydrogen peroxide (H₂O₂) via photo-induced electrons interaction with oxygen molecules and its further radiolysis under X-ray exposure.

Thus, depending on pre-treatment condition, we can change oppositely the redox properties of (Gd,Y)VO₄:Eu³⁺ NPs that makes this nanomaterials unique theranostic agents for RT enhancement allowing the problem of RT resistant hypoxic tumour to be overcome.

Acknowledgments: This research was supported by National Research Foundation of Ukraine for Leading and Young Scientists Research Support, Grant No. 2020.02/0052. The authors thank the Armed Forces of Ukraine for the opportunity to continue our research work.

⁽¹⁾ A. D. Paro et al. *Methods Mol. Biol.* 1530 (2017), 391.

⁽²⁾ N. Scher et al. *Biotechnol. Rep.* 28 (2020), e00548.

Synthesis, crystal structures of Cu(II), Ni(II), Co(II) and Cd(II) coordination complexes constructed by tetrazole and bi-pyrazole CN junction entities

Y. Bahjou,^{1,2} M. Cimpoesu,³ S. Radi,¹ Y. Garcia²

¹LCAE, Department of Chemistry, Faculty of Science, University Mohamed I, Oujda, Morocco

²Institute of Condensed Matter and Nanosciences, Molecular Chemistry, Materials and Catalysis(IMCN/MOST), Université catholique de Louvain, Belgium

³University of Bucharest, Faculty of Chemistry Inorganic Chemistry Department Panduri Road, Bucharest, Romania

email: yousra.bahjou@uclouvain.be

C-N junctional tetrazole and bi-pyrazole motif ligands can easily form different types of coordination networks (CCs/CPs) which have attracted much attention due to their variety of architectures and topologies,⁽¹⁾ as well as their wide potential applications, e.g. in molecular magnetism, photoluminescence and cancer therapeutics.^(2,3) A series of novel tetrazole and C,N-bipyrazole ligands, 2-(3,5,5'-trimethyl-1'H-[1,3'-bipyrazol]-1'-yl)acetonitrile (L1), and 1'-((1H-tetrazol-5-yl)methyl)-3, 5,5'-trimethyl-1'H-1,3'-bipyrazole (L2), were prepared and identified by different methods spectroscopy including ¹H-NMR, ¹³C-NMR, FT-IR and HRMS.

The reaction of L1 and L2 with several metals, Ni(II), Cu(II), Co(II) and Cd(II) lead to the formation of coordination complexes, namely: [Ni(L1)₃](ClO₄)₂ (1), Cd(L1)₂(Cl)₂ (2), [Cu(L2)₂](ClO₄) (3), Cu(L2)₂ (4) and Co₂(L2)₂Cl₃ (5). These different coordination complexes have been characterized by single-crystal X-ray diffraction and show different architectural structures due to the nature of the coordination of the metal ions and the structural features of the organic ligands as well as the effect of the counter anion.

⁽¹⁾ Y. Garcia. *Adv. Inorg. Chem.* 76 (2020), 121 – 153.

⁽²⁾ H. Benaïssa et al. *Cryst. Growth Des.* 21 (2021), 3562 – 3581.

⁽³⁾ A. Oulmidi et al. *RSC Adv.* 11 (2021), 34742 – 34753.

High magnetic anisotropy induced by unusual coordination in a pentanuclear star-like Ni₄Fe molecule

J. Bujakowska, M. Heczko, B. Nowicka

Faculty of Chemistry, Jagiellonian University, Kraków, Poland

Molecular magnetics are an attractive alternative to classic materials due to their potential multifunctionality. They can exhibit not only magnetic order, but also various combinations of desirable properties, e.g. low density, transparency or sensitivity to pressure, light and temperature. Single-molecule magnets (SMMs), which behave in a superparamagnetic manner and show magnetic hysteresis below blocking temperature, are one of the exceptional examples of molecular magnetics. High spin and high magnetic anisotropy are required to observe the SMM behavior. The two main sources of magnetic anisotropy are spin-orbit coupling and the molecule shape. Anisotropy can be increased by enforcing unusual coordination environment.⁽¹⁾ The purpose of this work was to synthesize high spin molecule with high magnetic anisotropy. We have chosen the [Ni(tmc)]²⁺ (tmc=1,4,7,11-tetramethyl-1,4,7,11-tetrazacyclotetradecane) and [Fe(CN)₆]³⁻ ions as building blocks. The macrocyclic tmc ligand coordinates in a folded conformation leaving only one position available for an additional ligand, and thus favors an unusual coordination number five. We expected the formation of a star-like molecule with Ni(II) ions arranged around the central hexacyanoferrate(III), bound by CN-bridges which are short, and mediate relatively strong magnetic interactions. During the synthesis the Fe(III) ions have been reduced to Fe(II) and the pentanuclear [Ni^{II}(tmc)]₄[Fe^{II}(CN)₆]⁴⁺ cation was formed. [Ni^{II}(tmc)]₄[Fe^{II}(CN)₆](ClO₄)₄·solv crystallizes in the orthorhombic system (space group *Pbca*). The core of the molecule consists of the Fe(II) ion connected by CN-bridges with four Ni(II) ions. Every Ni(II) ion is coordinated by a tmc ligand. The Continuous Shape Measure calculations show that the coordination geometry for all Ni(II) ions is close to the square pyramid (Fig. 1). Magnetic measurements and fitting of the ZFS parameters with the Phi software reveal that the compound shows paramagnetic behavior and high magnetic anisotropy.

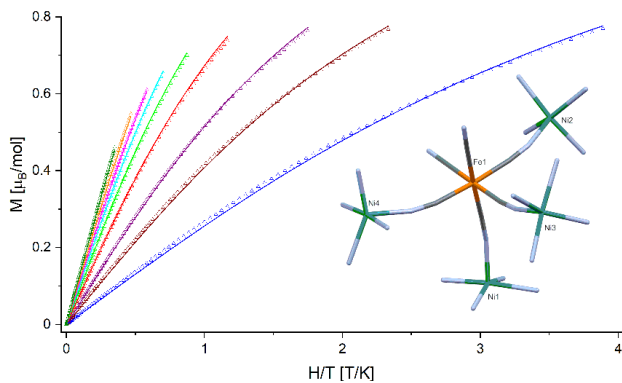


Figure 1. Reduced magnetization and structure fragment showing tetragonal pyramidal environment of Ni(II) ions in $[\text{Ni}^{\text{II}}(\text{tmc})]_4[\text{Fe}^{\text{II}}(\text{CN})_6](\text{ClO}_4)_4 \cdot \text{solv}$.

⁽¹⁾ B. Cahier et al. Eur. J. Chem. 23 (2017), 3648.

Inertial Lévy flights in bounded domains

K. Capała, B. Dybiec

Institute of Theoretical Physics, Jagiellonian University, Krakow, Poland

email: karol.capala@uj.edu.pl

The escape from a given domain is one of the fundamental problems in statistical physics and the theory of stochastic processes. In this talk we will explore properties of the escape of an inertial particle driven by Lévy noise from a bounded domain, restricted by two absorbing boundaries. The properties of the mean first passage time for the integrated Ornstein-Uhlenbeck process driven by Lévy noise will be compared to its Brownian counterpart i.e. randomly accelerated process. Mean first passage time considerations will be complemented by analysis of the escape velocity and energy along with their sensitivity to initial conditions.

Acknowledgments: This research was supported by the National Science Center (Poland) grant 2018/31/N/ST2/00598.

Norfloxacin-picolinic acid coamorphous/cocrystal: diffractometric study of a cocrystallization process through amorphous phaseG. P. Costa,¹ P. O. Ferreira,¹ A. C. de Almeida,¹ F. J. Caires^{1,3}¹Faculty of Science, São Paulo State University (UNESP), Bauru, Brazil²Institute of Chemistry, São Paulo State University (UNESP), Bauru, Brazil.

email: giovannadepaulacosta@hotmail.com

One of the biggest problems in the development of new drugs is the low solubility, a problem found even in drugs already marketed. ⁽¹⁾ Pharmaceutical cocrystals are an approach that improves this, among other properties. They are crystals formed from two or more components in stoichiometric proportions interacting mainly by hydrogen bonds. ⁽²⁾ Coamorphous, as well as cocrystals, have intermolecular interactions, but no crystalline arrangement. Some coamorphous are described as intermediates in the formation of cocrystals. ⁽³⁾ This work aimed to cocrystallize norfloxacin (NOR), a broad-spectrum antibiotic with low solubility and permeability, ^(4,5) with picolinic acid (PCA), focusing on improving the aqueous solubility of the drug. The coamorphous/cocrystal was synthesized by the mechanochemical method, characterized by thermoanalytical (DSC), spectroscopic (IR), and diffractometric (PXRD) techniques.

The DSC curve (Fig. 1a) of the synthesized system shows an exothermic event at 140°C followed by melting at 226°C, a temperature higher than that of the drug and the isolated coformers. The PXRD analysis (Fig. 1b) showed an amorphous pattern of the system, and the IR spectra (Fig. 1c) presents bands deviations, which confirms the formation of the NOR-PCA coamorphous system. PXRD heated until after the event observed in the DSC shows the crystalline pattern and proves cocrystallization with heating.

Acknowledgments: This study was financed in part by the FAPESP process No. 2022/00239-2, process No. 2020/07724-8, and Brazilian Federal Agency for Support and Evaluation of Graduate Education (CAPES-PrInt) process no 88887.571008/2020-00, process No. 88887.684961/2022-00.

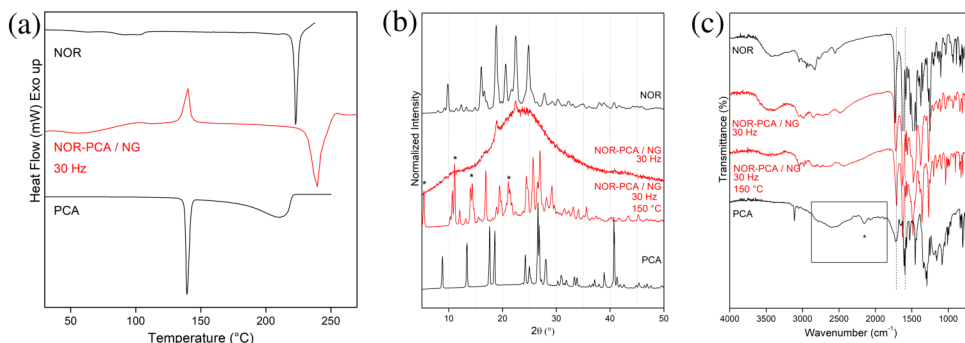


Figure 1. (a) he figure represents DSC curve of NOR, system formed. (b) The figure represents PXRD analysis of NOR, system formed. (c) The figure represents IR spectra of NOR, system formed.

- (1) S. Chaudhari et al. *J. Drug Deliv. Ther.* 8 (2019), 350.
- (2) O. N. Kavanagh et al. *Drug Discov. Today* 24 (2019), 796.
- (3) M. Karimi-Jafari et al. *Cryst. Growth Des.* 18 (2018), 6370.
- (4) M. De Souza. *Mini-Reviews Med. Chem.* 5 (2005), 1009.
- (5) D. T. Bearden and L. H. Danziger. *Pharmacotherapy* 21 (2001). 224S.

Effects of plasma irradiation on the three-dimensional cyanide-bridged network based on the Nb(IV) and Mn(II) ions

D. Czernia,¹ P. Konieczny,¹ D. Pinkowicz²

¹Institute of Nuclear Physics PAN, Cracow, Poland

²Jagiellonian University, Faculty of Chemistry, Cracow, Poland

email: dominik.czernia@ifj.edu.pl

Molecular magnets are a class of metal-organic materials exhibiting unique physical properties that can potentially play an essential role in developing modern technology, including spintronics, quantum computing, magnetic cooling, or bistable magnetic switches. On the one hand, one of the most apparent approaches to discovering new molecular compounds is a consistent synthesis that involves various building blocks. On the other hand, molecular magnets are often sensitive to external stimuli such as temperature, pressure, light, or the presence of guest molecules, which opens new ways of modification of magnetic properties.

Here, we report preliminary results obtained for the molecular magnet NbMn₂ based on the Nb(IV) and Mn(II) ions subjected to plasma irradiation under various conditions. NbMn₂ structure consists of the three-dimensional network, where the Nb(IV) and Mn(II) ions are alternately linked through cyanide bridges CN. The origin magnetic properties of NbMn₂ come from one Nb(IV) ion spin of $S=1/2$ and two Mn(II) ions spins of $S=5/2$. The antiferromagnetic exchange interaction between Nb(IV) and Mn(II) ions leads to the long-range ferrimagnetic order observed below $T_C=47.5$ K and confirmed by the saturation magnetization of 9 Bohr magnetrons per NbMn₂ formula unit.

Numerous samples of NbMn₂ were ground down and scattered on the adhesive tape to assure a large surface-to-volume ratio of exposed crystallites. Then, the samples were placed in the vacuum chamber and irradiated with plasma made of air, nitrogen, oxygen, and argon. Two other parameters were tested: plasma power (low, medium, high) and irradiation time (2 – 30 min). After the irradiation, all samples were protected from air and vacuum by an additional layer of adhesive tape put at the top of the samples. The reference sample was ground down and placed in the vacuum chamber as well to reproduce the same initial conditions as for other samples. The magnetic properties of the irradiated samples of NbMn₂ show a clear appearance of the second magnetic phase with T_C around 70 K. However, the changes in magnetic signal are observed only for samples irradiated with at least 10 minutes and medium power, indicating the presence of threshold effects. The choice of the gases used to create plasma is also an important parameter. The most extensive modification of the magnetic properties was observed for argon, then oxygen, nitrogen, and air (Fig. 1).

Although plasma irradiation is not a common approach to altering physical properties in molecular magnets, it indeed offers a promising way of obtaining new magnetic phases. Two other aspects of the presented results of NbMn_2 should be considered, namely, what the influence of heat generated during the plasma irradiation is and how the observed magnetic properties changes are related to the structural modifications of NbMn_2 after the plasma irradiation.

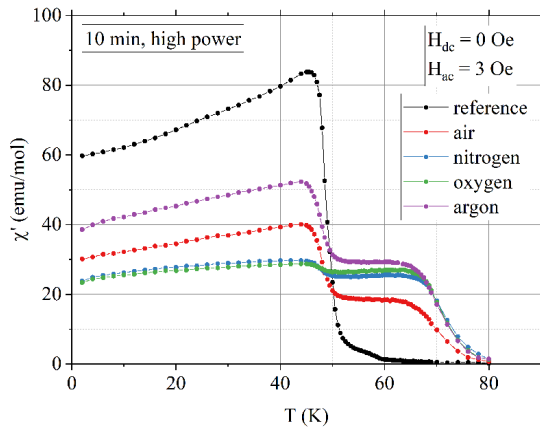


Figure 1. The real part of the AC magnetic susceptibility of NbMn_2 measured for samples irradiated for 10 minutes with high power air, nitrogen, oxygen, and argon plasma.

Effect of nonzero temperature on the process of penetration of the potential barrier through the kink

J. Gatlik,¹ T. Dobrowolski²

¹Doctoral School, Pedagogical University of Krakow, Krakow, Poland

²Institute of Physics, Pedagogical University of Krakow, Krakow, Poland

email: jacek.gatlik@doktorant.up.krakow.pl

The description of nonlinear phenomena is fundamental to the discovery of the laws of nature. Many physical systems are linear only within a particular area, however exhibit nonlinear behavior outside it. In such cases, to fully understand the dynamics of a physical system, a description of its nonlinearity should be included. A particular role for the modern description of nonlinear phenomena is played by structures such as solitons. In mathematical physics, the concept of the soliton appeared due to the work of N. Zabusky and M. Kruskal. At present, the concept of the soliton is used to describe many phenomena appearing in the field of physics. In 1962 the British physicist B. Josephson presented a model describing the tunnelling of Cooper pairs between two superconductors separated by a thin insulator layer. Currently, a system composed of two superconductors separated by a thin insulator layer is called a Josephson junction. In the description of the Josephson junction the equation (sine-Gordon) appears which also has soliton solutions including the so-called fluxon defined as the soliton carrying the magnetic flux quantum.

The research concentrates on the impact of thermal noise on kink motion through the curved region of the long Josephson junction. We consider the kink motion in the sine-Gordon model with the position dependent dispersive term

$$\partial_t^2 \phi + \alpha \partial_t \phi - \partial_x (F(x) \partial_x \phi) = -\Gamma$$

where the function $F(x)$ contains information about the curvature of the junction. The physical motivation for description of curvature effects in the framework of this model was described in detail in the article ref. (1). This research aimed at studying the effects of nonzero temperature of the system on the process of penetration of the potential barrier through the kink. We propose the analytical formula that describes the probability of transmission of the kink over the potential barrier based on the Fokker-Planck equation. The analytical results are compared with the simulations based on the field model. Due to potential applications in normal and in high-temperature superconductors, the comparison was made from zero to $T=50$ K, $T=20$ K, and $T=5$ K.

The Josephson junctions have found a wide variety of science and technical applications, and research into their possible further development is continuing. Fundamental for the preparation of junctions with specific properties are the descriptions of the soliton dynamics inside the junction. The results of the research could be the basis for future development of devices based on the Josephson junction and creation of electronics based on quantum effects occurring in the junction.

Acknowledgments: The studies were financially supported from the project WPBSD/2021/04/00010 funded by the Doctoral School of the Pedagogical University of Krakow.

⁽¹⁾ J. Gatlik, T. Dobrowolski. *Physica D: Nonlinear Phenomena* 428 (2021), 133061.

Menthol-valsartan low transition temperature mixtures (LTTMs): a thermoanalytical study

P. O. Ferreira,¹ J. A. Baptista,² A. C. Almeida,¹ G. de P. Costa,¹
L. T. Ferreira,³ M. E. S. Eusébio,² F. J. Caires,^{1,3} R. A. E. Castro^{2,4}

¹School of Sciences, São Paulo State University, Bauru, Brazil

²CQC/IMS, Chemistry department, University of Coimbra, Coimbra, Portugal

³Institute of Chemistry, São Paulo State University, Araraquara, Brazil

⁴Faculty of Pharmacy, University of Coimbra, Coimbra, Portugal

email: patricia.osorio@unesp.br

Menthol have been demonstrating the ability of coamorphization with drugs, giving rise to mixtures with below zero degree Celsius glass transitions,⁽¹⁾ which generate liquids in room temperature conditions. These systems have been classified as Low Transition Temperature Mixtures (LTTMs).⁽²⁾

This work presents the investigation of the formation of a LTTM between crystalline valsartan (VALc) and menthol (MENT) using binary solid-liquid phase diagram and applying the Gordon-Taylor equation.⁽³⁾ The API (active pharmaceutical ingredient) chosen for this work is valsartan, an antihypertensive drug, that has a low aqueous solubility, been classified by the Biopharmaceutical Classification System (BCS) as a class II drug (low solubility — high permeability drugs).⁽⁴⁾ The samples were prepared through mechanochemical synthesis and then characterized by Differential Scanning Calorimetry (DSC) and infrared spectroscopy (FTIR), and powder X-ray diffraction (PXRD).

The binary phase diagram, Figure 1a, was constructed using the first DSC heating curves, and shows a eutectic system, confirmed by the FTIR as no interaction prior the melting was observed. After melting cooling, the second heating reveals amorphous systems confirmed by PXRD, with single T_g events. LTTMs systems were observed in compositions below $x_{VALc}=0.4$. The experimental T_g temperatures of the different molar ratio mixtures are in good agreement with the predicted by the Gordon-Taylor equation, which suggests that the intermolecular interactions of menthol-menthol and valsartan-valsartan, have energy similar to intermolecular interactions of menthol-valsartan.⁽⁵⁾

Acknowledgments: This work was financed in part by the Brazilian Federal Agency for Support and Evaluation of Graduate Education (CAPES), in the scope of the Program CAPES-PrInt, Mobility number 88887.571008/2020-00. It was also supported by Portugal national funds through FCT — Fundação para a Ciência e a Tecnologia, I.P., under the project UIDB/00313/2020.

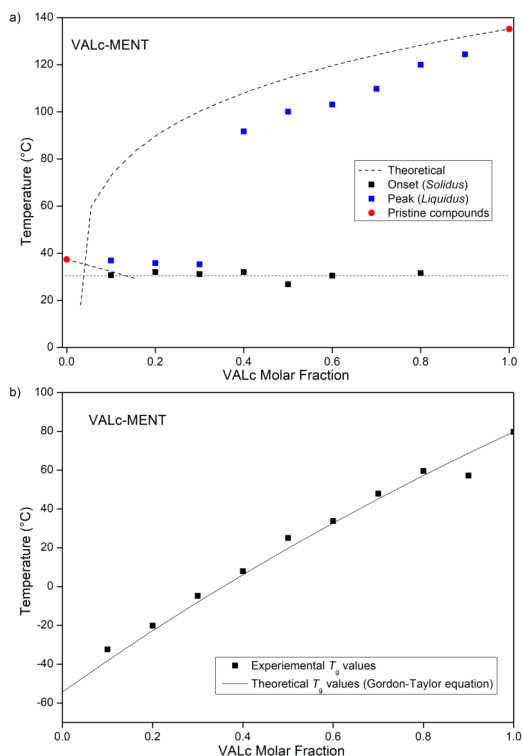


Figure 1. a) Binary phase diagram of VALc-MENT system b) Experimental glass transition temperatures (T_g) (black square) and prediction by Gordon Taylor equation (solid line) as a function of molar ratios of VAL.

- (1) M. S. Rahman et al. Mol. Liq. 321 (2021), 114745.
- (2) S. A. Mat Hussin et al. J. Mol. Liq. 308 (2020), 113015.
- (3) M. Gordon and J. S. Taylor. J. Appl. Chem. 2 (2007), 493.
- (4) R. Hamed, S. H. Alnadi. AAPS PharmSciTech 19 (2018), 2213.
- (5) T. Cordeiro et al. Mol. Pharm. 14 (2017), 3164.

Carbon structures fabricated by a versatile hydrothermal method: controllable synthesis and preliminary material characterization

A. Karczmarzka, M. Adamek, M. Laskowska

The Henryk Niewodniczański Institute of Nuclear Physics Polish Academy of Sciences, Kraków, Poland

email: agnieszka.karczmarzka@ifj.edu.pl, michal.adamek@ifj.edu.pl

A strongly developed specific surface area, an extensive pore system, high electrical conductivity, and excellent chemical stability make carbon materials practical for use in almost every branch of modern industry. Particularly fast-growing topics are those related to environmental protection, such as supercapacitors and catalytic support. Hydrothermal carbonization (HTC) is of great interest among the many methods of synthesizing carbon materials due to its mild operating conditions and low CO₂ emissions. It can be used to process various aqueous solutions of saccharides (e.g. glucose or sucrose) or biomass. Properly selecting the parameters of the hydrothermal process (temperature, solution concentration, duration, reactor filling) makes it possible to obtain carbon spheres of controlled size and morphology. In turn, carbonaceous materials obtained from biomass by appropriate activation (chemical and/or thermal) are materials with a huge specific surface area. The HTC method has also been successfully used to create mesoporous silica-carbon composites with a regular, homogeneous carbon internal layer. The three classes of carbon materials presented were characterized by the following research methods: scanning electron microscope (SEM), transmission electron microscopy (TEM), Raman and IR spectroscopy, isothermal sorption of nitrogen, and thermalgravity analysis (TGA). The results obtained confirm that the use of HTC is an efficient and effective method for the synthesis of carbon structures.

Investigation of structural, morphological and magnetic properties of $\text{Bi}_{1-x}\text{Gd}_x\text{Fe}_{0.85}\text{Mn}_{0.15}\text{O}_3$ solid solutions prepared via sol-gel method

D. Karoblis,¹ R. Diliautas,¹ K. Mazeika,² D. Baltrunas,² G. Niaura,³
M. Talaikis,⁴ A. Lukowiak,⁵ W. Strek,⁵ A. Zarkov,¹ A. Kareiva¹

¹Institute of Chemistry, Vilnius University, Vilnius, Lithuania

²Center of Physical Sciences and Technology, Vilnius, Lithuania

³Institute of Chemical Physics, Vilnius University, Vilnius, Lithuania

⁴Department of Bioelectrochemistry and Biospectroscopy, Institute of Biochemistry, Life Sciences Center, Vilnius, Lithuania

⁵Institute of Low Temperature and Structure Research, Polish Academy of Sciences, Wroclaw, Poland

email: Dovydas.Karoblis@chgf.vu.lt

Magnetolectric multiferroics are one of the most extensively studied multifunctional materials, due to possible application in different fields, including electric or magnetic field sensors, gyrators, magnetolectric phase shifters, photovoltaic solar cells,⁽¹⁾ etc. There are numerous multiferroics with different composition and structure, but BiFeO_3 are considered to be the most promising one. Despite demonstrating ferroelectric and antiferromagnetic properties at room temperature,⁽²⁾ this compound has some drawbacks, like thermal instability or disappearance of linear magnetolectric coupling.⁽³⁾ GdFeO_3 is another perovskite-type material with multiferroic properties. While magnetic ordering and ferroelectricity for BiFeO_3 occur due to separate mechanisms, electric polarization for GdFeO_3 is caused by exchange striction mechanism.⁽⁴⁾

In this work novel $\text{Bi}_{1-x}\text{Gd}_x\text{Fe}_{0.85}\text{Mn}_{0.15}\text{O}_3$ (where x varies in 0 – 1 interval) solid solutions were prepared by sol-gel synthetic approach using ethylene glycol as complexing agent. Different annealing temperatures (500, 650 and 800°C) were used in order to investigate structural, morphological and magnetic properties. It was observed, that solid solutions in the whole compositional range can form when heating temperature is 650 and 800°C. At lower temperature only 10% of Gd^{3+} ions can be intercalated into $\text{BiFe}_{0.85}\text{Mn}_{0.15}\text{O}_3$ structure, because amorphous compounds form at higher Gd content. Few different structural regions, like trigonal, trigonal+orthorhombic and orthorhombic, can be identified depending upon chemical composition and annealing temperature. Scanning electron microscopy (SEM) analysis revealed, that nearly all samples are composed of nanosized particles, which are necked to each other. Only two samples with the highest Bi content and annealed at 800°C consisted of larger grains with expressed grain boundaries. Magnetization of the obtained solid solutions can be explained by contribution of antiferromagnetically ordered Fe-Mn sublattice with weak ferromagnetism arising from nanosized grains.

Acknowledgments: The work has been done in frame of the project TransFerr. This project has received funding from the European Union's Horizon 2020 research and innovation program under Marie Skłodowska-Curie grant agreement no. 778070.

- (1) A. M. M. Vopson. *Crit. Rev. Solid State Mater. Sci.* 40 (2015), 223 – 250.
- (2) A. J. De-Chang et al. *J. Eur. Ceram. Soc.* 29 (2009), 3099 – 3103.
- (3) A. I. Sosnowska, B. A. K. Zvezdin. *J. Magn. Magn. Mater.* 140 (1995), 167 – 168.
- (4) A. Y. Tokura et al. *Rep. Prog. Phys.* 77 (2014), 076501.

Thermodynamic studies of the zeolitic imidazolate frameworks

L. A. Kotvytska,¹ R. Tarasenko,¹ R. Feyerherm,² S. Gabáni,³
O. Lyutakov,⁴ M. Orendáč,¹ A. Orendáčová¹

¹Institute of Physics P. J. Šafárik University, Košice, Slovakia

²Institut für Quantenphänomene in neuen Materialien Helmholtz-Zentrum Berlin GmbH, Berlin, Germany

³Institute of Experimental Physics of SAS, Košice, Slovakia

⁴University Chem & Technol., Dept. Solid State Engn, Prague, Czech Republic

email: liliia.kotvytska@student.upjs.sk

Metal–organic frameworks (MOFs), composed of organic linkers and metal nodes, are a new class of crystalline porous materials with significant application potentials.

Zeolite imidazolate frameworks (ZIFs) represent a relatively new class of MOFs with spreading three-dimensional networks formed by 3d transition metal ions connected by rigid imidazole (Im) linkers. The observed Zn-Im-Zn angles are close to the ideal Si-O-Si angle ($\approx 145^\circ$) in zeolites, therefore many ZIF structures have the same topology as inorganic zeolites.⁽¹⁾

This work is devoted to the study of the thermodynamic properties of two compounds [$\{\text{Zn}(\text{mIm})_2 \cdot 2\text{H}_2\text{O}\}_\infty$] known as ZIF-8 and [$\{\text{Cu}(\text{mIm})_2 \cdot 2\text{H}_2\text{O}\}_\infty$], abbreviated as Cu-ZIF-8 where $\text{HmIm} = 2\text{-methylimidazole} = \text{C}_4\text{H}_6\text{N}_2$. Previous structural studies of ZIF-8 were focused at the substitution Zn-Cu in the concentration up to 25% and they did not indicate any significant changes of the ZIF-8 crystal structure.⁽²⁾

The heat capacity of the samples was experimentally measured at temperatures nominally from 0.4 to 300 K. It was found that within experimental accuracy, both ZIF-8 and Cu-ZIF-8 data sets are nearly identical, suggesting that the lattice dynamics is not sensitive to the Cu-Zn substitution. At temperatures above 100 K, the rate of the increase of specific heat decelerates approaching quasi-linear behavior up to 300 K. There is no saturation at room temperature and the data achieve much lower values than the classical value of $3sR$ resulting from the equipartition principle.

At low temperatures the specific heat of the diamagnetic ZIF-8 drops down towards zero value while Cu-ZIF-8 data begin to rise slightly below 6 K forming a round maximum at a temperature of approximately 0.4 K in zero magnetic field. Since this increase begins to manifest itself already at a relatively high temperature of 6 K and in a zero magnetic field, we could basically rule out its origin in the nuclear magnetism of copper atom, which is characterized by a nuclear spin $I=3/2$.

The character of the low-temperature data is preserved also in the magnetic fields up to 5 T whereas the application of higher fields leads to the significant reduction of the maximum and its shift towards higher temperatures. Further studies at lower temperatures are required to clarify the origin of the observed behavior.

Acknowledgement: The work was supported by the project APVV-18-0197 and GAČR 20-01768S.

⁽¹⁾ K. S. Park et al. Proc. Nat. Acad. Sci. U.S.A. 103 (2006), 10186.

⁽²⁾ A. Schejn et al. Catal. Sci. Technol. 5 (2015), 1829.

Orbach-like which-way spin dephasing in self-assembled and gate-defined quantum dots

M. Kuniej,¹ K. Gawarecki,¹ and M. Gawełczyk^{1,2}

¹Department of Theoretical Physics, Faculty of Fundamental Problems of Technology, Wrocław University of Science and Technology, Wrocław, Poland

²Institute of Physics, Faculty of Physics, Astronomy and Informatics, Nicolaus Copernicus University in Toruń, Toruń, Poland

email: 245034@student.pwr.edu.pl

Achieving long coherence times of spin states in quantum dots (QDs) is crucial for spintronics and quantum information processing applications. Recently, it was shown that inequality of Zeeman splitting in orbital carrier states leads to spin pure dephasing during orbital relaxation.⁽¹⁾ Apart from direct processes, virtual excitations to excited states lead to Orbach-like thermally activated accumulation of this decoherence.

In this contribution, we theoretically study the impact of such processes on spin coherence in single and coupled self-assembled and gate-defined QDs. We present results for typical self-assembled InAs/GaAs, InAs/InP, InAs/AlGaInAs and gate-defined InAs/GaAs and GaAs/AlGaAs QDs. In single QDs, we calculate the spin dephasing rate for the electron and the hole due to excitations from the *s*-shell ground state to the *p*-shell one. In this case, for gate-defined QDs in a relatively weak magnetic field and at cryogenic temperatures, the rate of decoherence could still be higher than 1/ns. We also study the effect in tunnel-coupled nanostructures, especially in dense ensembles of asymmetric InAs/AlGaInAs QDs, where dephasing rates for holes are also significant.

We model the QDs assuming anisotropic harmonic confining potential. For tunnel-coupled QDs, we calculate the tunnel coupling constant using Bardeen's tunneling theory.⁽²⁾ The rate of phonon-induced orbital transitions is calculated using Fermi's golden rule,⁽¹⁾ including carrier-phonon coupling via piezoelectric effect and deformation potential. Calculating Zeeman splitting requires knowledge of *g*-factors for both electron and hole orbital states. For this, we integrate the Fourier-transformed carrier probability densities with *k*-dependent *g*-factors⁽³⁾ calculated for appropriately strained bulk using the eight-band *k* · *p* method.⁽⁴⁾

We find that most single, self-assembled QDs have very long spin dephasing times (rate lower than 10^{-12} ns⁻¹). The telecom application-relevant asymmetric InAs/AlGaInAs QDs are an exception.

Our results show that the effect is significant in gate-defined QDs, where transition energies are close to resonance with the phonon reservoir. It may surpass the homogeneous dephasing times due to hyperfine interaction (10^{-6} s).⁽¹⁾ Due to this, under certain conditions, the studied effect may be the process limiting spin coherence in QDs in a magnetic field.

⁽¹⁾ M. Gawęlczyk et al. Phys. Rev. B 98 (2018), 075403.

⁽²⁾ H. J. Reittu. Am. J. Phys. 63 (1995), 940.

⁽³⁾ K. Gawarecki, M. Zieliński. Sci. Rep. 10 (2020), 22001.

⁽⁴⁾ K. Gawarecki. Phys. Rev. B 97 (2018), 235408.

Nanocomposites based on liquid crystalline (S)-MHPOBC matrix and Au nanoparticles

S. Lalik,¹ O. Stefańczyk,² D. Dardas,³ D. Deptuch,⁴ T. Yevchenko,³
S. Ohkoshi,² M. Marzec¹

¹Institute of Physics, Jagiellonian University, Kraków, Poland

²Department of Chemistry, School of Science, Tokyo University, Tokyo, Japan

³Institute of Molecular Physics, Polish Academy of Sciences, Poznań, Poland

⁴Institute of Nuclear Physics, Polish Academy of Sciences, Kraków, Poland

email: sebastian.lalik@doctoral.uj.edu.pl

The influence of a small amount of Au nanoparticles (0.2 and 0.5 wt.%) on many chemical/physical parameters of antiferroelectric liquid crystal (S)-MHPOBC will be presented. The preparation of new composite materials which combining liquid crystalline matrix and nanoparticles is an alternative way to the chemical synthesis of materials with strictly defined parameters. The process of doping soft matter has been known for about fifteen years and concentrates mainly on the nematic phase and to a lesser extent on the SmC/SmC* phases. Until now, nobody has reported the influence of Au nanoparticles on the properties of antiferroelectric phase, which was the main motivation for us to fill this research gap. The low dopant concentration is intentioned to avoid degradation of liquid crystalline properties. Additionally, nanoparticles with a size of 2 – 4 nm was selected because it is comparable to the size of long axis of rod-like molecules building the liquid crystalline matrix. We chose (S)-MHPOBC as the matrix, the first antiferroelectric liquid crystal that exhibits an antiferroelectric SmC*_A phase over a wide temperature range and is commercially available. The preparation process of composites is multi-stage and basically requires only solvent and sonication system. By using complementary methods it was found that the effect of an admixture on the phase sequence is very small but the enthalpy changes were considerable for several transitions. Also the polymorphism of crystal state was found. The admixture does not affect the optical textures, while for larger concentration the inhibition of crystallization process as well as a wide temperature range of coexistence crystal and SmI*_A phases was found. The smectic layer thickness is not affected but the correlation length is slightly modified in the SmA* phase. In turn, the helix pitch increases in the high temperature range of the SmC*_A phase in comparison to pristine (S)-MHPOBC matrix. The contact angle for thin layer is strong changed after doping (even up to 17° in the SmC*_A phase). In turn, the switching time for larger Au nanoparticles concentration is shorter, but for lower concentration is longer than for pristine matrix.

The spontaneous polarization increases after doping at the high temperature range of the SmC^*_A phase, while below ca. 90°C no influence was observed. The increase in P_s results from the induction of the dipole moment of Au NPs under the influence of incident light. In addition, an increase in fluorescence after doping was noted. Moreover, high resolution optical microscopy revealed that with the increase in the concentration of NPs and after the composites annealing at high temperature, structures of the order of $0.5\ \mu\text{m}$ appeared, which may indicate agglomeration (despite the decoration of nanoparticles with thiol derivatives). The presented research results are the basis of our article.⁽¹⁾

⁽¹⁾ S. Lalik et al. *Molecules* (after review).

Numerical investigation of radiation-induced dynamics of solids in two-dimensional geometry

V. Lipp,^{1,2} B. Ziaja^{2,1}

¹Institute of Nuclear Physics, Polish Academy of Sciences, Krakow, Poland

²Center for Free-Electron Laser Science CFEL, DESY, Hamburg, Germany

email: vladimir.lipp@desy.de

We simulate the dynamics of silicon after its excitation by an X-ray laser in two-dimensional (2D) geometry. The approach combines classical Monte Carlo (MC)⁽¹⁾ with Two-Temperature-like model, nTTM.⁽²⁾ The MC takes into account X-ray absorption and electron cascading and provides the initial conditions for the nTTM, which takes into account Auger recombination and impact ionization, band gap evolution, ambipolar carrier diffusion, electronic and atomic heat conduction, and electron phonon coupling. To solve the nTTM system of equations in 2D, we developed a finite-difference integration algorithm based on Alternating Direction Implicit method with additional predictor corrector algorithm, which takes care of the nonlinearities. We show the first results of the model and discuss its possible applications. In particular, the approach should be applicable also for metals, various radiation sources (e.g. heavy ion beams), and extendable to three dimensions.

Acknowledgments: We thank Jan Grünert and Jia Liu for helpful discussions.

⁽¹⁾ V. Lipp et al. Proc. SPIE 10236 (2017), 102360H.

⁽²⁾ H. van Driel. Phys. Rev. B 35 (1987), 8166.

Polymorphism and physical stability of aripiprazole

N. Osiecka-Drewniak,¹ A. Deptuch,¹ A. Dziuba,²
E. Juszyńska-Gałązka,^{1,3} M. Jasiurkowska-Delaporte¹

¹Institute of Nuclear Physics Polish Academy of Sciences, Cracow, Poland

²Cracow University of Technology, Cracow, Poland

³Research Center for Thermal and Entropic Science, Osaka, Japan

email: Natalia.Osiecka@ifj.edu.pl

A complex phase behavior of the antipsychotic drug aripiprazole (AZP)⁽¹⁾ was studied by differential scanning calorimetry (DSC), polarized light microscope observations (POM), broad band dielectric spectroscopy (BDS) and X-ray diffraction (XRD). AZP has rich polymorphism.⁽²⁻⁴⁾ A primary sample crystallizes as a pure triclinic sample. Coexistence of a glassy state and a crystal phase occur during slow cooling of AZP sample. The structure and molecular dynamics of phases occurring upon slow cooling and subsequent heating will be presented. Two glass transitions associated with different dynamic disorder was revealed in BDS studied for sample after fast cooling. The kinetics of isothermal melt and cold crystallization process will be described in terms of Avrami and Avramov models.

⁽¹⁾ M. Greenaway, D. Elbe. *J. Can. Acad. Child Adol. Psych.* 18 (2009), 250.

⁽²⁾ D. E. Braun et al. *J. Pharm. Sci.* 98 (2009), 2010.

⁽³⁾ S. P. Delaney et al. *Cryst. Grow. Des.* 13 (2013), 2943.

⁽⁴⁾ J. B. Nanubolu et al. *Cryst. Eng. Com.* 14 (2012), 4677.

Environmental-friendly adsorbent based on pyridine blocks for removal of heavy metals

A. Oulmidi,^{1,2} R. Smaail,¹ Y. Garcia²

¹University Mohammed I, LCAE Faculty of Sciences, Oujda, Morocco

²Institut of Condensed Matter and Nanosciences Université Catholique de Louvain, Louvain La Neuve, Belgium

email: afaf.oulmidi@uclouvain.be

Nowadays, there is much more concern about the planet's future sustainability due to the increasing rate of pollution, and mainly the contamination of groundwater and oceans by heavy metal ions from industrial waste. That's why their removal is necessary or even primordial in order to preserve our environment.⁽¹⁾

The main objective of this work is the synthesis of functional mesoporous nanoparticles. It is achieved by grafting a novel synthesized ligand 2,6-bis(3,5-dimethyl-1H-pyrazol-1-yl)isonicotinic acid (L) on silica surface.

The choice of this natural support was based on its various characteristics,⁽²⁾ for instance, its high surface properties, its large pore channels, also for its attractive features such as optical, electrical or magnetic properties based on inorganic nanomaterials. Whereas for ligand L belonging to the NNN pincer family were and will always be the focus of extensive investigation in coordination chemistry and crystal engineering.⁽³⁾

Hybrid materials are used frequently in different fields as an example in catalysis, adsorption and separation. On our part, we intend to use them for environmental application to extract heavy metals from waste water. The obtained hybrid materials are characterized using IR-FT, TGA and EA.

Acknowledgments: Development Cooperation UCLouvain, CNRST Morocco, WBI, CMOL and LCAE laboratories.

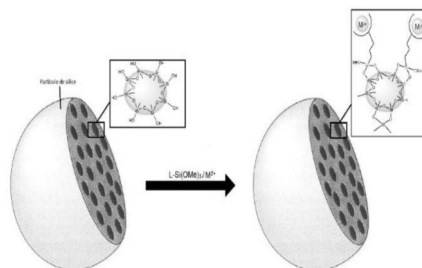


Fig.1 schematic representation of the incorporation of ligand L on the silica surface

(1) A. F. El-Kafrawy et al. Egyptian Journal of Petroleum 26 (2017), 23.

(2) S. Radi et al. Anal. Methods 8 (2016), 6923.

(3) T. R. Scicluna et al. CrystEngComm 12 (2010), 3422.

Emergence of a superglass phase in a Bose-Hubbard model with off-diagonal disorder

A. M. Piekarska, T. K. Kopeć

Institute of Low Temperature and Structure Research, Polish Academy of Sciences, Wrocław, Poland

email: a.piekarska@intibs.pl

The interplay between disorder and interactions in solid state systems is full of challenges and opportunities for both theoretical and experimental research. Disorder leads to the localization of the wave function, with the most known example being Anderson localization. On the other hand, interactions have an opposite effect, most notably pronounced in the phenomenon of Bose-Einstein condensation. The case, when the disorder lies in the potential energy is well explored. It was found that there is no direct Mott insulator to superfluid phase transition, as an intermediate Bose glass phase appears in between.⁽¹⁾ To broaden this research, it is vital to explore physics that emerge when the hopping amplitudes are disordered instead, which makes the system frustrated. It is also of particular interest, as with this kind of disorder, we make a connection to the once celebrated spin-glass systems.

In this contribution, we study a system of bosons with off-diagonal disorder,^(2,3) and show that it features an emergent superglass phase characterized by the competition of glassy and superfluid orders.

The system is modeled using the Bose-Hubbard Hamiltonian, in which the hopping terms are independent Gaussian-distributed random variables. We employ the replica trick and Trotter-Suzuki expansion to arrive at a set of self-consistent equations, which we then solve numerically. Using their solution, we evaluate critical line conditions, based on Landau theory and stability criterion,⁽⁴⁾ to find the phase diagrams of the system.

The computation requires calculating thermodynamical averages with an effective Hamiltonian. While the Monte Carlo method is usually effective in such cases, we have proved that our case suffers from a severe sign problem and thus requires us to perform a direct summation over all microscopic states of the system. We implement hybrid parallelization of the code and utilize a range of optimizations to make the computation feasible.

We find the phase diagrams for various choices of the system parameters and characterize the phases based on the values of the order parameters, compressibility, and behavior of dynamical correlations.⁽⁵⁾ With the two possible orderings present in the system, glassy and superfluid, we can identify four phases: disordered, glassy, superfluid, and the emergent superglass phase. In the latter, the two orders compete, as evidenced by the anticorrelation of their order parameters.

Acknowledgments: This work was supported by the Polish National Science Centre under Grant No 2018/31/N/ST3/03600. Calculations have been partially carried out using resources provided by Wroclaw Centre for Networking and Supercomputing (<http://wcss.pl>), grant No. 449.

- ⁽¹⁾ L. Pollet et al. *Phys. Rev. Lett.* 103 (2009), 140402.
- ⁽²⁾ A. M. Piekarska, T. K. Kopeć. *Phys. Rev. Lett.* 120 (2018), 160401.
- ⁽³⁾ A. M. Piekarska, T. K. Kopeć, *Phys. Rev. B* 105 (2022), 174203.
- ⁽⁴⁾ A. M. Piekarska, T. K. Kopeć. *arXiv:2202.06610* (2022).
- ⁽⁵⁾ A. M. Piekarska, T. K. Kopeć. *J. Stat. Mech.* 2020 (2020), 024001.

Phase situation of (E)-4-((4-alkyloxyphenyl)diazenyl)phenyl alkanooates and their mixtures with chiral mesogens

M. Piwowarczyk,^{1,2} E. Juszyńska-Gałązka,¹ N. Osiecka-Drewniak,¹
M. Gałązka,¹ Z. Galewski²

¹Institute of Nuclear Physics, Polish Academy of Sciences, Kraków, Poland

²Faculty of Chemistry, University of Wrocław, Wrocław, Poland

email: marcin.piwowarczyk@ifj.edu.pl

Thermotropic liquid crystals have proved to be excellent temperature sensors due to their unusual optical properties and their strong temperature dependence. Thousands of this kind of molecules were synthesized and described in literature.⁽¹⁾ For example, (E)-4-((4-alkyloxyphenyl)diazenyl)phenyl alkanooates (nOABOOCm, structure shown in Figure 1) homologues series with various numbers of carbon atoms in alkyloxy chain (n) and alkyl chain (m) were investigated. Occurrence of plenty mesophases was observed, e.g. nematic; smectic C, G and H phases. In addition, this group of compounds can absorb UV-Vis light thanks to the presence of diazenyl group.^(2,3) Although, for application purposes more suitable is using mixtures of liquid crystals (e.g. thermography).⁽⁴⁾

Phase situation of nOABOOCm (for $n=3, 5, 7, 8$ or 10 and $m=1-19$) compounds will be present. Results were obtained with Polarizing Optical Microscopy (POM), Thermo-Optical Analysis and Differential Scanning Calorimetry (DSC).

Phase diagrams and thermal properties, investigated using POM and DSC methods, of mixtures of selected nOABOOCm (for $n=7$ and $m=5$ or 8) compounds and chiral mesogenes (e.g. cholesterol pelargonate), which were prepared in various concentrations, will be shown in details. Induction of chiral mesophases will be discussed.

Acknowledgments: MP has been partly supported by the EU Project POWR.03.02.00-00-I004/16.

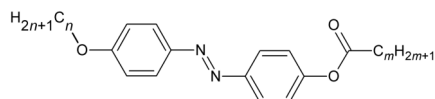


Figure 1. Structural formula of nOABOOCm compounds (for $n=3, 5, 7, 8, 10$ and $m=1-19$).

(1) D. Demus et al. Handbook of Liquid Crystals, Wiley-VCH (1998).

(2) I. Niezgoda et al. Phase Transit 87 (2014), 1038.

(3) M. Piwowarczyk et al. Phase Transit 92 (2019), 1066.

(4) J. Żmija et al. Wydawnictwo Naukowo-Techniczne (1989) [in Polish].

The effect of solvent on oxidation behavior of copper during laser irradiation of suspension, a reactive bond molecular dynamics study

M. S. Shakeri,¹ Z. Swiatkowska-Warkocka,¹ T. Itina²

¹Institute of Nuclear Physics Polish Academy of Science, Kraków, Poland

²Laboratory of Hubert Curien, University of Jean Monnet, Saint-Etienne, France

email: ms.shakeri@ifj.edu.pl

Pulsed laser irradiation of suspension (PLIS) is a promising method for synthesis of multicomponent powders i.e. composite materials and heterojunctions.⁽¹⁾ The process initiates with making a stable suspension following by laser irradiation. One of the advantages of this method is the production of completely spherical particles which are of great interest in high-tech applications. Beside the advantages of this method, there is an obstacle which restricts the usage of this method including the mechanism of phase formation. Laser irradiation increases the temperature of the suspension containing nano-powders; by the way, the exact temperature could not be easily determined due to the fastness and the excessive increasing of temperature during irradiation.⁽²⁾ Kinetics and thermodynamics rules play an important role in bond breaking and bond formation during laser irradiation of suspension. Hence, reactive bond molecular dynamics (RBMD) is considered as a suitable method for studying the atomic interactions in high temperatures and better understanding of PLIS. RBMD uses the conventional Newton's law to study the dynamic of a system, but, it is also contains bond orders for determination of bond breaking/formation procedure.⁽³⁾

In the present investigation, the effect of different kinds of solvent on oxidation behavior of copper has been evaluated using RBMD during PLIS. To determine the exact temperature of spheres, heating-cooling model has been utilized. The NVT simulations have been done for copper slabs exerted inside solvent molecule pack. Ethanol, ethyl acetate, toluene and acetone have been considered as the main solvents. Results of the investigation show that the solvent molecules firstly absorb on the copper surface. The oxidation behavior of copper is completely affected by the kind of solvent because each solvent decomposes to different species which play the role of oxidation or reduction agents. The top reactions, their network and timeline of oxidation process have also been reported.

Acknowledgments: This work was supported by the Polish National Science Center Program No. 2018/31/B/ST8/03043.

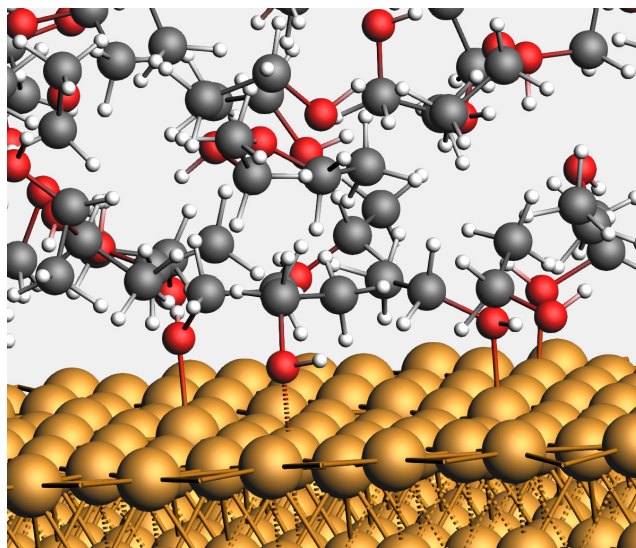


Figure 1. Absorption of ethanol molecules on Cu surface during the initiation of MD process.

- (1) S. Sakaki et al. *Chem. Phys. Chem.* 18 (2017), 1101 – 1107.
- (2) M. Dontgen et al. *J. Chem. Theory Comput.* 11 (2015), 2517 – 2524.
- (3) W. Zhu et al. *J. Phys. Chem. C* 124 (2020), 12512 – 12520.

Influence of He^+ irradiation and surface effects on compensation point in ferrimagnetic TbFe alloys

P. Sobieszczyk, M. Krupiński

Institute of Nuclear Physics Polish Academy of Sciences, Kraków, Poland

email: pawel.sobieszczyk@ifj.edu.pl

Over the last two decades, the interest of the 3d-transition metal (TM) — rare earth(RE) alloys has been emerged due to their possible applications in magneto-optical recording and ultrafast laser switching.⁽¹⁾ The most interesting properties for the magnetic reorientation process occurs at the compensation temperature (T_n) where the alloy shows no net magnetization. The value of the compensation point can be controlled through the composition, structure and thickness of the alloy thin film.⁽²⁾ In the studies, we explore other possibilities of tuning the compensation point, namely by He^+ ion irradiation and by surface to bulk ratio adjustment. We investigated a 20-nm-thick $\text{Tb}_x\text{Fe}_{1-x}$ alloy film with perpendicular magnetic anisotropy, irradiated with doses ranging from 5×10^{13} to 5×10^{15} ions per cm^2 . The changes in compensation point caused by the irradiation were explained with the help of atomistic simulation.^(3,4) Based on the same model we also studied the changing in compensation point in the nanospheres of $\text{Tb}_x\text{Fe}_{1-x}$ with diameters (D) ranging from 3 nm to 12 nm. We observed that T_n depends on the diameter of the nanoparticle as $1/D$, which may be attributed to changes in the spin direction on the particle surface. The results performed in atomistic approach were also confirmed with the mean-field approximation.

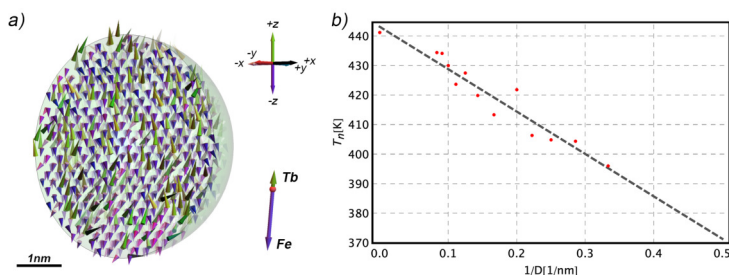


Figure 1. a) Distribution of spins in the ferrimagnetic $\text{Tb}_{24}\text{Fe}_{76}$ nanoparticle at $T=100$ K. b) Compensation point as a function of nanosphere diameter (D).

(1) S. Mangin et al. Nat. Mater. 13 (2014), 286.

(2) M. Heigl et al. AIP Advances 11 (2021), 085112.

(3) M. Krupiński et al. Phys. Rev. Mat. 5 (2021), 024405.

(4) T. A. Ostler et al. Phys. Rev. B 84 (2011), 024407.

The analysis of anisotropy in polydispersed multiphase composites

N. Rylko,^{1,4} M. Stawiarz,^{2,4} P. Kurtyka,^{3,4} V. Mityushev^{1,4}

¹Department of Applied Mathematics, Faculty of Computer Science and Telecommunications, Cracow University of Technology, Kraków, Poland

²Pedagogical University of Krakow, Doctoral School, Krakow, Poland

³Innerco sp. z o.o, Kraków, Poland

⁴Materialica+ ResearchGroup

email: mgstawiarz@gmail.com

The Al-Si-Cu/SiCp composite structure produced in the Friction Stir Processing is investigated. As a result of severe plastic deformation, the local anisotropy fields are obtained. This effect usually cannot be seen in the sense of direct observation. In this work we discuss a new two-dimensional polydisperse model for testing multiphase composites. The analyzes are carried out in order to study the influence of the separate phases redistribution on the anisotropy of the physical properties. The microstructure of examined composite is considered on the micro-, meso-, and macro levels. For these calculations, not only concentration but also the geometrical parameters of each particle is take into account. In this case, the results can be defined as the cumulative vector parameter corresponding to the two-point spatial correlation function of inclusions, but a significant reduction in computational costs is achieved.

First the new formula of polydispersed anisotropy coefficient κ is derived. Then $\kappa(x)$, a global coefficient, is computed as an anisotropy value over the all meso cells in spatial coordinates x . It leads to the determination of the principal axes of the effective conductivity tensor Λ , the angle of their inclination to the x -axis. It properly describes the anisotropy fields in composites modeling in particular thermal and electric conductivity, diffusion and elastic antiplane deformation. The relation between $|\kappa|$ and Θ is investigated. The results of the numerical experiments are analyzed using the Elbow Method and K-mean algorithm.

The geometrical properties of the analyzed structural elements are obtained with the use digital images analysis.

Serendipitous formation of a dumbbell-like CN-bridged Ni(II) dimer

A. Warzybok, M. Heczko, B. Nowicka

Faculty of Chemistry, Jagiellonian University, Krakow, Poland

email: adrian.warzybok@student.uj.edu.pl

Coordination assemblies based on cyanide bridges are susceptible to molecular engineering and often yield designed compounds. However, serendipitous formation of unexpected products with unusual properties sometimes occurs. In the presented case we have used $[\text{Cr}(\text{CN})_6]^{3-}$ together with $[\text{Ni}(\text{tmc})]^{2+}$ (tmc=1,4,8,11-tetramethyl-1,4,8,11-tetraazacyclotetradecane) in order to obtain a polynuclear molecule. The tertadendate tmc ligand coordinates in a folded conformation leaving only one position available for an additional ligand,⁽¹⁾ which was found to induce high magnetic anisotropy.⁽²⁾ However, during the synthesis the $[\text{Cr}(\text{CN})_6]^{3-}$ anionic building block decomposed, enabling the release of the cyanide ions, which resulted in the connection of two Ni(II) centers via a CN-bridge in a dumbbell-like dinuclear ion (Figure 1). The synthetic method was later optimized, with the direct use of NaCN to obtain the same product.

The structure of $\{[\text{Ni}(\text{tmc})]_2(\mu\text{-CN})\}(\text{ClO}_4)_3$ consists of two $[\text{Ni}(\text{tmc})]^{2+}$ complexes connected by a slightly bent cyanide bridge. Single-crystal X-ray structural analysis indicates a crystallization in the monoclinic system, space group $P21/C$ with a lattice constants of $a=15.6422(6)$ Å, $b=14.8690(5)$ Å and $c=18.1734(7)$ Å. The nickel ions have an unusual coordination number of 5, and their coordination sphere shows transitional geometry between vacant octahedron (vOC) and spherical square pyramid (SPY). Magnetometric measurements show complicated magnetic interactions, with narrow hysteresis loop, metamagnetic phase transition and very low magnetization value at 7 T. These results suggest antiferromagnetic coupling between Ni(II) ions through the CN-bridge and high magnetic anisotropy, which result in a low residual spin value of the dimer with strong directional preference.

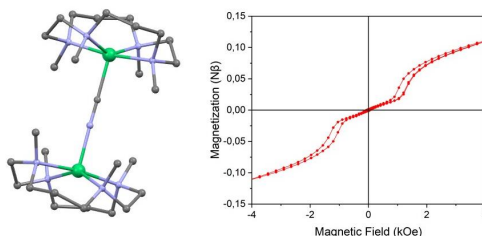


Figure 1. Structure of the $\{[\text{Ni}(\text{tmc})]_2(\mu\text{-CN})\}^{3+}$ dimer and magnetic hysteresis loop.

⁽¹⁾ B. Nowicka et al. In Bull. Chem. Soc. Jpn. 75 (2002), 2169 – 2175.

⁽²⁾ B. Cahier et al. Chemistry — A European Journal (2017), 3648 — 3657.

The lattice specific heat of metal-organic materials with chain-like crystal structure

O. Vinnik,¹ R. Tarasenko,¹ I. Potočný,¹ K. Zakuťanská,²
N. Tomašovičová,² M. Orendáč,¹ A. Orendáčová¹

¹Institute of Physics, P. J. Šafárik University, Košice, Slovakia

²Institute of Experimental Physics of SAS, Košice, Slovakia

email: olha.vinnik@student.upjs.sk

The current work is focused on the comparative study of lattice subsystem of Cu(II) based low-dimensional quantum magnets with a quasi-one-dimensional polymer structure Cu(en)₂SO₄, Cu(en)₂CrO₄, Cu(en)Cl₂ and Zn(en)Cl₂ (en = ethylenediamine = C₂H₈N₂). The temperature dependence of the specific heat was measured in zero magnetic field in the temperature range from 2 to 300 K. Structural phase transition was observed only in Cu(en)Cl₂ manifested as a sharp λ -like anomaly in the lattice specific heat at $T_c=138$ K, which is associated with the removing structural disorder of en rings.⁽¹⁾

A similar behavior was also expected for the Zn(en)Cl₂ material, but after structural analysis it turned out that while in Cu(II) compounds en coordinates as chelating ligand, in this material ethylenediamine forms bridging ligands resulting in the formation of zig-zag covalent chains. Concerning the isomorphous Cu(en)₂CrO₄ and Cu(en)₂SO₄ compounds, the comparison of specific heats revealed that S-Cr substitution caused larger differences in specific heats than Cu-Zn substitution in Cu(en)Cl₂ and Zn(en)Cl₂ which are characterized by different spatial groups. The differences indicate that the main contribution to the specific heat below room temperature is provided by intramolecular vibration modes. The study was completed by room-temperature infrared and Raman spectra, yielding information about the frequency range of lattice vibrations. Using phonon density of states approximated by a quadratic frequency dependence up to Debye frequency and the set of delta functions at Einstein frequencies taken directly from vibration spectra, the specific heats were described up to room temperature. The deviations from the Debye approximation with Debye temperatures $\Theta_D=100$ K, 94 K, 109 K and 103 K for Cu(en)₂SO₄, Cu(en)₂CrO₄, Cu(en)Cl₂ and Zn(en)Cl₂, respectively, covering the contribution of acoustic modes were observed nominally already below 15 K in all compounds. The effect of acoustic and optical modes on the magnetic correlations of these systems is discussed.

Acknowledgments: The financial support of the projects APVV-18-0197 and VEGA 1/0132/22 is acknowledged.

⁽¹⁾ M. Zabel et al. Journal Structural Chemistry 47 (2006), 585.

Luminescent synthetic opals for angle-dependent emissive colour

W. Zając,^{1,2} M. Czajkowski,¹ M. Zdończyk,^{1,2} J. Cybińska^{1,2}

¹Lukasiewicz Research Network — PORT Polish Center for Technology Development, Wrocław, Poland

²Faculty of Chemistry, University of Wrocław, Wrocław, Poland

email: weronika.zajac@port.lukasiewicz.gov.pl

The history of photonic crystals known to today's scientists began in 1987 with the works of Yablonovitch⁽¹⁾ and John.⁽²⁾ Photonic crystals are remarkably interesting and deeply-studied group of modern optical materials, because of their periodical arrangement of the forming elements, which gives such effects as chromatic dispersion of diffracted light (easy to notice on 2D crystals) or Bragg reflection (3D crystals).⁽³⁾ Nowadays, artificial opals consisted of monodisperse polymeric and silica nanospheres are relatively easy to synthesize. And what's more, a possibility of doping photonic crystals with various types of materials makes it possible to obtain compounds with unique optical properties.⁽⁴⁾ Use of these materials allows to design completely new and difficult to counterfeit security features.

We synthesized a series of colloidal photonic crystals, based on poly(methyl methacrylate) (PMMA) — undoped and doped with organic dyes. We have chosen the dyes with respect to high quantum efficiency and different spectral range of the emission. Structures of the selected dyes are presented in Figure 1. The size of the nanospheres forming the synthesized 3D opals was optimized in order to cover the emission range of the dye by the reflection band of the photonic crystal. We performed full spectroscopic characterization of the fabricated luminescent opals, including angle-dependent emission (Figure 2) of light at the output of the photonic crystal.

The fabricated luminescent opals showed unusual angle-dependent emission spectrum, covering three different spectral ranges.

These studies were supported by the National Centre for Research and Development (Poland) within the framework of the 12th edition of the LIDER programme — project contract no.LIDER/39/0203/L-12/20/NCBR/2021.

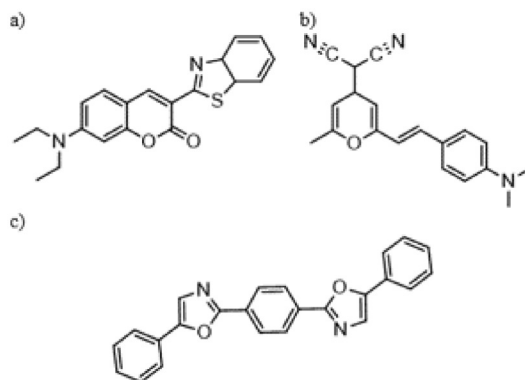


Figure 1. Chemical formula of selected dyes: a) Coumarin 6, b) DCM, c) POPOP.

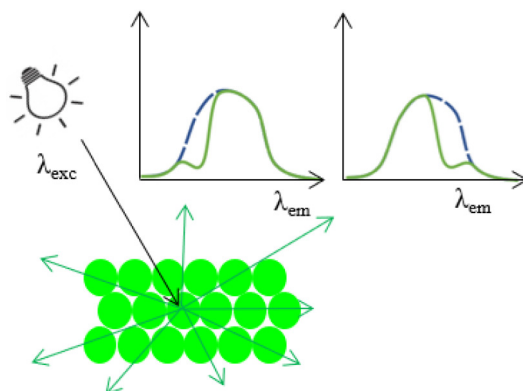


Figure 2. Schematic representation of emission measurement from different angles.

- (1) E. Yablonovitch. Phys. Rev. 58 (1987), 2059.
- (2) S. John. Phys. Rev. Lett. 58 (1987), 2486.
- (3) E. Armstrong, C. O'Dwyer. J. Mater. Chem. C 3 (2015), 6109.
- (4) Y. Yamada et al. Langmuir 25 (2009), 13599.

The TP-C isotherms of LaNi_5 and $\text{LaNi}_{4.75}\text{Pb}_{0.25}$ alloy at different temperatures statistical physics modeling of hydrogen sorption onto: microscopic state investigation, interpretation and comparison between alloys

M. Żurek

Institute of Nuclear Physics Polish Academy of Sciences, Krakow, Poland

email: michal.zurek@ifj.edu.pl

The theoretical model has been use in order to analyses absorption isotherms of hydrogen storage alloys LaNi_5 and $\text{LaNi}_{4.75}\text{Pb}_{0.25}$ at three different temperatures ($T=303$ K, 313 K, 323 K). The theoretical expressions of model base on statistical physics formalism and simplifying hypothesis. The model with highest correlation to the experimental data has been determined using numerical simulations. In the introduced model have fitted and then adjusted six parameters which corresponding to the numbers of hydrogen atoms per site denote n_α and n_β , the receptor site densities N_α and N_β and the energetic parameters P_α and P_β . The fitted parameters, were compare between Pb doped and non doped alloys in relationship to absorption isotherms temperature. Finally the established model parameters is further applied to calculate thermodynamic functions which govern the absorption mechanisms such as entropy, free enthalpy and internal energy.

⁽¹⁾ M. Khalfaoui. Science and Technology 20 (2002), 33 – 47.

⁽²⁾ N. Bouaziz. Physica B 525 (2017), 46 – 59.